Benghazi University
Faculty of Science
Department of Earth Sciences

Mineralogy and Geochemistry of the Beach Sands Along the Coast Between Al Kuwifia and Tolmeita, NE Libya.

A thesis
Submitted to Department of Earth Sciences,
University of Benghazi in Partial Fulfillment of the
Requirements for the Degree of Master of Science in Geology

By

Basem A. El-Werfalli

Supervised by

Professor Esam O. Abdulsamad

Assistant Professor Osama R. Shaltami

Academic Year (2015 - 2016)

جامعة بنغازي

كلية العلوم

قسم علوم الارض

الخصائص المعدنية والجيوكيميائية للرمال الشاطئية على طول الساحل من طلميثة إلى الكويفية، شمال شرق ليبيا.

أطروحة قدمت لقسم علوم الأرض، جامعة بنغازي في تحقيق جزئي لمتطلبات درجة الماجستير في علوم الارض

بواسطة الطالب:

باسم أحمد الورفلي

تحت اشراف:

استاذ دكتور: عصام عبد الصمد

استاذ مساعد: اسامة الشلطامي

السنة الدراسية (2015 - 2016)

Title of thesis

Mineralogy and Geochemistry of the Beach Sands Along the Coast Between Al Kuwifia and Tolmeita, NE Libya.

By

Basem A. El-Werfalli

Approved by:

Supervisor:

Professor Esam O. Abdulsamad…….

Dr. Osama R. Shaltami…….……..

Examination Committee:

External examiner:

Dr. Ahmed O. El-Werfalli.…….

Internal examiner:

Dr. Saad El Ebaidi……..……

Countersigned by

Dr. Omar B. Elfigih

(Head, Department of Earth Sciences)

…….

Dr. Houssien M. Elbaraasi

(Dean, Faculty of Sciences)

……

DEDICATION

To an epitome of kindness, patience, and optimism my dear mother;

To the Man with the big heart my dear father;

To those who have given me all support and encouragement my brothers and sisters;

To the source of love my wife;

To those who have been the reasons for my happiness my daughters;

To the people who paved my way of science and knowledge my teachers; and

to the people who lived with me the most beautiful moments my friends

I dedicate this research.

ABSTRACT

The present work aims to characterize the mineralogy, geochemistry and environmental geochemistry of the beach sands along the Mediterranean Coast from Al Kuwifia to Tolmeita, NE Libya. The microscopic examination and SEM-EDX indicate abundance of carbonates, quartz, feldspars, glauconite and evaporites. Carbonate grains are mainly represented by biogenic grains made of aragonite and/or calcite. Quartz is mostly monocrystalline with uniform and undulatory extinction. It occurs either in the form of angular grains or as rounded grains. The former type is the more abundant. The detected evaporites are gypsum and halite. Feldspars, glauconite and heavy minerals are controlled by terra rossa and only detected in the eastern side of the studied beach, while they are lacking in the western side. The recorded heavy minerals are zircon, augite, tourmaline, rutile, biotite, garnet, monazite, titanite, hornblende, pistachite, magnetite, ilmenite, hematite, goethite, limonite and pyrite. Based on the mineral composition, two distinct types or groups of sediments were extracted. The major oxides CaO and MgO are the main constituents of the carbonate minerals; calcite and aragonite. SiO_2 is mainly in the form of quartz. Sometimes a high quotient of SiO_2 together with the oxides; Al_2O_3, K_2O and partly of Na_2O, TiO_2 and Fe_2O_3 are essentially allocated within the structure of the feldspars. Part of Na_2O and the content of Cl belong mainly to halite. Part of Fe_2O_3 and TiO_2 may be accommodated as iron oxyhydroxides. Part of CaO and the content of SO_3 are allotted within the gypsum structure. Ba, Sr, Th, U and REE are basically controlled by the carbonate fraction, while Cu, Zn, V and Cr are strongly correlated with Al_2O_3. The prevailing well oxidizing coastal environments are well expresses by the low authigenic uranium and low U/Th, V/Cr and Cu/Zn ratios. ΔCe values are not correlated with U and CaO contents, which suggest that the ΔCe values are not related to the paleo-redox conditions. Metals analyzed in this study, except Cr and V in some locations, have $EF > 2$ suggesting that they are mainly of anthropogenic origin and that natural activities exert little influence on their abundances. The I_{geo} values suggest that the studied samples are unpolluted with Cu, Zn, V, Cr, Pb and Th, very lightly polluted to lightly polluted with As and lightly polluted with U.

الملخص العربي

تهدف هذه الدراسة إلى تقييم التكوين المعدني والجيوكيمياء البيئية للرمال الشاطئية على طول ساحل البحر المتوسط بين الكويفية وطلميثة، شمال شرق ليبيا. الدراسة باستخدام المجهر والأشعة السينية تدل إلى وفرة من الكربونات، الكوارتز، الفلسبار، جلوكونيت والمتبخرات. تتمثل الحبيبات الكربونية أساسا من الحبيبات الاحيائية المتكونة من الأراجونيت والكالسيت. المتبخرات المحللة تتمثل في الجبس والهاليت. الفلسبار، الجلوكونيت والمعادن الثقيلة متكونة من الرواسب القارية وموجودة في الجانب الشرقي فقط من الشاطئ المدروس. المعادن الثقيلة المحللة تتمثل في الزركون، الأوجايت، التورمالين، الروتيل، البيوتايت، الجارنت، المونازيت، التيتانيت، الهورنبلند، البيستاكيت، المجنتيت، إلمينيت، الهيماتيت، الجيوثايت، الليمونيت والبيريت. بناء على التركيب المعدني تم استخراج نوعين أو مجموعتين من الرواسب. أكاسيد الكالسيوم والمغنيسيوم هي المكونات الرئيسية للمعادن الكربونية (الكلسيت والأراجونيت). السليكا هي مكون اساسي في معدن الكوارتز. أحيانا نسب عالية من السليكا مع أكاسيد الالومنيوم، الصوديوم، الحديد والتيتانيت متكونة في معادن الفلسبار. جزء من اكسيد الصوديوم والكلور تنتمي أساسا إلى الهاليت. جزء كبير من اكاسيد الحديد والتيتانيوم موجودة في مكون اكاسيد وهيدرواكاسيد الحديد. جزء من أكسيد الكالسيوم وثالث اكسيد الكبريت داخل معادن الجبس. الكربونات هي المكون الاساسي للباريوم، الاسترانشيوم، الثوريوم، اليورانيوم والعناصر الأرضية النادرة، بينما المكون الاساسي للعناصر الثقيلة النحاس، الزنك، الفانديوم والكروم هو اكسيد الالومنيوم .النسب المنخفضة للنحاس الى الزنك، الكروم الى الفانيديوم، و اليورانيوم الى الثوريوم دلت على وجودها في بيئة مؤكسدة. لا يرتبط معدل تغير السيريوم مع اليورانيوم والتي تشير إلى ان قيم معدل تغير السيريوم السالبة لا تتعلق بالأكسدة القديمة. المعادن التي تم تحليلها في هذه الدراسة فيما عدا الكروم والفانيديوم في بعض المواقع لها معامل زيادة اكبر من 2 والذي يشير إلى أنها هي أساسا من مصادر صناعية وأن المصادر الطبيعية قليلة جدا. ويشير معامل التراكم الى أن العينات المدروسة هي غير ملوثة بالنحاس، الزنك، الفانيديوم، والكروم، والرصاص، وملوثة بشكل بسيط مع اليورانيوم والزرنيخ.

ACKNOWLEDGEMENT

Special thanks to Allah for giving me the strength to take up this Masters degree. I also thank my supervisors Prof. Esam Abdulsamad and Assistant Prof. Osama Shaltami for their support and constructive criticisms throughout the study period.

I would like to extend my thanks to all Members of the Department of Geology, Cairo University and Nuclear Material Authority for their kind assistance in the preparation and analysis of samples.

I remain greatly indebted to my parents, siblings and wife for their encouragement, support, and unconditional love.

I would never forget the inputs of Members of Staff of the Department of Earth Sciences and the Geology Management of Arabian Gulf Oil Company (AGOCO) to this piece of research. With all the gratitude within me, I thank you all.

CONTENTS

LIST OF FIGURES

LIST of TABLES

INTRODUCTION

This work aims to characterize the mineralogy, geochemistry and environmental geochemistry of the beach sands along the Mediterranean Coast from Benghazi outskirts (Al Kuwifia) to Tolmeita, NE Libya, with especial emphases on the provenance. Libya is bounded by Egypt in the east, Sudan, Chad and Niger in the south, Tunisia and Algeria in the west, and by the Mediterranean Sea in the north. It has an area of 1.8 million km^2 with coastline extending over 1900 km long. Libya includes four major sedimentary basins represented in Sirt, Muruzq, Alkufra and Ghadamis Basins.

North eastern Libya (referred to as Cyrenaica) is located on the southern margin of Mediterranean Sea and on the northern margin of the African plate. The study area is the coastal area of a part of the Cyrenaica extended from Benghazi to Tolmeita, between longitudes 20^o 06' and 21^o 00' E and latitudes 32^o 12' and 32^o 45' N (Fig. 1.1).

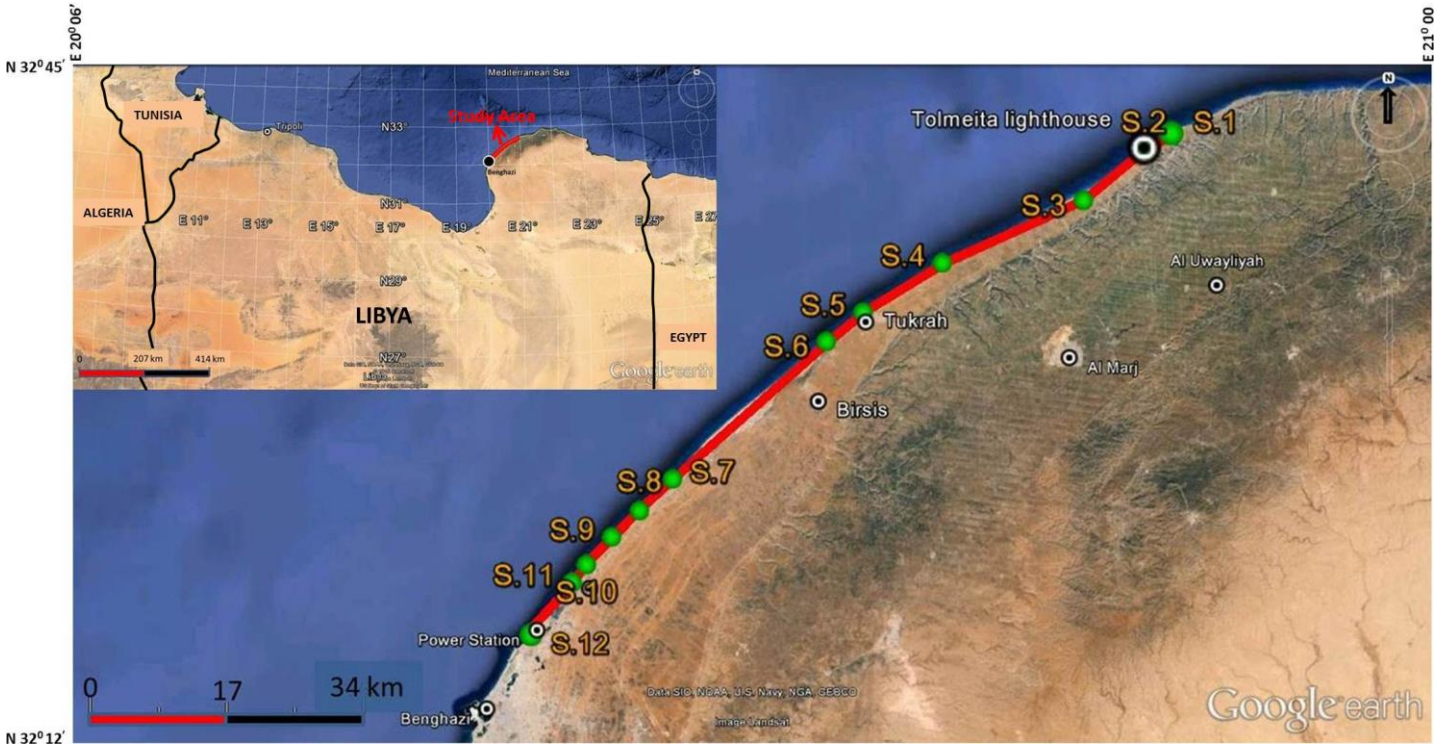

Fig. 1.1: Location map of Libya showing the study area and the location of the sampled stations

Twelve stations were sampled along the beach of the study area (S1-S12). This beach is surrounded by Al Jabal Al Akhdar (Green Mountain) from the first to the forth stations (S1-S4), and it is getting to be open from the fifth station (S5) to the southwest (Fig. 1.1). There are two beach types; sandy and rocky beaches (Figs. 1.2-3).

Fig. 1.2: Sandy beach at station no.2 (Tolmeita)

Fig. 1.3: Rocky beach at station no.5 (Toukrah)

1.1. Geology of the area between Benghazi and Tolmeita

The Cyrenaica covers an area of about 150.000 km^2 of northeastern Libya. The arms of the Sirte rift complex and its offshore extension into the Gulf of Sirte bound it to the west and to the south. To the east it extends into the Marmarica Platform of the Western Desert of Egypt. The Cyrenaica consists of two distinct tectonic provinces, which are separated by the Cyrenaican Fault System. These are the North Cyrenaica Inverted Basin, referred to as the Al Jabal al Akhdar, and the Cyrenaica Platform to the south (Fig. 1.4) (El Hawat and Pawellek, 2005).

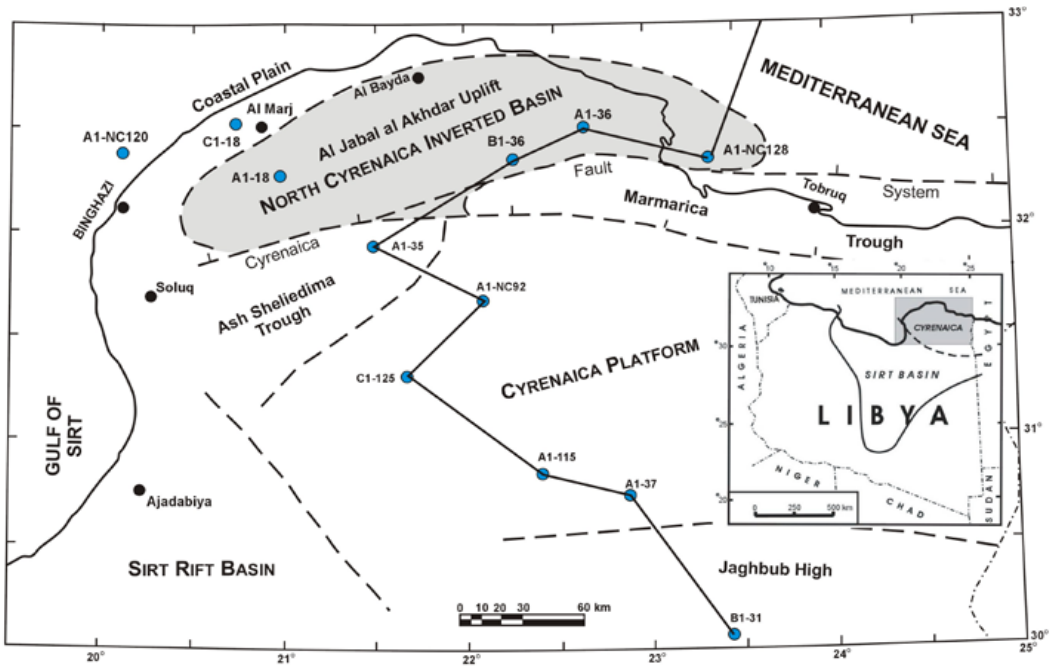

Fig. 1.4: Map of the Cyrenaica showing the main tectonic provinces (after El Hawat and Pawellek, 2005)

The inversion of north Cyrenaica Basin during the Upper Cretaceous was a direct result of the compressive forces induced by the convergence between the African – European and Aegean plates. These are also reflected on the stratigraphic record of the northern Cyrenaica. Evidence of repeated syn-depositional mass movement of sediments, unconformities, as well as post-depositional deformation structures extends from the Upper Cretaceous to the present demonstrating these recurring compressive events. Major slump structures, slides, debris flows and turbidites are commonly observed in surface outcrops of the Cretaceous, the Eocene, and the Oligocene.

The northern coastal margin of Cyrenaica exhibits successive elevated wave-cut erosional terraces with residual Pleistocene beach-dune calcarenite depositional complexes are observed in place up to 150 m elevation above the present day sea level (Fig. 1.5-6). These terraces were elevated not only as result of the relative Pleistocene eustatic sea-level change, but were uplifted after the Pleistocene by uplifting as indicated by the associated knee folds of the older rocks (Fig. 1.6), where the footwall was pushed upward in relation to the hanging wall. All of these events and signatures are testament to the ongoing tectonic activity of Cyrenaica since the Late Cretaceous inversion to the present day (El Hawat and Abdulsamad, 2004).

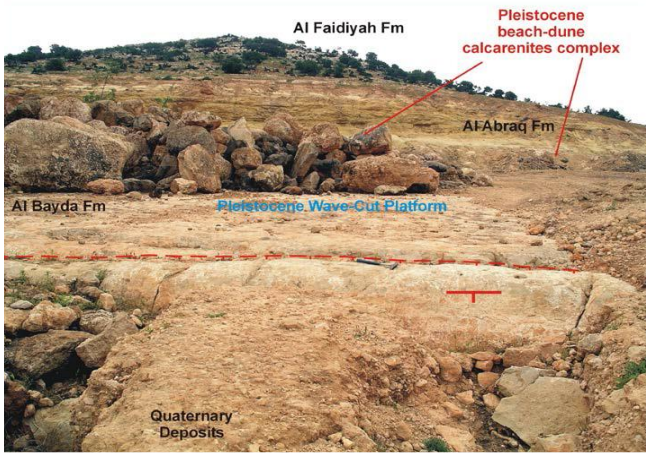

Fig. 1.5: Benghazi Plane fault system, uplifted Pleistocene wave-cut platform, and associated calcarenite beach-dune deposits (now at 130 m above sea level) (after El Hawat and Pawellek, 2005)

Fig. 1.6: Panoramic view from the first escarpment road overlooking Susah showing fault elevated wave-cut terraces and associated Pleistocene beach-dune calcarenites (after El Hawat and Abdulsamad, 2004)

The exposed facies surrounded the study area range in age from the Lower Eocene which is represented by the Apolonia Formation, to the Upper Miocene which is represented by the Wadi al Qattarah Formation (Figs. 1.7-8). All these formations are mainly consisted of carbonates rich in fossils which are different from a formation to another.

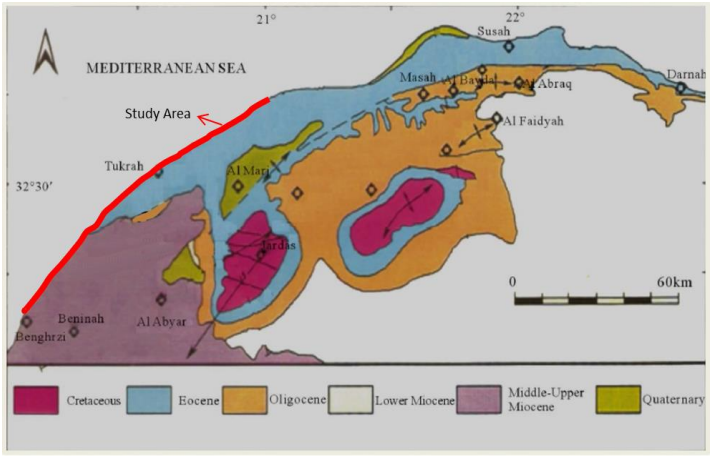

Fig.1.7: Surface geological map of Al Jabal Al akhdar (modified after El Werfalli et al, 2000)

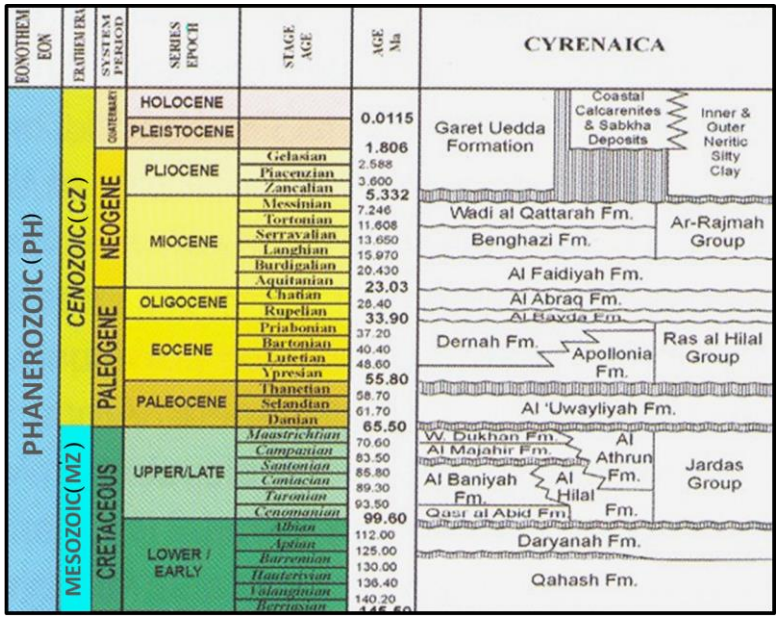

Fig.1.8: Stratigraphic chart of northern Cyrenaica (after El Hawat el al., 2004)

Much of northern Cyrenaica is occupied by Al Jabal Al Akhdar, a mass of limestone hills rising to heights of more than 800 meters. On its north side it falls steeply to the sea making a high and well-defined escarpment, this feature also continues round the west side of the Al Jabal Al Akhdar. At frequent intervals along the whole of its length the escarpment is notched by wadis, most of them dry at all times except for a few days of violent flooding each year. Perennial springs are rare, and only a few are copious enough to maintain a stream as much as a kilometer in length (Hey, 1963).

In these wadis and along the coastal escarpment various Pleistocene deposits are found of which an account was given by Mcburney and Hey (1955). With regard to the non-marine deposits,

Hey (1963) concluded that they belonged to two distinct phases of deposition، both subsequent to the Last Interglacial. First, much calcareous marls were laid down in some wadis, together with small amounts of gravel. The climate of this time he believed to have been wet and temperate. Then, after a period of down-cutting, great quantities of gravel were laid down, forming terraces in almost all the wadis and alluvial fans on the coastal plains. These, which he called the Younger Gravels, he attributed to frost-shattering under conditions much colder than those of today.

The Pleistocene deposits in the coastal areas consist of lagoonal clays, sabkha carbonates evaporites, and beach-dune calcarenite complexes (El Hawat and Abdulsamad, 2004).

The Tertiary carbonate rocks which surround the study area from northeast to southwest are covered by Quaternary deposits. The Quaternary deposits observed in the study area are extended along the coastal plain to the shoreline. These deposits are represented in red soil, loose gravels, beach sands and calcarenites (Figs. 1.2-3 & 1.9).

Fig. 1.9: Quaternary deposits (calcarenite) at station no.12 (Al Kuwifia)

1.2. Previous work

As far as the author is aware, the published data on the beach sands of the study area and their environmental geochemistry are very insufficient. The studies on the Quaternary are less numerous than those on the Tertiary rocks. Most geological publications on the study area deal with the sedimentary succession of the Al Jabal Al Akhdar. The present thesis attempts to contribute to the available knowledge on the mineral and chemical compositions and the environmental geochemistry of the beach sands along the Mediterranean Coast from Benghazi outskirts (Al Kuwifia) to Tolmeita, Northeast Libya. The following, is a brief survey on the published data

especially those dealing with the mineralogy, geochemistry and environmental geochemistry in other areas in Libya.

Desio (1970) studied the major element geochemistry of the Sabkha of Marada, Southwest Libya. He found that the differences in the chemical composition of the salts characterizing the various sabkhas can be explained to the different composition of the sediments through which flow the underground water feeding the sabkhas and to which owes the saline inflow. He also found that the high concentration of potassium in the Miocene series of Sirte seems to be in close relation to the lagoonal character of some Oligocene and Miocene levels of Sirte.

Maksimovic and Eskangi (1978) studied the trace elements in groundwater of the Alkufra Basin, Southeast Libya. They considered that the studied water is of excellent quality, because only a few wells have anomalous content of Pb and Zn, and in some of them small amounts of Cd have been detected. They also added that these anomalous water wells are not dangerous in the Alkufra area, because of a very low percentage of clay minerals in soils, which might adsorb heavy metals.

Krinsley and Tovey (1978) used CL (Cathodoluminescence) technique to study dune sands from Libya and gravelly sands from England. They identified six textural characteristics on the basis of CL: (1) absence of CL; (2) lack of CL contrast; (3) narrow band structures (fractures); (4) diffuse dark areas; (5) dark areas with sharp bound arises; and (6) mottled CL textures. They suggested that these fractures reflect the complex geological history of the quartz grains clearly a reference to provenance.

El-Amamy *et al.*, (1982) studied the chemical and mineralogical properties of some Libyan glauconitic soils in the Barce Plateau region, Northeast Libya. There are three soil types, Elabiar clay loam, Elmarj silty clay, and Hamama clay, were selected to represent a weathering sequence. The cation exchange capacities (CEC) of these soils were found to increase with increasing weathering intensity. They studied the effect of potassium (K) depletion in clay and silt fractions on chemical and mineralogical properties of the soil glauconite. A relationship between equilibrium K concentration in the extracting solution and weathering degree was established. Although it exists in all size fractions, glauconite (10.0, 5.0Å) was found at higher concentrations in fine silt and coarse clay fractions. Elabiar clay loam contained more glauconite and less K-depleted glauconite than Hamama clay. Total K values were proportional to the amount of glauconite in each of the soil

separates. The results of equilibrating the clay and silt fractions with 1N NaCl indicated that more than 90% of total K was exchangeable with an equivalent increase in CEC. When the replaced K was allowed to accumulate in the extracting solution, the exchange process continued until K concentration reached a certain equilibrium level. The equilibrium K concentration was a function of K depletion regardless of particle size, solution density, or both. Because of their larger surface areas and the shorter diffusion paths, the finer fractions had shorter equilibration times and more rapid exchange rates. The K depletion resulted in expanding the 10Å glauconite to 14 and to 15Å when Mg-saturated. Glycolation of the Mg-treated samples did not affect the 14 to 15Å K-depleted mineral. The results confirm those of previous research with glauconite specimens that, upon weathering, the soil glauconite produced vermiculite- rather than a smectite-type mineral.

Jakovljevic (1984) studied the characteristics of soil in A1 Awaynat area, Southwest Libya. He found that the studied soil is characterized by moderate alkaline reaction, absence of calcite, extremely low content of organic matter and very high salt content.

Golik *et al.,* (1988) studied the pelagic tar in the Mediterranean Sea. They found that the distribution of the tar content indicates that the most tar contaminated sea is in the northeast between Cyprus and Turkey and in the Gulf of Sirte off the coast of Libya, where the mean tar content was 1847 and 6859 μg m^{-2}, respectively. The least polluted areas were the western Mediterranean, 236 μg m^{-2}, and the northern Ionian Sea as far east as halfway between Crete and Cyprus with mean tar concentration of 150 μg m^{-2}. A comparison between pelagic tar data collected in 1969, in 1974 and this 1988 data shows a sharp decline in tar concentration with time, from 37,000 μg m^{-2} in 1969 to 9700 μg m^{-2} in 1974 and to 1175 μg m^{-2} in 1987. The increased activity of the oil terminal in Iskenderun Bay, Turkey, and the activity of oil loading at the terminals in Libya still leave a high level of tar pollution in the Mediterranean water off these coasts.

Hamouda and Wilson (1989) studied the levels of the heavy metals in surface sediments along the Benghazi Bay, Northeast Libya. They found that the ranges of concentration were 1.03 % - 1.96 % (dry wt) for organic content and 64.7 % - 93 % for calcium carbonate while the ranges of the heavy metals concentration (μg g^{-1} dry wt) were 8.7 - 42 for Cu, 2.3 - 27.3 for Zn, 5.7 - 19 for Ni, 37 - 76.7 for Mn, and below the detection limit (< 1.73 ppm) for Cd. They also found that the Pollution Load Index (PLI) score for the control site was 9.51 and the score for the overall studied area was 7.51 indicating a very clean environment.

El Hinshery and Kumar (1992) studied the Pb levels in settled dusts of Tripoli, Northwest Libya. The samples collected near small streets, playgrounds, gas stations and main streets in the Tripoli area. They found that the overall mean values observed were 417, 533, 553 and 797 μg g^{-1} dry wt for the above locations, respectively. The overall mean concentration for main streets was significantly higher ($P < 0.05$) than for other sites.

Shenber and Eriksson (1993) studied the sorption behavior of Cs in 19 different soils from various regions of Sweden and Libya. They found that the sorption behavior of Cs was complex. The distribution coefficient, the Kd value, was strongly reduced after small additions of stable Cs. However, at increasing concentrations of stable Cs the effect became much less. They also found that some of the Libyan soils have higher Kd values than the Swedish soils with similar clay content.

Assaf *et al.*, (1994) studied the surficial uranium mineralization in Zarzaitine Formation sediments, A1 Awaynat, Southwest Libya. They found that the studied sediments, in particular the silt and clay units are believed to be partially formed of volcanic ash, which are known to be one of the main sources of U. The concentration of U, from these sediments, is thought to occur through devitrification and the leaching action of groundwater. The restriction of this uraniferous mineralization to the surface of the Zarzaitine Formation is attributed to the lithological characteristics of these sediments rather than their intrinsic origin.

Ali *et al.*, (1998) studied the organics in the Libyan beach sand and water. Forty-three samples from fifteen locations extending along 200 kilometers from near the Tunisian borders to 20 kilometers east of Tripoli harbor were examined for their organic contents. Sampling was conducted under the following specifications. 1- Dry beach sand, 3-4 meters away from water. 2- Wet beach sand, obtained from 1 meter depth. 3- Beach water. Known amounts of sand and beach water were extracted with a suitable volume of chloroform. Organics in the extracts were determined gravametricly by complete evaporation of chloroform. The residue was further examined by gas chromatography, and the distribution of carbon numbers in each sample was assessed. Alternatively, a direct determination of organics concentration in CHCl3 solution was obtained spectrophotometrically from calibration curves of absorptions at 410nm and 260nm. Infrared study on organics isolated from different locations enabled an assessment of the degree of oxidation that affected each sample. This was obtained by comparing the relative absorption values at 1736 and

1712cm^{-1}, normalized with respect to 2925 cm^{-1}: C-H stretching vibration; to rule out effects due to concentration. Organics concentration in shore water ranged from 0.05 to 9.50ppm, depending on the anthropogenic activities, while much higher concentrations, ranging from 50-1500 ppm were detected in dry and wet beach sand samples.

Younis *et al.,* (1999) studied the characterization of iron in soils from the Al Jabal Al Akhdar region of North East Libya. The studied soils have been investigated by X-ray diffraction, chemical analysis and Mössbauer spectroscopy. Quartz, kaolinite and illite were the main components identified by XRD in all specimens. Total and poorly ordered iron oxides were estimated using dithionite–citrate–bicarbonate (DCB) and oxalate extraction methods, respectively. In all cases, the oxalate-extractable iron represents a relatively minor fraction. Mössbauer spectroscopy showed the presence of substantial quantities of hematite and goethite, both in microcrystalline forms, but there was no systematic relationship between the relative proportions of these phases and the geographical origins of the soils.

Pirrone *et al.,* (2001) studied the Hg emissions to the atmosphere from natural and anthropogenic sources in the Mediterranean region. They found that on a country-by-country basis, France is the leading emitter country with 22.6 tyr^{-1} followed by Turkey (16.1 tyr^{-1}), Italy (11.4 tyr^{-1}), Spain (9.1 tyr^{-1}), the former Yugoslavia 7.9 (tyr^{-1}), Morocco (6.9 tyr^{-1}), Bulgaria (6.8 tyr^{-1}), Egypt (6.1 tyr^{-1}), Syria (3.6 tyr^{-1}), Libya (2.9 tyr^{-1}), Tunisia (2.8 tyr^{-1}) and Greece (2.7 tyr^{-1}), whereas the remaining countries account for less than 7 % of the regional total. They also found that natural and anthropogenic sources in the Mediterranean region release annually about 215 t of Hg, which represents a significant contribution to the total mercury budget released in Europe and to the global atmosphere.

Shenber *et al.,* (2001) studied the radioactivity levels of the Sirte Gulf. The paper presents the result of measurements on air and soil samples collected for their natural and artificial radioactivity content. The radionuclides studied under this program are ^{7}Be and ^{137}Cs. Average activity concentrations in surface air of ^{7}Be and ^{137}Cs were found to be 1920 and 2.1 μBq m^{-3}, respectively. ^{137}Cs activity concentration in surface soil is found to be 450 m Bq kg-1. Estimated effective doses to adult from inhaled ^{7}Be and ^{137}Cs were found to be 1 and 0.13 nSv y^{-1}, respectively. The average outdoors absorbed dose rate in air, 1 m above the ground level was found to be; 48 ± 4.0 nGy h^{-1}, based on analysis data of thermo-luminescence dosimeters.

Lashhab *et al.,* (2002) studied the origin and diagenesis of the evaporites in the Jir Formation, Jabal Waddan and Western Sirte Basin, Libya. They found that the Eocene evaporites of the Jir Formation consist of gypsum, anhydrite, halite, celestite with dolomite. The gypsum crystals are commonly subhedral; some are pseudomorphs after anhydrite. The crystals are well interlocked with irregular interfaces. A few irregular lenses of anhydrite occur in the Jir Formation in samples from the Wadi Faras type-section. This is an indication that the Jir Formation gypsum is secondary and is a near surface replacement of anhydrite. Most of the gypsum nodules in the Jir Formation at Wadi Faras are randomly aligned and surrounded by microcrystalline dolomite. The nodules are mostly small in size, ranging up to approximately 3 cm in length. Some of the gypsum nodules are composed of crystals exhibiting porphyrotopic and granotopic secondary gypsum with minor amounts of anhydrite laths. It is possible that primary gypsum nodules were converted into anhydrite by burial diagenesis and were later transformed into secondary gypsum. As erosion re-exposed the Jir Formation, rainwater and dew dissolved gypsum and reprecipitated it as the water evaporated to form gypcrete.

El-Ghawi *et al.,* (2005) studied the arable soils in different regions in Libya. They found that the epithermal neutron activation is a useful technique for reducing the major activity from the matrix in soil samples, and analytical sensitivities are significantly improved for many elements for medium-lived radionuclides. The determination of the primary nutrients, potassium and micronutrients, molybdenum in these selected soils is very important for fertilizers management. The results show that trace metal concentrations in clay surface soil (Derna) are higher than in the sandy soil (South of Libya). The soil to plant transfer factor should be determined, because the transfer factor is one of the important parameters used to estimate the possible accumulation of toxic elements especially radionuclides through food ingestion.

Abu El-Ella (2006) studied the mineralogy, geochemistry and environmental geochemistry of the Quaternary soils of the coastal area in the Jifarah plain, Northwestern Libya. She found that the mineralogical composition of the whole soil is chiefly composed of variable proportions of carbonates, quartz, feldspars, rock fragments, evaporites, clay minerals and heavy minerals. The detected non-opaque heavy minerals are zircon, tourmaline, rutile, epidote, garnet, augite, hornblende, staurolite, kyanite, monazite, anatase and biotite. The opaque minerals are represented mainly by ilmenite, magnetite, hematite, limonite and few grains of pyrite. The increase in the K_2O/Al_2O_3 ratio indicates more illitic character of the soil, while the normalization of Mg by

alumina may measure the relative increase of dolomite content. The statistical treatment of data indicates that Zr and Cr, as indicators of terrestrial influence, are not loaded in the same factor. The studied coastal area seems to be somewhat polluted by Cd, Pb, Cr and Cu.

Atkinson and Waugh (2007) studied the morphology and mineralogy of the red desert soils in the Libyan Sahara. They found that the mineralogy investigation of the soils and the underlying parent rocks strongly suggest that the properties of the soils are largely dependent on the parent material. Both have identical patterns of kaolinite content, hematite as the main ferric oxide, and similar proportions of quartz silt and coarse quartz sand. Therefore, the use of kaolinite and ferric oxides in interpreting past soil-forming climates in arid regions needs to be carried out with caution, for in the present case such an interpretation would be unreliable.

El-Ghawi *et al.,* (2007) studied the level of trace elements in different arable regions in Libya. They used instrumental neutron activation analysis for the determination of 10 elements, namely; Ba, Ce, Co, Cr, Cs, Fe, Sc, Se, Th, and Zn, using their long-lived radionuclides. They found that in the Libyan soil, Se concentration is somewhat lower than in other countries. They also found that trace metals concentration in Libyan clay surface soil are higher than the sandy soil.

Shaltami (2007) studied the characteristics of the heavy metals in the red soil (terra rossa) along the coastal plain of Al Jabal Al Akhdar, Northeast Libya. He found that the data are positively skewed for Co, Zn, Mo, Pb and Cd but negatively skewed for Cu and V. This conclusion indicates that these elements have lognormal distribution. In his study area he found that several sources of the heavy metals, the natural sources include chemical weathering and wadi sediments, while the anthropogenic sources are expected to be trivial because of the harsh governmental supervision and the absence of large industries or substantial mining activities in the study area. However, the most important sources of anthropogenic heavy metals in his study area are the use of commercial products such as fertilizers. His results revealed that the studied soil is severely contaminated by Cu, Zn, Mo, Pb and Cd. All stations display low Cu/Zn ratio, as a result of strong oxidizing conditions.

Voegborlo and Chirgawi (2007) studied the heavy metals accumulation in roadside soil and vegetation along a major highway in Libya. The analysis was done by atomic absorption spectrophotometry. The concentrations of Pb, Cd, Ni, Zn, Cu, Cr and Mn in soil and vegetation decrease with distance from the road, indicating their relation to traffic. The concentration of these

metals decreases also with depth in the soil profile indicating that the source of the metals was aerial deposition from motor vehicles. Inter-relationships between metals in the soil were highly significant ($p < 0.05$) suggesting a common source for these metals. Pb and Zn were found to be deposited more than the other metals. Average values for citrus lemon leaves were generally 30 - 65 % of those for Olea europaea leaves. In most cases, between 20-40% of the metals was removable by simple washing with water, indicating that a significant, but not predominant fraction of the metals is in the form of easily-removed particulate matter. Discussion of the results of this study is based on statistical treatment of the data.

El-Kameesy *et al.*, (2008) studied the natural radioactivity of beach sands in the Tripoli Region, Northwest Libya, using high resolution γ-ray spectroscopy. Collection of samples was carried out during low tide, where it was possible to collect sediments from the wet region that was covered by sea water during high tide. From the measured γ-ray spectra, elemental concentrations were determined for ^{226}Ra, ^{232}Th, ^{40}K, and ^{210}Pb at depths 5-10 and 50-70 cm from the surface. The activity concentration ratio of $^{210}Pb/^{226}Ra$ for some samples was calculated to show disequilibrium between ^{210}Pb and its parent nuclei ^{226}Ra in the coastal marine sediments. The mean value of the absorbed dose rates in air obtained in the studied area was 4.4 ± 1.3 nGy h^{-1}, which is lower than the world average (55 nGy h^{-1}).

Shaltami (2012) studied the mineral composition and environmental geochemistry of the beach sands along the Mediterranean Coast from Benghazi to Bin Jawwad, Northeast Libya. He found that the studied beach sands are basically a mixture of carbonate and non-carbonate materials. The microscopic examination and the X-ray powder diffraction on bulk samples indicate abundance of carbonates, quartz, feldspars and evaporites with other minor minerals. In the western part of his study area, sediments are characterized by their green color most probably due to algal activity. The heavy minerals in the eastern and central parts of his study area are extremely rare, while the sediments in the western beach stretch of his study area are characterized by medium to high concentration of the heavy minerals. The recorded heavy minerals are zircon, titanite, amphibole, monazite, garnet, epidote, tourmaline, rutile, kyanite, biotite, pyroxene and opaques. Based on the dendrogram cluster analysis, three distinct types or groups of sediments were extracted. The distribution of CaO is clearly opposite to that of both SiO_2 and MgO. Silica is likely to represent mineral components especially quartz, while lime may be mainly derived from shell fragments, which are abundant in the studied beach. The abundance of Ba and Sr is basically controlled by the

carbonate fraction which includes shell fragments and clastics of limestone. The Sr/Ca ratio ranges from $33*10^{-4}$ to $92*10^{-4}$. The latter value coincides with the high Sr aragonitic carbonates. The analyzed silt size is enriched in the LREE over the HREE. The total REE budget and the chondrite-normalized REE patterns differentiate markedly between the sediments of the three provinces under consideration. The prevailing well oxidizing coastal environments are well expresses by the low Cu/Zn, V/Cr, V/Ni and U/Th ratios and authigenic U (0.85, 1.81, 1.1, 0.01 and 4 in average, respectively). Metals analyzed in his study, except Co, Cr and V in all provinces and Ni and U in province one, have EF > 2 suggesting that they are mainly of anthropogenic origin and that natural activities exert little influence on their abundances. The I_{geo} values suggest that the studied samples are lightly polluted with As and Th (grade 3, $2 < I_{geo} < 3$), very lightly polluted with Cd and Sb (grade 2, $1 < I_{geo} < 2$) and unpolluted with other metals (grade 1, $I_{geo} < 1$).

1.3. Objectives and Plan of Study

The study aims to evaluate the mineral and chemical composition of the beach sands along the Mediterranean Coast from Benghazi to Tolmeita, with especial emphasis on provenance. The study aims also to evaluate the present environmental status and possible sources of pollution in the study area. The work is done according to the following plan:

1- Sampling interval of the beach sands was between 5 and 25 km, it depends on access to the studied beach. The weight of each sample was about 18 kg and represented the uppermost 30 cm of the sands.
2- Samples preparation including grain size analysis and separation of the heavy mineral fraction.
3- Quantitative mineralogy using petrographic microscope and SEM-EDX investigations.
4- Chemical analysis of major oxides and trace elements using ICP-MS technique, with focusing on the environment-sensitive elements.
5- Evaluating the present environmental status from the geochemical and mineralogical points of views and discussing the possible sources of pollution in the study area.
6- Summary and conclusions.

1.4. Methodology

Sampling: Samples were collected from the beach sands along the Mediterranean Coast from Benghazi outskirts (Al Kuwifia) to Tolmeita, northeast Libya, from 12 stations (three samples of each station) at sampling interval between 5 and 25km, it depends on access to the studied beach

(Fig. 1.1). The traverse is parallel to the studied coast. Samples were essentially taken from the surface sands to represent the uppermost 30cm of the beach sands. Each sample was split into two parts; the first part was processed by gravimetric methods in order to concentrate heavy minerals, whereas the second part was kept as a reserve for further separation and chemical analysis.

Sample Preparation: The sample preparation procedure varies to meet the requirements of each technique. The following is, however summary of the main procedures used in the present work:

1- Grain size analysis of the studied samples. The silt size was considered for the analysis of the chemical composition, while the very fine sand size was collected to examine their mineral composition.

2- Grain size fraction in the range 125-63μm was subjected to gravitational heavy mineral separation using bromoform (specific gravity 2.87). The light and heavy fractions were mounted in Canada balsam for examination under transmitted light microscopy.

3- The opaque minerals in the heavy fractions in the grain size fraction 125 - 63μm were mounted in resin, ground and polished.

1.5. Analytical techniques

Scanning-Electron Microscope (SEM): A scanning-electron microscope, housed at the Nuclear Materials Authority of Egypt, was used in the present study. The scanning electron microscope (SEM) uses a focused beam of high-energy electrons to generate a variety of signals at the surface of solid specimens. The signals that derive from electron-sample interactions reveal information about the sample including external morphology (texture), chemical composition, and crystalline structure and orientation of materials making up the sample. The SEM was also capable of performing analyses of selected point locations on the sample (Fig 1.10).

Fig. 1.10: Scanning electron microscope (SEM) instrument

Loss on Ignition (LOI): Loss on Ignition (LOI) analysis is used to determine the organic matter content (OM %) of the sand samples. It does not involve the use of any chemicals, only the use of a muffle furnace. LOI calculates OM % by comparing the weight of a sample before and after the soil has been ignited. Before ignition, the sample contains OM, but after ignition all that remains is the mineral portion of the soil. The difference in weight before and after ignition represents the amount of the OM that was present in the sample (Roberstone, 2011, Fig 1.11). The analysis was done in the Nuclear Materials Authority of Egypt.

Preparation:

1- Weigh the crucible empty…….A.
2- Weigh the crucible + sample ……B.
3- Install B into oven and heated up to 1000° for an hour.
4- Weigh the crucible after heating ……..C.
5- B-A = weigh of sample…….D.
6- Weight loss = B – C = E.
7- LOI % = E / D100.

Fig. 1.11: Loss on Ignition (LOI) instrument

Inductively Coupled Plasma-Mass Spectrometry technique (ICP-MS): About 12 major oxides and 27 trace elements were analyzed by the ICP-MS technique (Fig. 1.12), which is widely used, at present, for determination of elements in various materials with high precision. The analytical procedure depends on the decomposition of exact weight of 0.2 g powdered fine sand size sample in 50 ml Teflon beaker. Decomposition was done by 4 ml HNO_3, 3 ml $HClO_4$ and 5 ml HF, and evaporated to dryness under 200^oC. The residue was dissolved with 5 ml (1:1) HNO_3 by heating and 5 ml of 4 ppm indium solution was added as an internal standard. The sample, as well as reference,

solutions were introduced by peristaltic pump with 0.18 rpm. Before each measurement, nebulizer and spray chamber were washed by introducing the solution for 3 min with 0.5 rpm and 30 seconds with 0.18 rpm. The analysis was done in the Nuclear Materials Authority of Egypt. The obtained data are given in tables (3.1 a, b, c and d, *see* chapter three).

Fig. 1.12: Inductively Coupled Plasma-Mass Spectrometry (ICP-MS) instrument

MINERALOGY

The present study is a detailed mineralogical investigation on the very fine size fraction (125-63μm) of the beach sands under consideration. The studied fraction is subjected to gravitational heavy mineral separation using bromoform (specific gravity 2.87). The fractions of both the light- and heavy-minerals were mounted in Canada balsam for transmitted light microscopy. The opaque minerals in the heavy fraction were mounted in resin, ground and polished. Scanning electron microscope with an energy dispersive X-ray attachment (SEM-EDX) was applied to shed light on the geochemical characteristics of the mineral composition.

2.1. Light minerals

The distribution and morphological properties of light minerals have persuaded many geoscientists to study them with respect to depositional environment and provenance (e.g. Trevena and Nash, 1979; Carranza-Edwards *et al.*, 1998; Garzanti *et al.*, 2006; Margineanu *et al.*, 2014). The studied beach sands are basically a mixture of carbonate and non-carbonate materials. The microscopic examination indicates abundance of carbonates, quartz, glauconite, feldspars and evaporites. Tables (2.1-2) and Fig. (2.1) show the relative frequency of the light minerals constituents in the very fine sand fraction.

2.1.1. Carbonates

According to Schwartz (2005), carbonate beaches have a significant proportion of the sediment fabric of biogenic origin, and carbonate in composition. Carbonate beaches are, therefore, wave deposited accumulations of sediment (sand to boulder in size) deposited on shores where a near shore supply of biogenic debris is available. Carbonate beaches exist in tropical and temperate locations, including some in relatively high latitudes. The main prerequisite for a carbonate beach is a source of carbonate-producing detritus, and a mechanism to erode and/or transport it to the shore. Bird and Schwartz (1985) recorded 32 tropical and 14 temperate countries where carbonate beaches and beach and/or dune calcarenite exist. Table (2.3) provides a summary of major beach carbonate sources and materials in tropical and temperate regions. The table and even the locations recorded by Bird and Schwartz (1985) are by no means exhaustive, as sediment characteristics are only available in the literature from a small minority of the world's beaches.

Table 2.1: Frequency distribution of the light minerals (wt %) of the studied beach sands (from east Tolmeita to west Tukrah, size range: 125-63µm)

Location	East Tolmeita	Tolmeita	West Tolmeita	East Tukrah	Tukrah	West Tukrah
Quartz	9.12	8.74	6.63	6.21	7.08	5.55
Aragonite	45.35	46.00	47.41	47.90	47.08	48.93
Calcite	39.57	40.09	40.66	41.03	40.95	41.71
Microcline	0.88	0.43	0.30	0.30	0.22	0.27
Orthoclase	0.67	0.55	0.29	0.30	0.35	0.44
Glauconite	0.66	0.32	0.45	0.19	0.27	0.38
Halite	1.39	1.67	2.11	1.96	1.83	1.22
Gypsum	2.09	1.96	2.07	1.88	1.94	1.36

Table 2.2: Frequency distribution of the light minerals (wt %) of the studied beach sands (from Daryana to Al Kuwifia, size range: 125-63µm)

Location	Daryana	West Daryana	East Sidi Khalifa	Sidi Khalifa	West Sidi Khalifa	Al Kuwifia
Quartz	2.45	1.79	2.66	1.52	1.81	2.81
Aragonite	48.11	48.72	47.94	49.05	48.66	48.04
Calcite	45.46	45.59	45.39	45.43	45.48	45.54
Microcline	0.00	0.00	0.00	0.00	0.00	0.00
Orthoclase	0.00	0.00	0.00	0.00	0.00	0.00
Glauconite	0.00	0.00	0.00	0.00	0.00	0.00
Halite	2.05	1.93	1.96	2.07	2.11	1.81
Gypsum	1.89	1.91	1.80	1.90	1.92	1.65

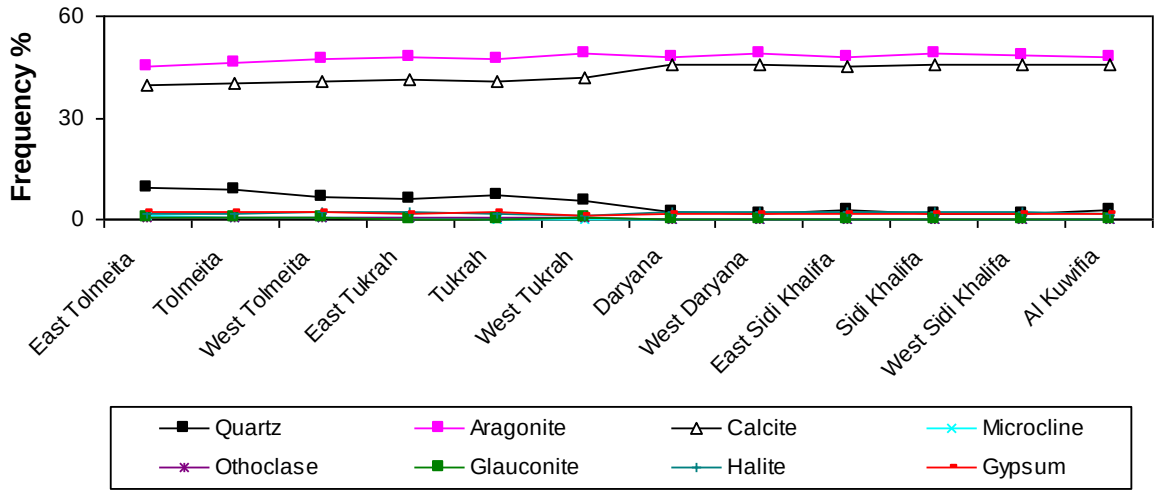

Fig. 2.1: Distribution of light minerals along the study area

Table 2.3: Location, sources, and form of carbonate beach systems (after Bird and Schwartz, 1985)

	Source	Material	Beach morphology
Tropical			
Open coast	coral-algae reefs	coral-algae fragments	reflective
Deltaic coasts	tidal sand/ mud flats	molluscs	cheniers, beach ridges
Shallow tropical seas	carbonate banks	ooids, skeletal, peloidal, pellets, aggregate sands	beach ridges
Temperate			
rocky coast	encrusting organisms	rocky shore biota	variable
low energy	sea grass meadows, tidal sand flats	molluscs, red algae foraminifera, bivalve fragments,	reflective/sand flats
high energy	inner shelf	molluscs, red algae, encrusting bryozoans, echinoids	low to high energy + dune calcarenite

In the studied samples, carbonate grains are mainly represented by biogenic grains made of aragonite and/or calcite. In agreement with Shaltami (2012), the author believes that the hydrodynamic system is one of the main factors that are responsible for the variation in the total carbonate contents. The distribution of the carbonates varies also according to the biological communities incorporated in the beach sands. Biogenic grains are composed of whole shell fragments of macrofauna (mollusks) and microfaunal shells, mostly of foraminifera and algae and other, not clearly classifiable biogenic fragments.

Chave (1962) mentioned that the contributions of calcite and Mg-calcite mostly belong to foraminifers, corals, echinoids and algae, while the contributions of aragonite mostly belong to corals, bryozoans, mollusks and benthic algae. Calcite and low-Mg calcite indicates older, reworked and diagenetically transformed material, while aragonite and high-Mg calcite indicates younger sediments (Preda and Cox, 2005). In agreement with Potter, (1994); Luzar-Oberiter *et al.*, (2008), the carbonate material that is present in the beach sands is more commonly composed of recent shell fragments or redeposited foraminifera than detrital carbonate grains. Carbonate sediments are composed largely or wholly of the skeletons of marine organisms. Contributions of $CaCO_3$ from pre-existing limestones or by inorganic precipitation from sea water appear to be relatively insignificant in most environments. Skeletons, and therefore the sediments derived from them, are composed of a variety of minerals: calcite, aragonite, and a spectrum of magnesium calcites (Chave, 1954b). The carbonate skeletal materials of marine

organisms are commonly unstable. Aragonite and magnesium calcite are more abundant in most marine environments than calcite. Aragonite is metastable mineral and it transforms during the diagenesis into calcite, only when aragonite is incorporated in the shells and skeletons of some marine organisms its stability is increased so that it can be preserved for a longer period.

In the present study, aragonite occurs as ooids and tritiform (Fig. 2.2). Calcite occurs as rectangular and irregular shapes. It is usually colorless (Figs. 2.3-4) and exhibits gleaming interference colors of very high orders.

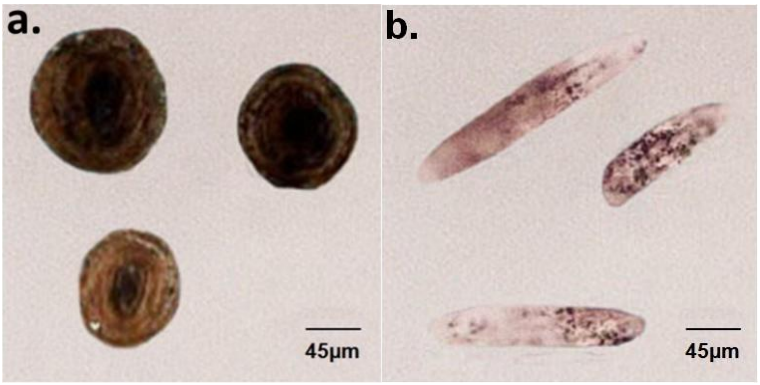

Fig. 2.2: Photomicrographs showing (a) aragonite ooids (sample 2b) and (b) aragonite tritiform (sample 10a) (size: 125-63µm)

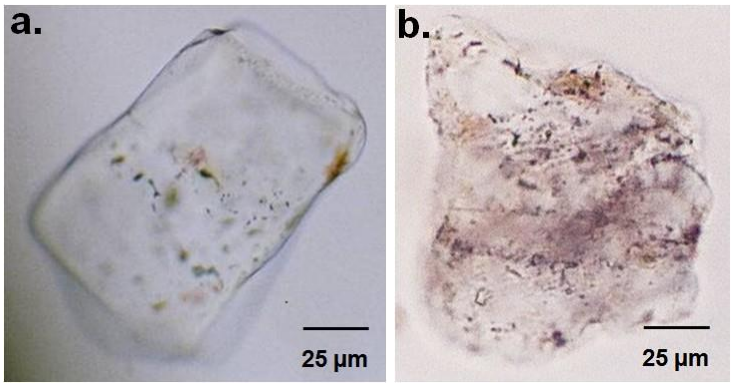

Fig. 2.3: Photomicrographs showing (a) rectangular calcite grain (sample 12b) and (b) irregular calcite grain (sample 1a) (size: 125-63µm)

The EDX microanalysis shows that calcite is an excellent accumulator of barium, strontium and yttrium (Table 2.4). According to Tucker (2001), the requisite Mg/Ca ratios are < 1.2 for low-Mg calcite (< 4 mole % Mg substituting for Ca); 1.2 to 5.5 for high-Mg calcite, and > 2 for aragonite. Generally, high-Mg calcite and aragonite are the predominant mineralogies of organisms in modern seas (Mg/Ca ratio=5.2) (Zankl, 1993). The EDX microanalysis shows that the detected calcite is low-Mg calcite. Pyokari (1997) and Shaltami (2012) found that low-Mg

calcite is the most common mineral in the carbonate beach sands. Kitano and Furutsu (1959) showed that Mg, the major impurity in marine carbonates, exists in the calcite crystal structure as a solid solution series between calcite and dolomite, and that as the Mg content increases in the solid solution series, the solubility of the calcite increases and eventually becomes greater than that of aragonite. As Mg exists in calcite and is incompatible with aragonite, the crystal type of calcium carbonate exerts a major control on the solution of natural carbonates.

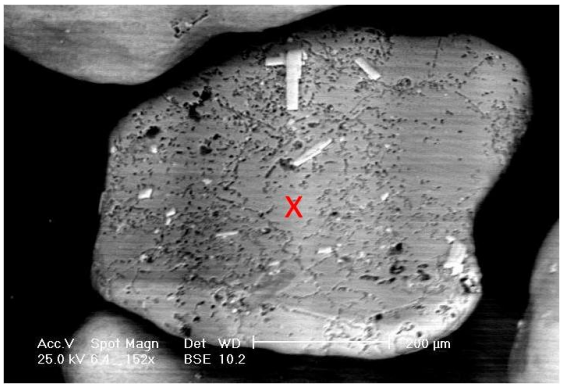

Fig. 2.4: BSE image showing irregular calcite grain (sample 12a) (size: 125-63µm)

Table 2.4: EDX microanalysis data (relative wt %) of calcite picked from grain size; 125-63 µm (carbon and oxygen are excluded)

Elements	Location
	Al Kuwifia
Si	3.18
Al	1.46
Fe	1.92
Mg	0.72
Ca	55.35
P	0.44
S	0.27
Cl	0.19
Sr	23.23
Ba	12.11
Y	1.09
Mg/Ca	0.01

2.1.2. Quartz

Quartz is one of the most abundant minerals in igneous, metamorphic and sedimentary rocks that make it useful for roundness and provenance analysis due to its relative durability and diverse varieties (Basu *et al*., 1975; Basu, 1985; Madhavaraju and Ramasamy, 1999; Kasper-Zubillaga *et al*., 2005; Kasper-Zubillaga, 2009). In the present study, quartz is commonly colorless and contains inclusions, namely, opaques (Fig. 2.5). It is mostly monocrystalline with uniform and undulatory extinction. However, polycrystalline quartz grains are observed in some

samples. According to Cherian *et al.,* (2004), the reduced percentage of the polycrystalline quartz is probably due to dilution by a fresh supply of monocrystalline quartz. Moreover, polycrystalline quartz grains are expected to disintegrate during the course of transportation from the source.

In the studied samples, quartz occurs either in the form of angular grains or as rounded grains (Fig. 2.5). The former type is the more abundant. Roundness is an attribute in quartz that can be used to infer transport and abrasion in different sedimentary environments (Folk, 1978; Sagga, 1993; Kasper-Zubillaga *et al.,* 2005). According to Shine (2006), the rounded and well rounded quartz grains owe their shape largely to a longer distance of transportation and/or the multi-cycle origin of clastic sediments. On the other hand, moderate to high degree of sphericity of the quartz grains are indication of derivation from crystalline and older sedimentary rocks exposed in regions far from the basin of deposition (Rahman *et al*., 2004). In agreement with Sanderson (1984) and Dickinson and Milliken (1995), the author believes that the presence of dust rims in most quartz grains has long been recognized as an indicator for sediment recycling. Some quartz grains show cracks, which could either be the feature inherited from the source material or could be due to long distance of transportation.

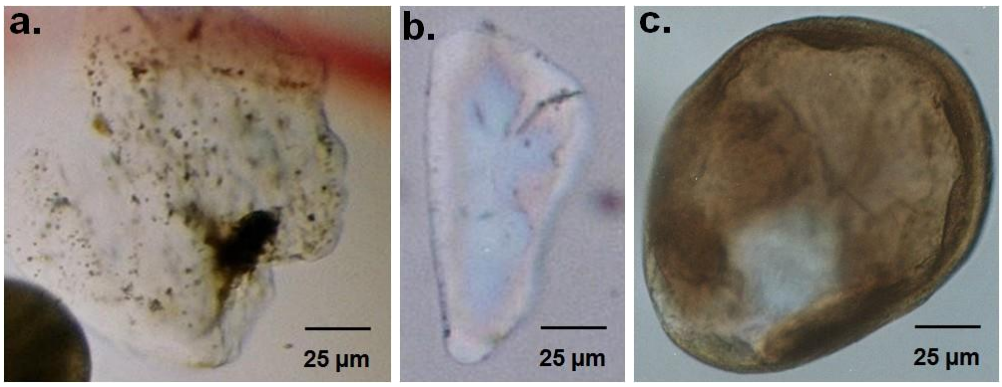

Fig. 2.5: Photomicrographs showing (a) quartz grain contains opaque inclusion (sample 1a), (b) angular quartz grain (sample 5a) and (c) rounded quartz grain (sample 1b) (size: 125-63µm)

2.1.3. Feldspars

In the present study, feldspars are only detected in the eastern side (from east Tolmeita to west Tukrah) of the studied beach, while they are lacking in the western side. Microcline and orthoclase are common feldspars. Microcline is mainly colorless and rectangular (Fig. 2.6). While orthoclase grains appear as turbid (Fig. 2.6). According to Muhs (1982), Nebsitt and Markovics (1997) and Mikesell *et al.,* (2004) there are many mineralogical indicators of weathering and maturity. The most common mineralogical indicator is the ratio of a resistant

mineral (or minerals) to one (or more) that is more susceptible to weathering. The most common minerals used in this regard are quartz (Q) and feldspar (F). The high ratio can be interpreted to more maturity of the sediments. The quartz/feldspar ratio of the examined sands (from east Tolmeita (station no. 1) to west Tukrah (station no. 6)) ranges between 5.88 and 12.42. The variation in the ratio is related to feldspars % rather than quartz %.

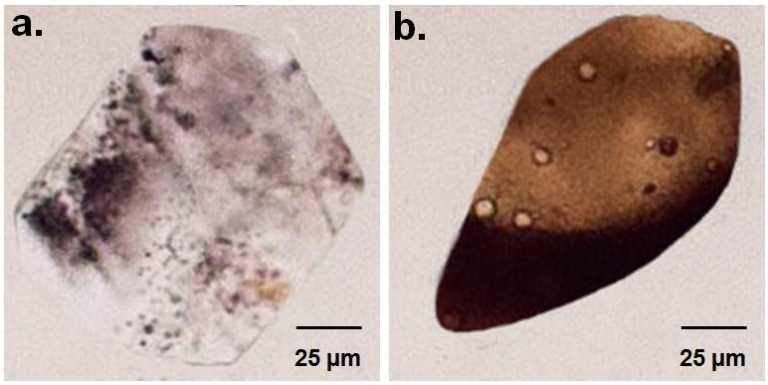

Fig. 2.6: Photomicrographs showing (a) rectangular microcline grain characterized by cleavage (sample 1a) and (b) turbid orthoclase grain (sample 1a) (size: 125-63µm)

2.1.4. Evaporites

In the present study, the detected evaporites are gypsum and halite. Gypsum occurs as prismatic grains (Figs. 2.7-8). While halite occurs as cubic grains (Figs. 2.7 and 2.9). The EDX microanalyses show that gypsum and halite are good accumulators of Ni (Tables 2.5-6).

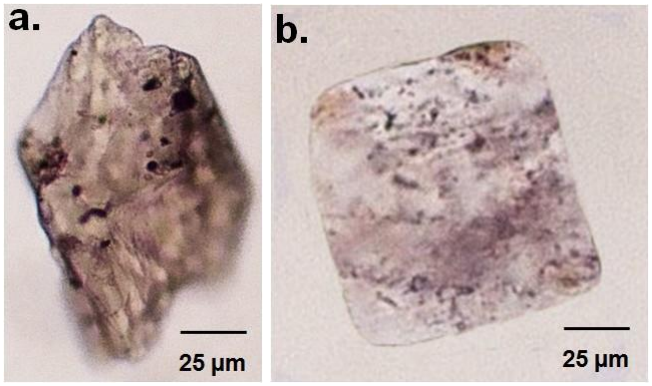

Fig. 2.7: Photomicrographs showing (a) prismatic gypsum grain (sample 11a) and (b) cubic halite grain (sample 10b) (size: 125-63µm)

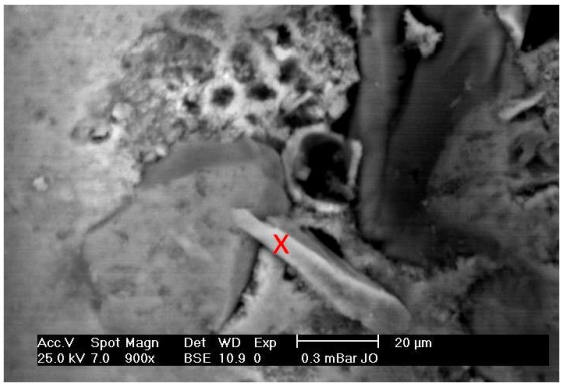

Fig. 2.8: BSE image showing prismatic crystal of gypsum (sample 12a) (size: 125-63µm)

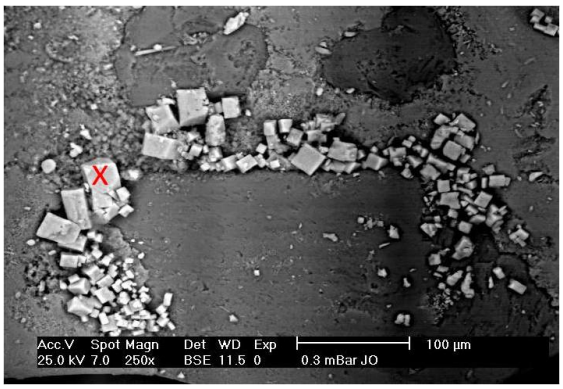

Fig. 2.9: BSE image showing cubic halite grains (sample 12a) (size: 125-63µm)

Table 2.5: EDX microanalysis data (relative wt %) of gypsum picked from grain size; 125-63 µm (carbon and oxygen are excluded)

Elements	Location
	Al Kuwifia
Si	2.00
Mg	16.15
Ca	34.71
Na	3.43
K	0.88
S	34.89
Cl	7.21
Ni	0.55

Table 2.6: EDX microanalysis data (relative wt %) of halite picked from grain size; 125-63 µm (carbon and oxygen are excluded)

Elements	Location
	Al Kuwifia
Si	3.33
Ca	2.00
Na	44.11
Cl	50.00
Ni	0.32

2.1.5. Glauconite

Glauconite is usually a component of sandstones. It occurs in sand-sized granules in marine sandstones (Skiba *et al.,* 2014). Glauconite may also occur in carbonate rocks. According to Chang *et al.,* (2008), glauconite may be abundant component of beach sand if green beds are exposed in a coastal cliff. In the present study, glauconite is only detected in the eastern side (from east Tolmeita to west Tukrah) of the studied beach, while it is lacking in the western side. It occurs as irregular dark green grains (Fig. 2.10).

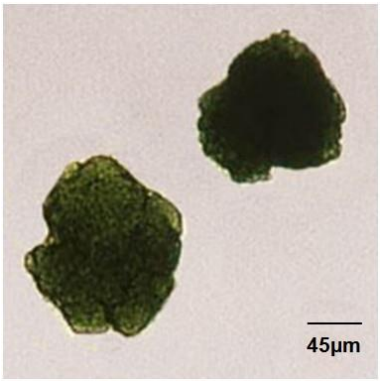

Fig. 2.10: Photomicrograph showing two irregular dark green glauconite grains (sample 1a) (size: 125-63µm)

2.2. Heavy minerals

Heavy minerals have been utilized by numerous authors to define provinces and to identify source rocks (Frihy and Komar, 1993; Pavicic *et al.,* 2000; Nilgun and Betel, 2005; Carranza-Edwards, *et al.,* 2009; Garzanti *et al.,* 2014; among others). Some studies (e.g., Pilkey, 1963; Morton and Hallsworth, 1999) demonstrate that particular association of heavy minerals do not necessarily reflect the mineralogy of the source area, because transport, weathering and post-depositional solution can appreciably modify them. The formation of heavy mineral placers on beaches is achieved through mineral segregation by entrainment processes as a result of the greater susceptibility of the lighter minerals to fluid shear stress, allowing lighter minerals to be winnowed from more stable, heavier minerals (Peterson *et al.*, 1986). Some heavy minerals are unstable during chemical weathering but stable against physical weathering, thereby influencing the distribution of the heavy minerals. For example, garnet is less stable to chemical weathering under acidic pH conditions, but more stable to transportation (Polozek and Ehrmann, 1998). Zircon is extremely stable during both chemical and physical weathering, and develops roundness only after substantial recycling. Under most conditions epidote is stable to moderately stable. Pyroxenes and amphiboles are influenced by most kinds of weathering (Polozek, 2000). At beaches, heavy minerals are often concentrated in rather localized spots usually in the swash

zone of the wave run-up or at eroding cliffs. Heavy minerals concentration on a beach can often be recognized from their dark color (red, purple or even black) (de Meijer *et al.*, 2001). Heavy minerals such as rutile, zircon, garnet and tourmaline provide greater constraints on possible source rocks because of their narrow parageneses (Fipke, 1991; Lihou and Mange-Rajetzky, 1996). Heavy mineral analysis benefits from the general chemical and mechanical stability of the minerals, although variations in properties exist. To be most effective, suites of minerals with similar hydrodynamic behavior (size, shape and density) should be used (Morton and Hallsworth, 1994). According to Carranza-Edwards *et al.*, (2001) the content of heavy minerals is not related to grain size, sorting, or sand provenance. Its variation is probably related to settling conditions of particles and local sedimentologic processes. The lack of mineralogical information can lead to incorrect assumptions with disastrous consequences (Reyneke and Van Der Westhuizen, 2001).

In the present study, heavy minerals are only detected in the eastern side (from east Tolmeita to west Tukrah) of the studied beach, while they are lacking in the western side (Table 2.7 and Fig. 2.11). The microscopic examination shows that the detected heavy minerals in the study area are opaques, zircon, augite, tourmaline, rutile, biotite, garnet, monazite, titanite, hornblende and pistachite. Table (2.7) and Fig. (2.11) show the relative frequency of the heavy minerals constituents in the very fine sand fraction.

Table 2.7: Frequency distribution of the heavy minerals (wt %) of the studied beach sands (from east Tolmeita to west Tukrah, size range: 125-63µm)

Location	East Tolmeita	Tolmeita	West Tolmeita	East Tukrah	Tukrah	West Tukrah
Opaques	36.25	33.52	39.39	38.21	33.71	36.11
Zircon	26.66	30.93	25.31	27.26	30.67	26.93
Titanite	18.67	21.22	20.19	20.97	21.15	18.56
Augite	2.54	3.00	2.61	2.73	2.87	2.61
Biotite	3.16	2.11	2.77	1.97	2.33	2.96
Hornblende	2.55	1.90	1.59	1.45	1.74	2.75
Monazite	1.76	0.94	1.00	0.79	0.88	0.97
Pistachite	1.53	0.88	1.11	0.89	0.91	1.78
Rutile	1.67	1.55	1.92	1.73	1.43	1.94
Garnet	1.37	0.91	0.88	0.90	0.98	1.55
Tourmaline	3.64	3.03	2.93	2.88	3.29	3.80

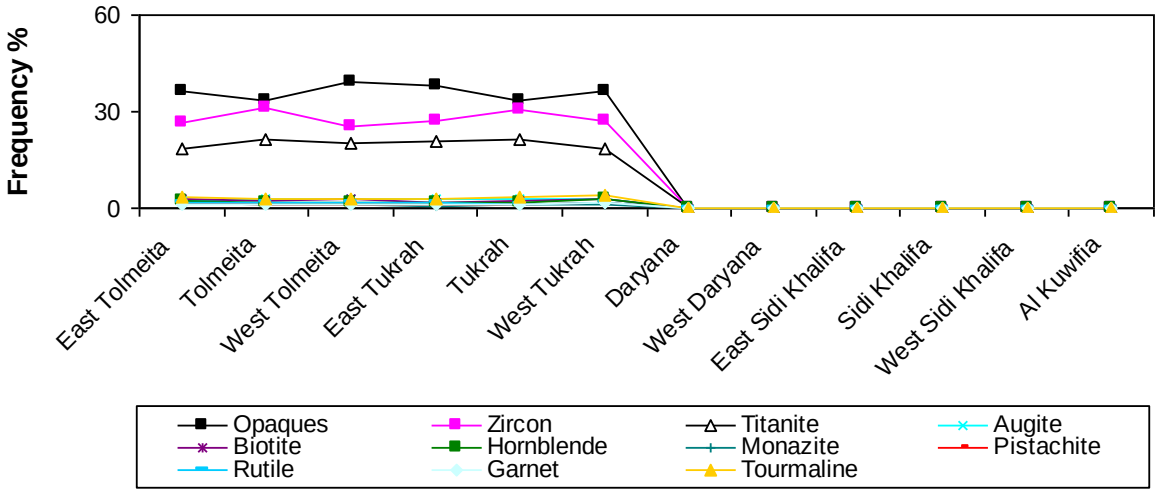

Fig. 2.11: Distribution of heavy minerals along the study area

2.2.1. Non-opaque minerals

2.2.1.1. Zircon

Zircon is among the most stable minerals commonly found in rocks (Speer, 1982; Pointer *et al.*, 1988). It is a remarkable mineral because of its ubiquitous occurrence in crustal igneous, metamorphic and sedimentary rocks (Schwartz and Gromet, 2004). Sedimentary zircon is predominantly derived from weathered igneous and metamorphic rocks. Detrital zircon in sedimentary rocks and sediments is highly durable and records age information of crustal units that contributed to the sediment load. In mature sediments where zircon may be one of a few, or the only, remaining heavy-mineral, information on source-rock compositions is largely lost, and may only be attainable through interpretation of zircon composition. Detrital zircons may be recycled many times, and multicycle sands may contain zircons from a variety of ultimate source rocks (Patyk-Kara *et al.*, 2007). It is thought that there is a close relationship between zircon morphology and the petrogenetic features of the host rock (Pupin, 1985).

In the studied samples, zircon represents the most abundant heavy mineral among the non-opaques (Table 2.7 and Fig. 2.11). Microscopic observations of zircon in the studied samples enabled the recognition of different shapes of zircon, such as; the oval with zoned structure, prismatic with bipyramidal terminations and broken (Figs. 2.12-13). It occurs as colorless and smoky grains (Fig. 2.12). The shape of heavy minerals is generally a sensitive indicator to the intensity of abrasion. Euhedral zircon is generally derived from intrusive granitoids, whereas rounded zircon may be derived from schists or from sedimentary rocks and occasionally may be caused by magmatic corrosion. Zircon with bipyramidal habit indicates an

extremely alkaline origin, where prismatic forms may be derived from granite. According to Angusamy *et al.,* (2004), the prolific presence of broken zircon in the beach sand of southern coast of Tamil Nadu, east coast of India, indicated that they had been subjected to rigorous energy conditions by waves, due to repeated swash and backwash and by littoral currents.

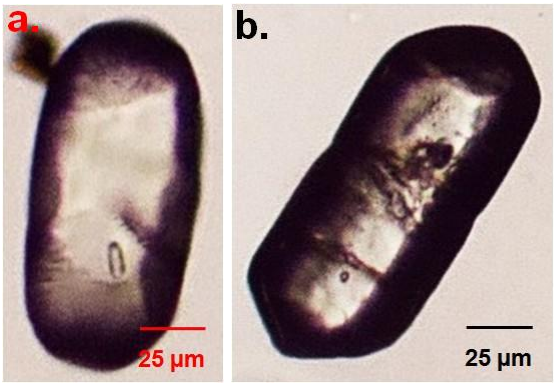

Fig. 2.12: Photomicrographs showing (a) oval shaped zircon grain with zoned structure (sample 5b) and (b) smoky prismatic zircon grain with bipyramidal terminations (sample 2a) (size: 125-63µm)

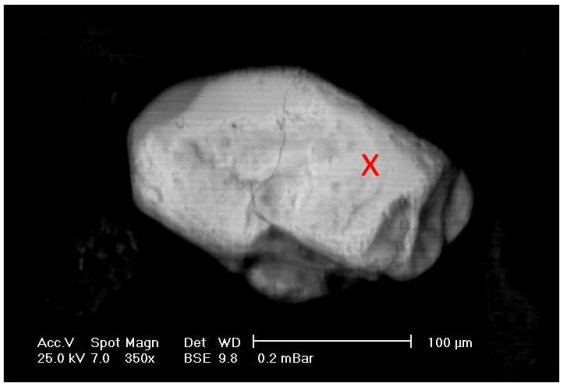

Fig. 2.13: BSE image showing broken zircon grain (sample 5b) (size: 125-63µm)

The EDX microanalysis data (Table 2.8) shows that zircon is enriched in uranium, thorium and heavy rare earth elements (ytterbium). Zircon is one end member of the zircon-hafnon solid solution series (Curtis *et al.,* 1954). Within the normal range, Hf composition of zircon is almost invisible to sedimentary processes (Owen, 1987). Crystal size, morphology and density are unrelated to Hf content (Lipova and Mayeva, 1971) except in rare cases of extreme Hf enrichment (Pupin and Turco, 1970). The Hf/Zr ratio in zircon provides a further proof to its origin. Hf is known to substitute for Zr in zircon; the Hf/Zr ratio varies generally from 0.01 to 0.05 (corresponding to an Hf weight percentage of 0.6 to 3.0) (Ahrens and Erlank, 1969). Despite the similarities between Hf and Zr, slight segregation may occur during crystallization in igneous rocks. A positive correlation apparently exists between Hf content of zircons and the

rock types in which they were formed (Butler and Thompson, 1965). El-Hinnawi (1964) found that the Hf/Zr ratio in zircons from Rosetta black sands were 0.033 for the colorless variety and 0.048 for colored ones. Abdel Gawad (1966), however, found a lower Hf/Zr ratio of 0.019 for the colorless zircons and 0.022-0.035 for colored varieties (the higher the ratio the higher the magnetic susceptibility of the zircon grains). Owen (1987) pointed out that the concentration of Hf in detrital zircons is a reliable indicator of petrogenesis. The frequency distribution of Hf is statistically similar for zircons in sands that were derived from the same source. Color may also bear important sign where the purple coloration of some zircons has been attributed to prolonged radioactive decay and consequently the intensity of shades increases with the amount of radioactive elements, as well as with geologic age (Mange and Maurer, 1992). The EDX data show that the Hf/Zr ratio is about 0.03 (Table 2.8).

Table 2.8: EDX microanalysis data (relative wt %) of zircon picked from grain size; 125-63µm (carbon and oxygen are excluded)

Elements	Location
	Tukrah
Si	22.09
Ti	0.55
Al	1.34
Fe	1.66
Mg	1.11
Ca	4.56
Na	0.23
K	0.09
Zr	65.00
Hf	1.93
Th	0.33
U	0.24
Yb	0.44
Hf/Zr	0.03

2.2.1.2. Titanite

Titanite is an accessory mineral which occurs in a wide range of igneous rocks (Smith, 1970; Nakada, 1991), in low to medium grade metamorphic rocks (Force, 1991; Frost *et al.*, 2000), and occasionally in sedimentary rocks (Morton and Hallsworth, 1999). In the present study, it is the second common non-opaque mineral (Table 2.7 and Fig. 2.11). The honey titanite is the only detected type (Fig. 2.14). It is uncommon, imperfect cleavage is observed in few titanite grains (Fig. 2.14).

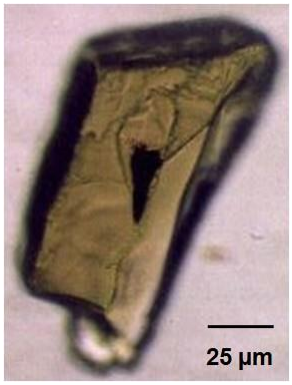

Fig. 2.14: Photomicrograph showing honey titanite grain with imperfect cleavage (sample 4a) (size: 125-63µm)

2.2.1.3. Tourmaline

In the studied samples, most of tourmaline grains are subrounded to well rounded but sometimes prismatic in shape (Fig. 2.15). The author believes that the occurrence of a rounded to well rounded tourmaline variety suggests that the sediments were reworked from older sedimentary precursor. In the present work, the majority of grains are zoneless. The yellowish brown and brown tourmalines are the only detected types (Fig. 2.15). It is characterized by its strong pleochrism.

Fig. 2.15: Photomicrographs showing (a) subrounded tourmaline grain (sample 5a) and (b) prismatic tourmaline grain (sample 1a) (size: 125-63µm)

2.2.1.4. Monazite

It is a widespread accessory mineral in felsic igneous rocks and amphibolite and granulite-facies metamorphic rocks, particularly politic schists and gneisses (Overstreet, 1967; Chang *et al.*, 1996; Rasmussen and Muhling, 2007). In the present study, it is pale yellow in color (Fig. 2.16) with very weak birefringence. It occurs as rounded grains (Fig. 2.16).

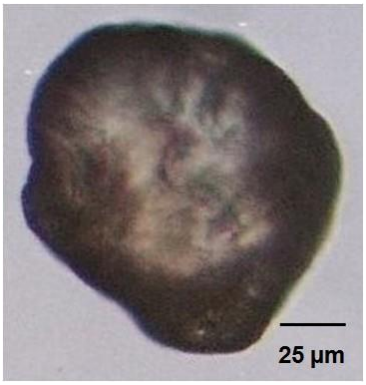

Fig. 2.16: Photomicrograph showing rounded monazite grain (sample 3a) (size: 125-63µm)

2.2.1.5. Rutile

It is among the most stable detrital minerals in sedimentary systems (Force, 1980; Morton, 1984; Margineanu *et al.*, 2014). Information contained in rutile is therefore of prime importance especially in the study of mature sediments where most diagnostic minerals are no longer stable (Zack *et al.*, 2004). Rutile grains can survive multiple weathering cycles and consequently become rounded in shape (Turner, 2005). In the studied samples, it occurs as prismatic grains (Fig. 2.17). It is characterized by deep reddish brown color (Fig. 2.17). According to Shaltami (2012) the presence of rutile suggests relative dominance of mafic sources in the hinterland.

Fig. 2.17: Photomicrograph showing deep reddish brown prismatic rutile grain (sample 4a) (size: 125-63µm)

2.2.1.6. Augite

In the studied sediments, augite is the only detected pyroxene mineral. It is mostly prismatic in shape (Fig. 2.18). It has yellowish brown color (Fig. 2.18) and exhibits perfect cleavage.

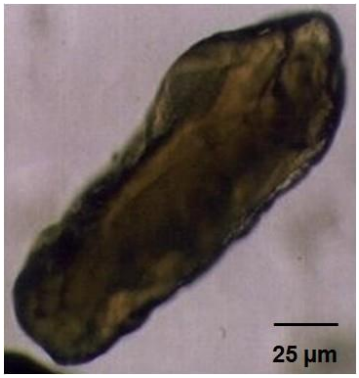

Fig. 2.18: Photomicrograph showing prismatic augite grain (sample 3c) (size: 125-63µm)

2.2.1.7. Garnet

Natural garnets are an important group of orthosilicate minerals that occur in a wide variety of geologic environments (Locock, 2008). It is an important rock-forming mineral of various magmatic, metamorphic and metasomatic rocks (Carlson and Schwarze, 1997; Sabeen *et al.*, 2002; Perchuk *et al.*, 2009). According to Anfuso *et al.*, (1999), in the coastal sand between Sanlucar de Barrameda and Rota, Cadiz, southwest Iberian Peninsula, garnet is more abundant in the coarsest fractions. The encountered garnet grains are cubic form but occasionally prismatic (Fig. 2.19-20). The most common grains are colorless. The EDX microanalysis shows that garnet mostly of almandite variety (Table 2.9).

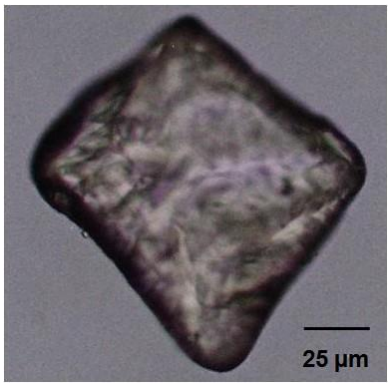

Fig. 2.19: Photomicrograph showing cubic garnet grain (sample 3a) (size: 125-63µm)

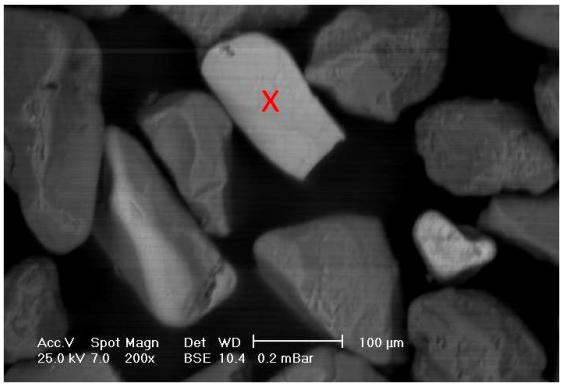

Fig. 2.20: BSE image showing prismatic garnet grain (sample 5b) (size: 125-63µm)

Table 2.9: EDX microanalysis data (wt %) of garnet picked from grain size; 125-63µm (carbon and oxygen are excluded)

Elements	Location
	Tukrah
Si	33.00
Al	18.51
Fe	34.11
Mn	1.09
Mg	5.87
Ca	6.56
U	0.23
Cr	0.54

2.2.1.8. Pistachite

According to Anfuso *et al.*, (1999), in the coastal sand between Sanlucar de Barrameda and Rota, Cadiz, southwest Iberian Peninsula, epidote is accumulated in the finer fraction. In the present study, pistachite is the only detected epidote mineral. It occurs mostly as sub-rounded to rounded grains (Figs. 2.21-22). It is commonly pale yellowish green in color. The EDX microanalysis (Table 2.10) indicates that pistachite contains more Fe than Mg. It has Ca/Mg ratio about 3.29 and relatively rich in Ti, where the Ti/Al ratio measures 0.41.

Fig. 2.21: Photomicrograph showing sub-rounded pistachite grain (sample 4b) (size: 125-63µm)

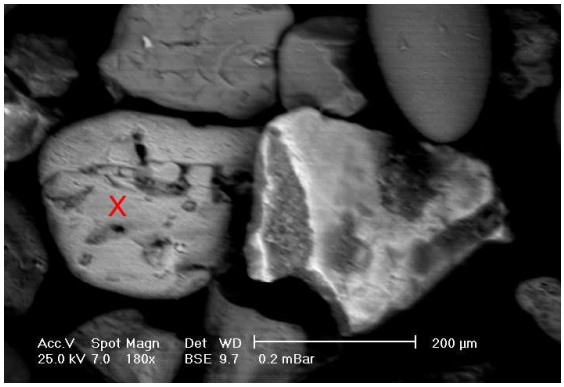

Fig. 2.22: BSE image showing sub-rounded pistachite grain (sample 5b) (size: 125-63µm)

Table 2.10: EDX microanalysis data (wt %) of pistachite picked from grain size; 125-63µm (carbon and oxygen are excluded)

Elements	Location
	Tukrah
Si	38.09
Ti	4.11
Al	9.92
Fe	10.33
Mg	8.55
Ca	28.13
Cr	0.22
Ni	0.17
V	0.10
Ca/Mg	3.29
Ti/Al	0.41

2.2.1.9. Biotite

In the present study, biotite is commonly light brown (Fig. 2.23). It is mostly sub-rounded in shape (Fig. 2.23). Fine inclusions of opaque minerals are sometimes frequent (Fig. 2.23).

Fig. 2.23: Photomicrograph showing sub-rounded biotite grain (sample 3c) (size: 125-63µm)

2.2.1.10. Hornblende

Hornblende is the only detected amphibole mineral in the studied samples. It is commonly light green (Fig. 2.24). It displays diagnostic perfect cleavage that appears imperfect in some cases (Fig. 2.24). It is mostly prismatic in shape. The presence of hornblende in the sediments is often considered as an indication of chemical immaturity of the lithogenic sediments (Blatt *et al.*, 1972; Morton and Hallsworth, 1999; Parra *et la.*, 2012).

Fig. 2.24: Photomicrograph showing prismatic hornblende grain (sample 3b) (size: 125-63µm)

2.2.2. Opaque minerals

According to Ozdemir and Dunlop (2000) and Weibel and Friis (2004), the importance of opaque minerals is often neglected when investigating the diagenetic evolution of sediments. The opaque detrital minerals can often be some of the most sensitive minerals to environmental change and, therefore, give detailed information about the diagenetic conditions. In particular, iron-rich detrital minerals, such as hematite and magnetite are sensitive to reducing/oxidizing conditions during alteration (Weibel, 1998).

The detected opaque minerals in the study area are magnetite, ilmenite, hematite, goethite, limonite and pyrite.

2.2.2.1. Magnetite

Magnetite has been very important in understanding the conditions under which rocks form and evolve (Ozdemir and Dunlop, 2000). Magnetite reacts with oxygen to produce hematite, and the mineral pair forms a buffer that can control oxygen fugacity. According to Ineson (1989) magnetite commonly alters to hematite and goethite. In the studied samples, magnetite occurs as homogeneous and altered grains. Homogeneous magnetite is commonly pale grey in color with pinkish tint (Fig. 2.25).

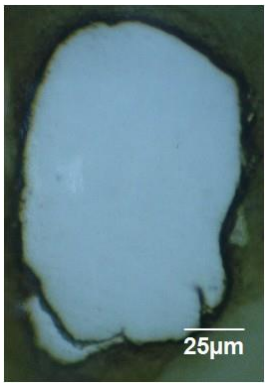

Fig. 2.25: Photomicrograph of homogeneous magnetite grain (sample 1b) (size: 125-63µm)

Magnetite is altered forming some characteristic textures of both pre-and post-depositional varieties. Several authors show that alteration of magnetite is more persistent than that of ilmenite (e.g., Shaltami, 2006). Akimoto *et al.*, (1984) suggested that the alteration process is linked to both the mobility of cation and the oxidation condition. In the studied samples, the pre-depositional textures of magnetite are martitization, replacement by titanite and alteration to rutile and hematite (Fig. 2.26), while the post-depositional texture is alteration to goethite and limonite (Figs. 2.27-28). According to Ineson (1989) and Shuster *et al.*, (2012) hematite commonly results from secondary processes. Martites are pseudomorphs after magnetite. Martitization usually starts at the grain borders and proceeds inwardly either parallel to the octahedral planes of magnetite or grow irregularly along cracks. In martitization the martite appears as broads lamellae or bands traversing the whole grain and forming uniform pattern of line network parallel to the (111) planes of original magnetite.

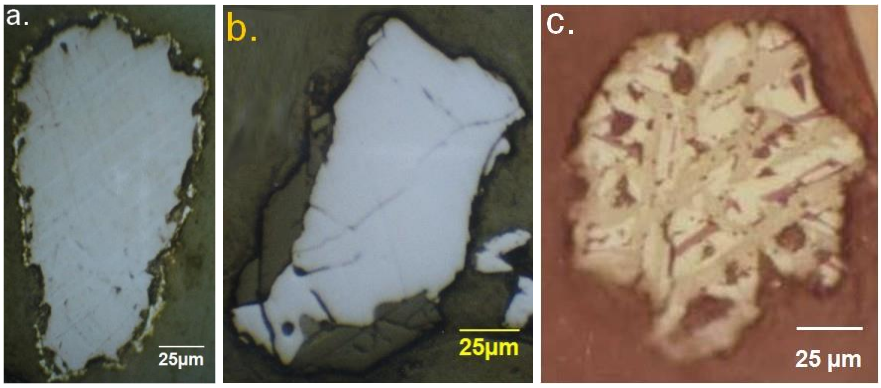

Fig. 2.26: Photomicrographs showing (a) martite (martitized magnetite) grain (framboidal pyrite replaces martite along its boundaries) (sample 3b), (b) magnetite replaced by titanite (sample 3a) and (c) magnetite altered to rutile and hematite (sample 3a) (size: 125-63µm)

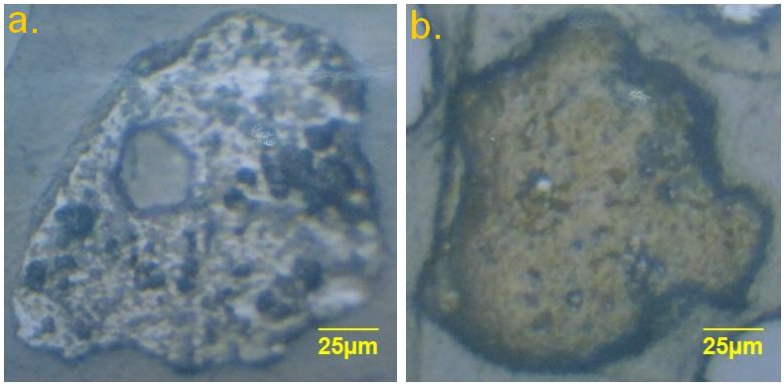

Fig. 2.27: Photomicrographs showing (a) magnetite replaced by goethite and limonite (sample 3a) and (b) magnetite completely replaced by limonite (sample 3a) (size: 125-63µm)

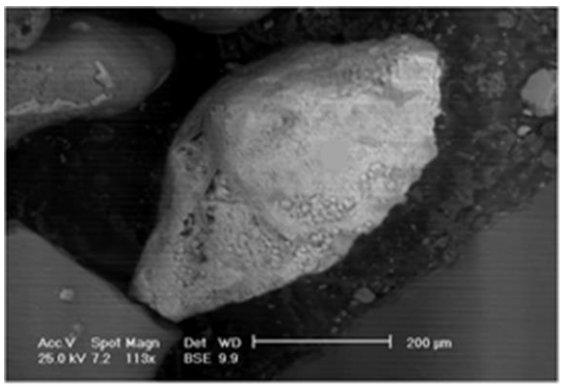

Fig. 2.28: BSE image showing magnetite completely replaced by goethite (sample 5b) (size: 125-63µm)

2.2.2.2. Ilmenite

In the present study, ilmenite occurs as homogeneous and altered grains. Homogeneous ilmenite is usually paler in color being grey with brownish tint (Fig. 2.29). It is commonly prismatic in shape (Fig. 2.29).

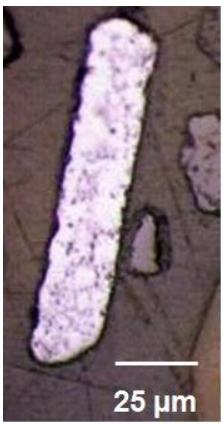

Fig. 2.29: Photomicrograph of homogeneous prismatic ilmenite slightly pitted (sample 1a) (size: 125-63µm)

There are many recent publications on ilmenite alteration (e.g., Frost *et al.*, 1983; Hugo and Cornell, 1991; Sukumaran and Nambiar, 1994; Premaratne and Rowson, 2003; Hegde *et al.*, 2006; Sundararajan *et al.*, 2009; Mohapatra *et al.*, 2015). In the present study, alteration of ilmenite could be classified into two main groups, the pre-depositional and the post-depositional alterations. The pre-depositional texture of ilmenite is alteration to rutile and hematite (Fig. 2.30), while the post-depositional texture is alteration to goethite and limonite (Fig. 2.31).

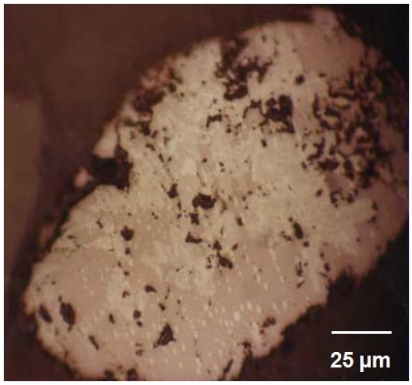

Fig. 2.30: Photomicrograph showing ilmenite altered to rutile and hematite (sample 5b) (size: 125-63µm)

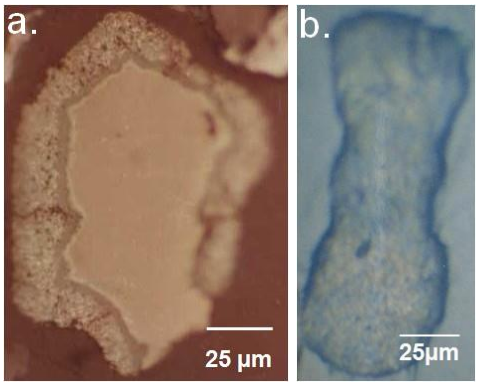

Fig. 2.31: Photomicrographs showing (a) ilmenite replaced by goethite and limonite (sample 5b) and (b) ilmenite completely replaced by limonite (sample 5a) (size: 125-63µm)

2.2.2.3. Pyrite

In the present study, the detected pyrite is framboidal pyrite. It commonly replaces magnetite grains along their boundaries (Fig. 2.26a), replaces magnetite along their cracks (Fig. 2.32) or completely replaces goethite (Fig. 2.33). According to Wilkin and Barnes (1997) pyrite framboid formation may be the result of four consecutive processes: (1) nucleation and growth of initial iron monosulfide microcrystals; (2) reaction of the microcrystals to greigite (Fe_3S_4); (3) aggregation of uniformly sized greigite microcrystals, i.e., framboid growth; and (4) replacement of greigite framboids by pyrite. In anoxic environments, which are typical of deeper strata, the hydrogen sulfide (H_2S) needed for the formation of iron sulfides is produced by biogenic reduction of sulfate (SO_4^{2-}), either by degradation of organic matter or by oxidation of methane (CH_4) (Garming *et al.,* 2005). According to Skiba *et al.,* (2014), glauconite may occur together with pyrite. They both need reducing conditions to form which is probably caused by the presence of decaying organic matter which consumes all free oxygen.

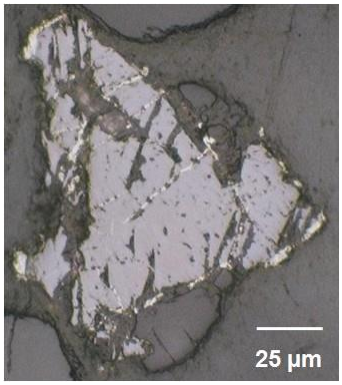

Fig. 2.32: Photomicrograph showing framboidal pyrite replaces magnetite along their cracks (sample 5b) (size: 125-63 µm)

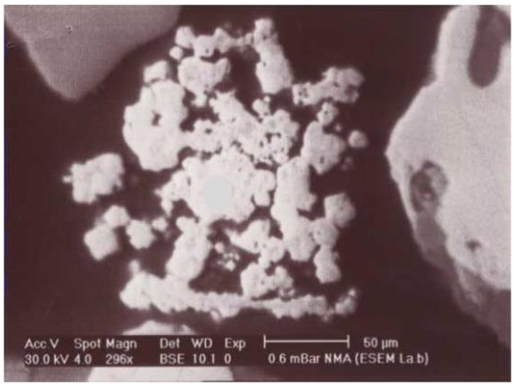

Fig. 2.33: BSE image of goethite completely replaced by framboidal pyrite (sample 5b) (size: 125-63µm)

2.3. Sediment type

Mixes of carbonate and clastic sediments, which are commonly encountered in the recent coastal sediments, require careful analysis if they are to be correctly interpreted (Carter, 1982). Various methods have been used to identify mixed carbonate-clastic sediments. Mount (1985) pointed out that carbonate sediments incorporate more than 10 % terrigenous constituents are considered to be of a mixed carbonate-clastic character. On the other hand, varied levels of $CaCO_3$ content were proposed to identify the transition region between the terrigenous and carbonate provinces, commonly ranging from 25 to 75 % (Hernandez Arana *et al.*, 2005).

Emelyanov (1986) pointed out that the Mediterranean Sea accumulations are dominantly non calcareous and low calcareous terrigenous sediments about 75% of the bottom, with magmatic rocks in parts. They show marked difference in mineral composition as they originate from different source areas (Fig. 2.34).

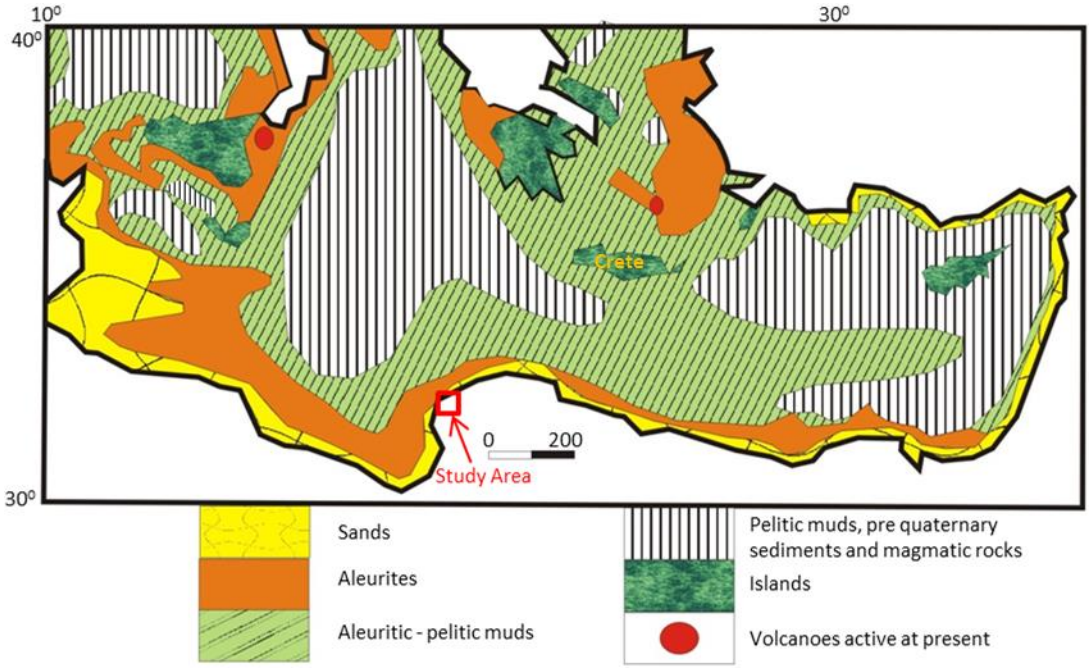

Fig. 2.34: The types of bottom sediments (0-5 cm) of the Mediterranean Sea (modified after Emelyanov, 1986)

Many islands are distributed in the Mediterranean Sea. The closest one from the study area is the Crete Island (Fig. 2.34). The surface geology of the Crete Island is dominantly sedimentary and metamorphic rocks, with some igneous rocks distributed in some parts of the island (Fig. 2.35).

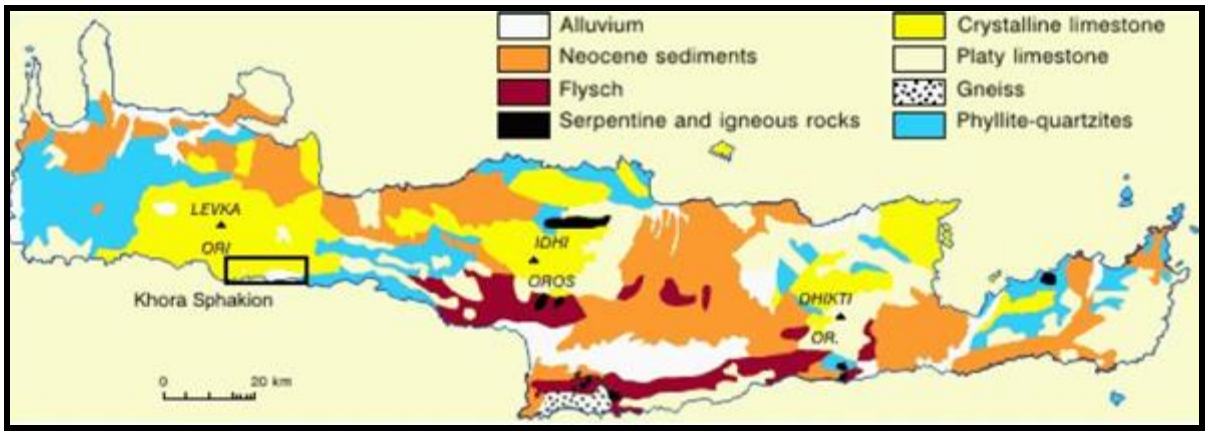

Fig. 2.35: Surface geological map of the Crete Island (after http://www.geocaching.com/geocache/GC2HV60_spilion-tou-xepitira)

In the present study, based on the mineral composition, two distinct types or groups of sediments were extracted and defined as:

Province One (from East Tolmeita (Station No. 1) to West Tukrah (Station No. 6)): This province contains high concentration of quartz (from 5.55 to 9.12). It is also characterized by the presence of feldspars, glauconite and heavy minerals.

Province Two (Daryana (Station No. 7) to Al Kuwifia (Station No. 12)): This province contains low concentration of quartz (from 1.52 to 2.81). It is also characterized by the absence of feldspars, glauconite and heavy minerals.

Based upon the difference in minerals concentrations between the two provinces, and regards to the mineralogy of the surrounded areas, the author believes that the beach sands of province one (closed beach) are derived from the sea accumulation (carbonates &evaporates), surrounded carbonate rocks (glauconite) and terra rossa (quartz, Fig. 2.36), while the beach sands of province two (open beach) are mainly derived from the sea accumulation. While bearing in mind that the provenance of the heavy minerals and some light minerals (feldspars) can be derived from the eolian sands which have been produced by weathering of the igneous and metamorphic rocks that are distributed in many part of Libya such as Jabal Al Tibisti, Harouj, As Sawda, etc. These eolian sands can be transported by wind from the source and deposited on the surrounded rocks, and then to the beach as terra rossa?.

Fig. 2.36: Terra rossa near the beach sands at station no. 1 (east Tolmeita)

GEOCHEMISTRY OF SILT SIZE FRACTION

3.1. Introduction

Grain size plays a significant role in determining elemental concentrations in sediments (Szefer *et al.,* 1996). It is recommended that a particle size fraction of < 63μm should be applied for analysis since it is the most equivalent to materials carried in suspension, the most important system for transport of sediments (Chen *et al.,* 1994). Elemental concentrations in sediments result from the competing influences of provenance, weathering, diagenesis, and sediment sorting (Quinby-Hunt *et al*., 1991). Trace element concentrations usually increase as grain size decreases, due to the higher ability of the fine particles to collect heavy metals. Fine-grained sediments have a greater surface area and provide a more efficient environment for the adsorption of metals. In the present work, the clay size fraction is trivial or even absent in many samples as a result of reworking by sea wave and currents. Accordingly, the silt size has been considered, instead of the scarce clay fraction for chemical analysis. The present geochemical study is based on complete chemical analysis data of the silt size fraction of 36 beach sand samples. Analysis of major oxides and trace elements was done by ICP-MS (inductively coupled plasma-mass spectrometry) technique. The data include 12 major oxides and 27 trace elements, as quoted in tables (3.1 a, b, c and d).

3.2. Statistical Treatment

The statistical treatment of the obtained data involves descriptive statistics and correlation matrix using the SPSS© program. The correlation matrix (Table 3.2) suggests that the heavy metals are possibly of different sources. The Th and U as well as the REE and Y are essentially related to marine and terrestrial inputs.

Table (3.3) indicates that the studied silt size fractions may contain unusually high concentrations of some elements such as Ba (398.75 ppm), Sr (5239.39 ppm), As (13.55 ppm), Th (42.1 ppm), U (14.6 ppm), Y (1015.88 ppm) and REE (25.27 ppm). These maximum values, besides the very high standard deviation values represent derivation from multi-sources and possible contribution from mineralized sources at the hinterland in addition to enhanced anthropogenic input.

Table 3.1a: Chemical analysis data (major oxides in wt %, trace elements in ppm) of the silt size of the studied beach sands (from east Tolmeita to west Tolmeita)

Location	East Tolmeita			Tolmeita			West Tolmeita		
Sample No.	**1a**	**1b**	**1c**	**2a**	**2b**	**2c**	**3a**	**3b**	**3c**
SiO_2	7.22	7.39	8.00	6.61	6.44	6.73	3.54	3.42	3.38
TiO_2	0.19	0.21	0.18	0.11	0.14	0.16	0.22	0.25	0.27
Al_2O_3	1.25	1.15	1.11	1.67	1.90	1.66	1.08	1.12	1.22
Fe_2O_3	0.84	0.89	0.77	0.47	0.52	0.57	0.92	0.95	0.98
MnO	0.02	0.02	0.02	0.01	0.01	0.01	0.02	0.02	0.02
MgO	0.48	0.46	0.49	0.43	0.38	0.44	0.55	0.60	0.58
CaO	49.28	49.23	48.37	49.00	49.15	49.11	51.28	51.35	51.30
Na_2O	0.09	0.09	0.09	0.09	0.08	0.08	0.06	0.05	0.05
K_2O	0.69	0.60	0.57	0.82	0.90	0.80	0.51	0.59	0.65
P_2O_5	0.13	0.11	0.14	0.46	0.42	0.41	0.16	0.16	0.13
SO_3	0.28	0.23	0.26	0.56	0.59	0.55	0.17	0.16	0.16
Cl	0.09	0.09	0.09	0.08	0.08	0.08	0.05	0.05	0.06
LOI	39.43	39.39	39.56	39.16	39.29	39.25	40.70	40.84	40.73
Total	99.99	99.86	99.65	99.47	99.90	99.85	99.26	99.56	99.53
Ba	333.11	331.94	331.00	328.28	331.09	330.33	345.45	348.23	346.00
Sr	3822.34	3818.61	3809.55	3700.22	3778.27	3717.18	4121.73	4137.36	4133.44
Cu	86.95	86.74	87.06	91.53	91.44	91.19	59.30	62.08	63.16
Zn	88.16	87.99	88.13	99.27	99.44	99.53	91.76	93.67	94.38
V	31.29	31.08	31.14	52.19	52.34	52.03	34.71	34.77	34.57
Cr	22.56	22.76	22.63	33.82	33.51	33.68	24.19	24.43	24.14
Pb	139.00	139.56	140.43	128.09	127.57	122.67	129.59	128.95	130.34
As	4.08	3.95	3.36	5.61	6.00	5.49	7.23	7.39	7.76
Zr	34.77	34.88	34.70	33.64	33.72	33.87	36.75	36.87	36.92
Hf	3.56	3.61	3.54	3.54	3.62	3.71	3.62	3.73	3.76
Th	27.93	27.75	27.86	27.69	27.89	27.82	28.72	28.65	28.88
U	10.44	10.33	10.38	10.27	10.41	10.31	10.63	10.61	10.66
Y	904.89	904.55	904.00	904.11	904.18	904.08	906.14	906.55	905.40
La	0.88	0.81	0.72	0.61	0.49	0.39	2.08	1.87	1.66
Ce	1.11	1.00	0.97	0.76	0.69	0.59	2.23	2.00	1.93
Pr	0.19	0.16	0.13	0.11	0.10	0.09	0.80	0.68	0.55
Nd	0.50	0.45	0.40	0.35	0.32	0.27	1.31	1.08	1.00
Sm	0.62	0.61	0.60	0.59	0.58	0.57	0.97	0.86	0.81
Eu	0.03	0.03	0.03	0.01	0.01	0.01	0.21	0.17	0.13
Gd	0.66	0.64	0.62	0.61	0.61	0.60	1.03	0.91	0.87
Tb	0.02	0.02	0.02	0.01	0.01	0.01	0.13	0.11	0.08
Dy	0.08	0.06	0.05	0.04	0.04	0.03	0.43	0.35	0.29
Ho	0.03	0.03	0.03	0.02	0.02	0.02	0.16	0.12	0.09
Er	0.06	0.05	0.04	0.04	0.04	0.04	0.22	0.19	0.15
Tm	0.02	0.02	0.02	0.01	0.01	0.01	0.03	0.03	0.03
Yb	0.04	0.04	0.03	0.03	0.03	0.03	0.22	0.19	0.14
Lu	0.02	0.02	0.02	0.01	0.01	0.01	0.03	0.03	0.03

Table 3.1b: Chemical analysis data (major oxides in wt %, trace elements in ppm) of the silt size of the studied beach sands (from east Tukrah to west Tukrah)

Location	East Tukrah			Tukrah			West Tukrah		
Sample No.	**4a**	**4b**	**4c**	**5a**	**5b**	**5c**	**6a**	**6b**	**6c**
SiO_2	3.11	3.00	3.19	3.71	4.22	3.84	2.64	3.15	2.77
TiO_2	0.13	0.17	0.18	0.26	0.25	0.32	0.22	0.24	0.20
Al_2O_3	1.33	1.41	1.23	1.08	1.00	1.04	1.11	1.05	1.00
Fe_2O_3	0.50	0.55	0.61	0.97	0.95	1.00	0.95	0.98	0.88
MnO	0.01	0.01	0.01	0.01	0.01	0.01	0.01	0.01	0.01
MgO	0.53	0.54	0.56	0.51	0.49	0.52	0.65	0.61	0.63
CaO	51.22	51.10	51.16	51.19	51.08	51.12	51.52	51.41	51.45
Na_2O	0.05	0.06	0.05	0.07	0.06	0.07	0.07	0.07	0.07
K_2O	1.21	1.26	1.18	0.52	0.48	0.50	0.56	0.51	0.49
P_2O_5	0.33	0.38	0.29	0.32	0.29	0.30	0.41	0.44	0.40
SO_3	0.23	0.24	0.24	0.24	0.24	0.26	0.27	0.31	0.33
Cl	0.05	0.05	0.05	0.06	0.06	0.06	0.07	0.06	0.06
LOI	40.65	40.53	40.59	40.62	40.50	40.55	40.95	40.83	40.88
Total	99.35	99.30	99.34	99.56	99.63	99.59	99.43	99.67	99.17
Ba	340.69	337.92	339.88	340.34	337.39	339.67	362.66	359.59	361.18
Sr	4036.77	4010.47	4029.66	4033.48	4000.52	4023.59	4244.12	4223.54	4237.09
Cu	89.50	89.95	89.89	61.05	60.76	60.87	62.27	61.98	62.09
Zn	95.94	96.09	96.18	81.84	81.55	81.73	83.06	82.77	82.95
V	40.34	40.13	40.46	22.86	22.55	22.53	44.08	46.88	51.01
Cr	26.95	26.77	27.08	18.38	18.70	18.85	21.76	22.72	23.18
Pb	137.41	138.90	138.98	141.08	142.57	141.89	142.95	143.87	143.67
As	4.95	5.09	5.44	6.02	5.80	5.53	7.94	8.05	8.76
Zr	32.22	32.40	32.48	36.88	36.92	36.97	32.19	32.37	32.42
Hf	3.49	3.53	3.55	3.62	3.73	3.76	3.49	3.53	3.55
Th	28.42	28.78	28.33	28.00	28.09	28.21	28.79	28.73	28.92
U	10.56	10.64	10.48	10.46	10.48	10.54	10.63	10.61	10.69
Y	906.11	906.00	906.03	905.07	904.98	906.00	907.00	906.85	906.91
La	1.51	1.38	1.22	1.13	1.08	1.00	2.39	2.51	2.69
Ce	1.55	1.46	1.33	1.21	1.17	1.13	3.00	3.20	3.39
Pr	0.43	0.40	0.37	0.33	0.26	0.23	1.32	1.43	1.51
Nd	0.85	0.80	0.69	0.64	0.60	0.55	2.72	2.95	3.11
Sm	0.72	0.68	0.65	0.64	0.63	0.63	1.12	1.24	1.30
Eu	0.11	0.08	0.05	0.05	0.04	0.04	0.22	0.25	0.26
Gd	0.83	0.78	0.71	0.68	0.67	0.67	1.16	1.27	1.35
Tb	0.06	0.04	0.02	0.02	0.02	0.02	0.16	0.20	0.24
Dy	0.19	0.15	0.11	0.10	0.09	0.09	0.50	0.58	0.63
Ho	0.07	0.05	0.03	0.03	0.03	0.07	0.20	0.26	0.33
Er	0.12	0.10	0.08	0.07	0.07	0.07	0.31	0.38	0.43
Tm	0.02	0.02	0.02	0.02	0.02	0.02	0.03	0.03	0.03
Yb	0.10	0.08	0.06	0.05	0.05	0.05	0.29	0.34	0.38
Lu	0.02	0.02	0.02	0.02	0.02	0.02	0.03	0.03	0.03

Table 3.1c: Chemical analysis data (major oxides in wt %, trace elements in ppm) of the silt size of the studied beach sands (from Daryana to East Sidi Khalifa)

Location	Daryana			West Daryana			East Sidi Khalifa		
Sample No.	7a	7b	7c	8a	8b	8c	9a	9b	9c
SiO_2	1.13	1.11	1.00	0.92	0.95	0.98	1.17	1.13	1.06
TiO_2	0.01	0.01	0.01	0.01	0.01	0.01	0.02	0.02	0.02
Al_2O_3	0.23	0.26	0.21	0.19	0.17	0.21	0.25	0.28	0.23
Fe_2O_3	0.18	0.21	0.21	0.29	0.34	0.40	0.30	0.27	0.28
MnO	0.01	0.01	0.01	0.02	0.02	0.02	0.01	0.01	0.01
MgO	0.79	0.80	0.78	0.69	0.72	0.70	0.68	0.67	0.67
CaO	54.89	54.60	54.96	54.81	54.93	54.73	54.55	54.26	54.69
Na_2O	0.04	0.04	0.04	0.07	0.07	0.08	0.06	0.06	0.07
K_2O	0.16	0.19	0.15	0.16	0.14	0.19	0.19	0.21	0.16
P_2O_5	0.38	0.59	0.43	0.33	0.26	0.28	0.61	0.72	0.66
SO_3	0.22	0.22	0.19	0.13	0.13	0.11	0.12	0.14	0.15
Cl	0.04	0.04	0.03	0.07	0.07	0.07	0.05	0.06	0.06
LOI	41.91	41.73	41.97	41.87	41.95	41.55	41.71	41.59	41.84
Total	99.99	99.81	99.99	99.56	99.76	99.33	99.72	99.42	99.90
Ba	385.11	384.00	385.30	393.44	395.08	393.10	375.08	373.00	376.23
Sr	4970.77	4966.38	4973.64	5026.26	5031.55	5023.27	4565.29	4555.43	4578.17
Cu	50.89	50.47	50.70	40.30	40.69	40.54	60.07	60.03	60.20
Zn	76.25	76.63	76.51	68.19	68.06	67.95	81.84	81.95	81.85
V	22.97	23.09	23.15	22.07	21.94	21.85	25.19	25.43	25.30
Cr	18.42	18.20	18.51	17.26	17.14	17.13	19.06	19.19	19.34
Pb	107.80	107.00	107.69	108.73	108.77	109.08	110.96	111.37	111.00
As	7.55	7.91	7.75	8.49	9.00	8.90	9.66	9.71	9.13
Zr	32.85	33.08	32.72	24.65	24.61	24.72	29.95	29.73	29.81
Hf	3.52	3.56	3.49	3.25	3.25	3.28	3.45	3.50	3.43
Th	32.30	32.42	32.16	32.11	31.94	31.80	31.87	32.06	31.93
U	13.57	13.58	13.54	13.51	13.42	13.36	13.13	13.45	13.25
Y	1007.66	1007.50	1007.85	999.70	999.93	999.00	997.11	996.93	997.09
La	4.97	5.19	5.07	3.80	4.08	4.24	3.77	4.00	4.17
Ce	5.12	5.39	5.29	4.52	4.81	4.92	4.49	4.75	4.88
Pr	1.08	1.15	1.10	0.77	0.83	1.00	0.75	0.79	0.95
Nd	3.65	3.88	3.66	2.61	3.00	3.45	2.55	2.92	3.14
Sm	1.45	1.52	1.45	1.15	1.21	1.35	1.14	1.16	1.32
Eu	0.16	0.20	0.17	0.04	0.09	0.13	0.02	0.06	0.11
Gd	1.49	1.53	1.51	1.17	1.27	1.37	1.15	1.24	1.32
Tb	0.20	0.23	0.21	0.12	0.16	0.18	0.11	0.14	0.17
Dy	0.98	1.05	1.00	0.63	0.72	0.91	0.60	0.66	0.88
Ho	0.27	0.30	0.28	0.16	0.20	0.24	0.14	0.17	0.22
Er	0.69	0.74	0.70	0.38	0.51	0.60	0.36	0.41	0.54
Tm	0.08	0.09	0.09	0.05	0.05	0.06	0.04	0.04	0.05
Yb	0.51	0.65	0.56	0.31	0.34	0.37	0.29	0.33	0.35
Lu	0.08	0.08	0.08	0.04	0.05	0.05	0.04	0.04	0.05

Table 3.1d: Chemical analysis data (major oxides in wt %, trace elements in ppm) of the silt size of the studied beach sands (from Sidi Khalifa to Al Kuwifia)

Location	Sidi Khalifa			West Sidi Khalifa			Al Kuwifia		
Sample No.	**10a**	**10b**	**10c**	**11a**	**11b**	**11c**	**12a**	**12b**	**12c**
SiO_2	0.81	0.88	0.90	0.90	0.93	0.96	1.11	1.09	0.98
TiO_2	0.01	0.01	0.02	0.02	0.01	0.02	0.01	0.01	0.01
Al_2O_3	0.13	0.11	0.15	0.16	0.15	0.18	0.21	0.24	0.19
Fe_2O_3	0.24	0.28	0.26	0.22	0.24	0.24	0.16	0.19	0.18
MnO	0.02	0.02	0.02	0.03	0.03	0.02	0.01	0.01	0.01
MgO	0.86	0.88	0.90	0.81	0.85	0.84	0.73	0.77	0.78
CaO	55.18	55.31	55.07	55.11	55.20	55.00	54.87	54.56	54.93
Na_2O	0.04	0.05	0.05	0.06	0.05	0.05	0.04	0.03	0.04
K_2O	0.09	0.07	0.11	0.12	0.11	0.13	0.14	0.17	0.13
P_2O_5	0.11	0.07	0.10	0.20	0.14	0.21	0.53	0.60	0.54
SO_3	0.08	0.07	0.10	0.09	0.12	0.11	0.19	0.17	0.16
Cl	0.04	0.04	0.05	0.05	0.04	0.05	0.03	0.03	0.03
LOI	42.19	42.26	42.13	42.11	42.15	42.09	41.88	41.70	41.95
Total	99.80	100.05	99.86	99.88	100.02	99.90	99.91	99.57	99.93
Ba	398.39	398.75	398.04	397.00	397.51	396.34	390.33	388.56	392.00
Sr	5228.17	5239.39	5222.43	5129.48	5137.32	5119.43	5005.29	5000.12	5013.62
Co	35.34	35.16	35.27	38.82	38.30	38.51	48.53	48.73	48.85
Ni	61.45	61.30	61.15	70.04	69.86	69.74	74.34	74.57	74.71
V	21.75	21.87	21.93	22.63	22.51	22.30	22.75	22.52	22.71
Cr	17.20	16.98	17.29	17.77	17.55	17.42	17.77	17.97	18.05
Pb	124.24	123.48	125.09	133.92	133.00	134.36	187.94	188.05	188.63
As	9.97	10.44	11.80	10.11	9.93	10.08	13.00	13.55	13.13
Zr	27.53	27.48	27.46	30.40	30.45	30.52	28.55	28.68	28.53
Hf	3.39	3.27	3.27	3.47	3.51	3.56	3.43	3.48	3.43
Th	41.91	42.03	42.10	32.10	32.53	32.34	31.96	32.10	31.91
U	14.04	14.48	14.60	13.48	13.59	13.56	13.29	13.48	13.19
Y	1015.35	1015.88	1015.00	1011.40	1011.85	1011.15	1005.35	1005.00	1005.66
La	5.33	5.52	5.71	5.27	5.48	5.63	4.92	5.13	5.00
Ce	5.52	5.70	5.82	5.46	5.67	5.73	5.00	5.33	5.20
Pr	1.20	1.26	1.41	1.18	1.23	1.33	1.05	1.11	1.08
Nd	4.31	4.48	4.61	4.23	4.44	4.56	3.63	3.67	3.65
Sm	1.58	1.63	1.73	1.55	1.60	1.66	1.40	1.49	1.43
Eu	0.24	0.28	0.33	0.22	0.25	0.30	0.14	0.18	0.15
Gd	1.55	1.62	1.67	1.54	1.59	1.64	1.45	1.52	1.50
Tb	0.25	0.29	0.37	0.24	0.27	0.32	0.19	0.22	0.20
Dy	1.09	1.11	1.18	1.07	1.10	1.13	0.96	1.03	0.98
Ho	0.33	0.38	0.48	0.31	0.36	0.41	0.26	0.29	0.27
Er	0.78	0.82	0.92	0.75	0.80	0.84	0.63	0.72	0.68
Tm	0.09	0.09	0.09	0.09	0.09	0.09	0.06	0.09	0.08
Yb	0.71	0.78	0.86	0.68	0.74	0.80	0.39	0.60	0.51
Lu	0.08	0.09	0.09	0.08	0.09	0.09	0.06	0.08	0.08

Table 3.2: Correlation matrix of the studied samples

Oxides and Elements	SiO_2	TiO_2	Al_2O_3	Fe_2O_3	MnO	MgO	CaO	Na_2O	K_2O	P_2O_5	SO_3	Cl	LOI	Ba	Sr	Cu	Zn	V	Cr	Pb	As	Zr	Hf	Th	U	Y	REE
SiO_2	1.00																										
TiO_2	0.67	1.00																									
Al_2O_3	0.85	0.80	1.00																								
Fe_2O_3	0.64	0.97	0.72	1.00																							
MnO	-0.09	-0.18	-0.30	-0.08	1.00																						
MgO	-0.87	-0.75	-0.91	-0.70	0.33	1.00																					
CaO	-0.95	-0.81	-0.95	-0.77	0.21	0.93	1.00																				
Na_2O	0.72	0.43	0.55	0.50	0.07	-0.69	-0.67	1.00																			
K_2O	0.67	0.66	0.90	0.55	-0.32	-0.79	-0.81	0.37	1.00																		
P_2O_5	-0.24	-0.28	-0.11	-0.32	-0.74	-0.02	0.18	-0.15	-0.08	1.00																	
SO_3	0.73	0.43	0.80	0.34	-0.48	-0.73	-0.75	0.52	0.61	0.22	1.00																
Cl	0.77	0.46	0.59	0.52	0.10	-0.71	-0.71	0.95	0.41	-0.22	0.52	1.00															
LOI	-0.97	-0.71	-0.93	-0.66	0.23	0.94	0.98	-0.71	-0.78	0.11	-0.80	-0.75	1.00														
Ba	-0.89	-0.83	-0.94	-0.76	0.33	0.95	0.96	-0.58	-0.85	0.08	-0.70	-0.61	0.94	1.00													
Sr	-0.88	-0.83	-0.95	-0.77	0.34	0.96	0.97	-0.63	-0.83	0.03	-0.72	-0.66	0.94	0.99	1.00												
Cu	0.84	0.58	0.88	0.49	-0.40	-0.88	-0.89	0.54	0.89	0.09	0.74	0.58	-0.90	-0.91	-0.91	1.00											
Zn	0.73	0.66	0.90	0.56	-0.40	-0.87	-0.84	0.40	0.87	0.14	0.71	0.44	-0.83	-0.90	-0.91	0.92	1.00										
V	0.60	0.52	0.83	0.47	-0.34	-0.65	-0.73	0.45	0.75	0.09	0.81	0.45	-0.71	-0.67	-0.72	0.74	0.77	1.00									
Cr	0.72	0.47	0.88	0.38	-0.30	-0.76	-0.79	0.45	0.82	0.04	0.85	0.48	-0.81	-0.77	-0.78	0.85	0.88	0.90	1.00								
Pb	0.11	0.19	0.12	0.13	-0.18	-0.07	-0.14	-0.21	0.11	0.09	0.07	-0.24	-0.10	-0.09	-0.09	0.09	0.07	0.06	0.00	1.00							
As	-0.80	-0.67	-0.77	-0.64	0.11	0.80	0.82	-0.63	-0.74	0.27	-0.53	-0.68	0.81	0.85	0.82	-0.78	-0.69	-0.48	-0.59	0.28	1.00						
Zr	0.66	0.81	0.71	0.74	-0.21	-0.66	-0.73	0.22	0.55	-0.15	0.46	0.25	-0.66	-0.79	-0.76	0.59	0.71	0.40	0.48	0.10	-0.66	1.00					
Hf	0.58	0.75	0.66	0.65	-0.23	-0.62	-0.65	0.14	0.50	-0.04	0.47	0.20	-0.61	-0.72	-0.70	0.53	0.70	0.39	0.48	0.17	-0.53	0.93	1.00				
Th	-0.64	-0.66	-0.72	-0.62	0.32	0.82	0.73	-0.49	-0.64	-0.19	-0.58	-0.49	0.72	0.76	0.79	-0.71	-0.80	-0.54	-0.56	-0.18	0.64	-0.64	-0.67	1.00			
U	-0.83	-0.91	-0.95	-0.86	0.28	0.92	0.95	-0.56	-0.84	0.13	-0.67	-0.58	0.89	0.95	0.96	-0.83	-0.86	-0.73	-0.73	-0.20	0.78	-0.77	-0.72	0.82	1.00		
Y	-0.82	-0.93	-0.95	-0.89	0.26	0.90	0.95	-0.56	-0.85	0.18	-0.64	-0.59	0.88	0.95	0.95	-0.81	-0.83	-0.73	-0.72	-0.16	0.78	-0.76	-0.69	0.76	0.99	1.00	
REE	-0.87	-0.80	-0.91	-0.73	0.27	0.97	0.93	-0.63	-0.83	0.11	-0.66	-0.67	0.93	0.97	0.96	-0.88	-0.85	-0.60	-0.73	-0.06	0.85	-0.69	-0.64	0.77	0.92	0.92	1.00

Table 3.3: The descriptive statistics of the studied samples (major oxides in wt %, trace elements in ppm)

Oxides and Elements	N	Minimum	Maximum	Mean	Std. Deviation
SiO_2	36	0.81	8.00	2.79	2.24
TiO_2	36	0.01	0.32	0.11	0.10
Al_2O_3	36	0.11	1.90	0.72	0.56
Fe_2O_3	36	0.16	1.00	0.52	0.31
MnO	36	0.01	0.03	0.01	0.01
MgO	36	0.38	0.90	0.65	0.15
CaO	36	48.37	55.31	52.69	2.35
Na_2O	36	0.03	0.09	0.06	0.02
K_2O	36	0.07	1.26	0.43	0.34
P_2O_5	36	0.07	0.72	0.33	0.18
SO_3	36	0.07	0.59	0.22	0.13
Cl	36	0.03	0.09	0.06	0.02
LOI	36	39.16	42.26	41.08	0.98
Ba	36	328.28	398.75	365.61	26.35
Sr	36	3700.22	5239.39	4490.67	540.49
Cu	36	35.16	91.53	60.53	19.13
Zn	36	61.15	99.53	81.13	11.39
V	36	21.75	52.34	30.47	10.53
Cr	36	16.98	33.82	21.34	4.87
Pb	36	107.00	188.63	132.74	21.04
As	36	3.36	13.55	8.02	2.61
Zr	36	24.61	36.97	31.74	3.61
Hf	36	3.25	3.76	3.51	0.14
Th	36	27.69	42.10	31.03	3.84
U	36	10.27	14.60	12.05	1.59
Y	36	904.00	1015.88	955.79	51.22
REE	36	2.67	25.27	13.75	7.86

3.3. Major Oxides:

The major elements are generally considered somewhat mobile during weathering, transportation, and post-depositional processes (McLennan *et al.*, 1993). According to Petersen *et al.,* (2004), Zaghlou *et al.,* (2009) and Albardeiro *et al.,* (2014), provenance interpretations using major elements are not considered definitive, if there is more than one source area. In the study area, the geochemistry of the major oxides is essentially controlled by the mineral composition of the studied beach sands which, in turn, roles the mutual abundance and distribution of the trace elements.

Lime, silica, alumina and magnesia are the main constituents of the studied samples. The graphical presentation of the correlation coefficients among the analyzed major oxides points to the intimate coherence among them, except for lime and magnesia (Fig. 3.1). Silica, alumina, iron oxides, soda and potash are most probably accommodated within silicate clastics. Lime, which expresses the carbonate sediments in the studied coastal zone, seems to be the main diluents of the terrestrial admixture.

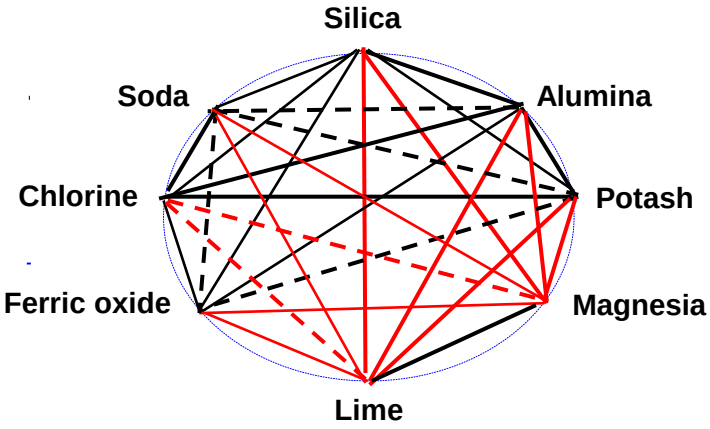

Fig. 3.1: Correlations among the major oxides in the studied samples (intensity of lines corresponds to the strength of the correlation coefficient (< 0.4 to > 0.8)) (red line means inverse relation)

The plot of silica versus alumina (Fig. 3.2) suggests that silica and alumina are strongly correlated in province two, while their weak correlated in province one. This reflects the occurrence of silica in both silicate and free silica modes. Preda and Cox (2005) found that quartz and shell-rich sediments tend to have smaller amounts of Al in the shallow marine sediments in the Gulf of Carpentaria, Northern Australia.

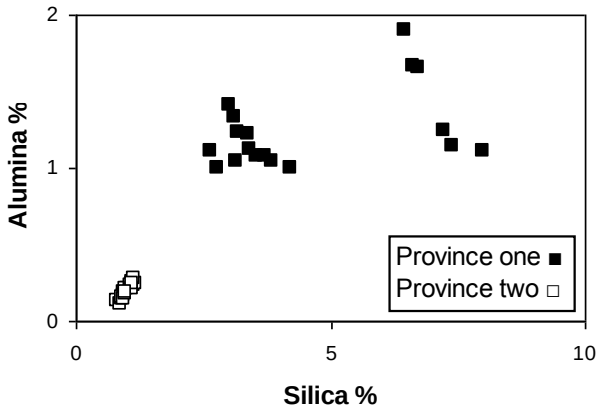

Fig. 3.2: Relationship between silica and alumina in the study area

The distribution of CaO is clearly opposite to that of SiO_2 (r = -0.95, Fig. 3.3). Silica is likely to represent mineral components especially quartz, while lime may be mainly derived from shell fragments, which are abundant in the studied beach.

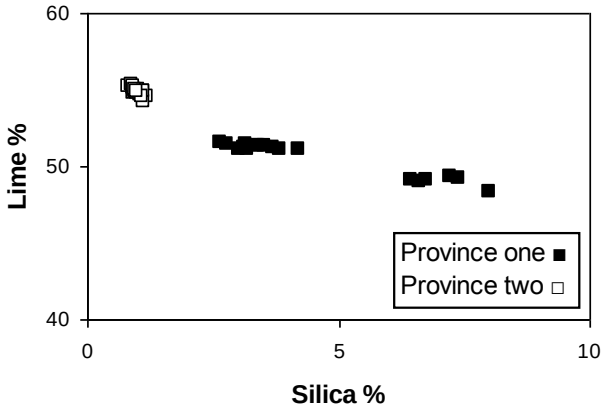

Fig. 3.3: Relationship between silica and lime in the study area

In the present study, CaO is strongly correlated with MgO (r = 0.93, Fig. 3.4). The relationship means that calcite is the sole carrier of MgO. The studied samples show very low MgO/CaO ratio (~0.01). This low value indicates that the studied samples are not dolomitized, because dolomitization would necessarily cause a marked increase in the MgO/CaO ratio of the limestone.

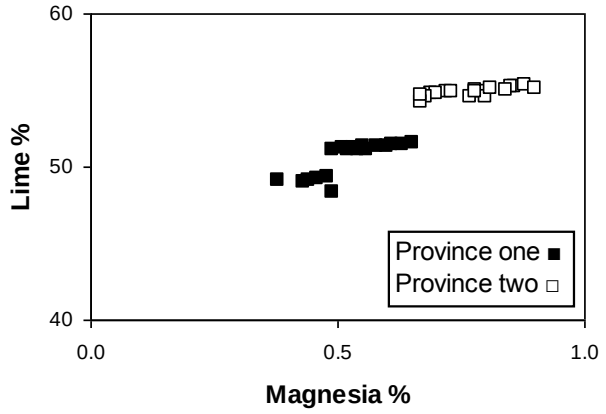

Fig. 3.4: Relationship between magnesia and lime in the study area

Aluminum concentration is a reasonably good measure of detrital influx. Macquaker *et al.*, (1997) noticed that during weathering ferric iron and aluminum accumulate relative to other common elements because of the extreme insolubility of their oxides and hydroxides. The studied samples show lower concentrations of Al_2O_3 than the siliciclastic contaminated carbonates (Al_2O_3 concentration of 1.59 %, in Veizer, 1983).

In the studied samples, K_2O is strongly correlated with Al_2O_3 (r = 0.90, Fig. 3.5) suggesting, in agreement with Zhang (2004) and Nagarajan *et al.*, (2007), that these elements are almost entirely associated with detrital admixture.

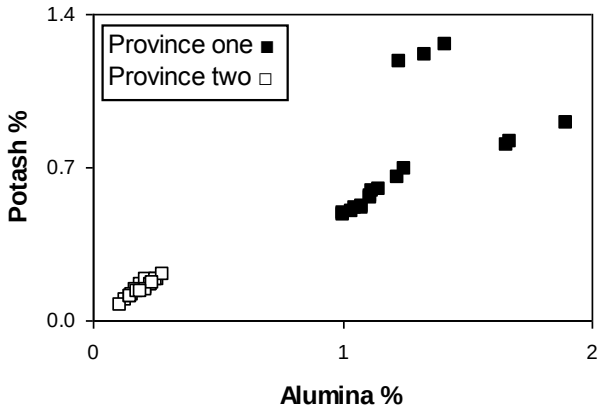

Fig. 3.5: Relationship between alumina and potash in the study area

The K_2O/Al_2O_3 ratio is important in sedimentary rocks in understanding the source of aluminum and its distribution between clay and feldspars minerals (Katongo *et al.*, 2004). The K_2O/Al_2O_3 ratios for clay minerals and feldspars are different (0.0 to 0.3, 0.3 to 0.9, respectively; Cox *et al.*, 1995). In province one, the K_2O/Al_2O_3 ratio ranges from 0.47 to 0.96, indicates that feldspars have a major role in the distribution of aluminum in this province.

Many authors (e.g., Gandhi and Raja, 2014) suggest that Na present in the original carbonate sediments can be modified greatly during diagenesis. The strong positive correlation between Na_2O and Cl (r = 0.95, Fig. 3.6) supports their accommodation in the form of halite.

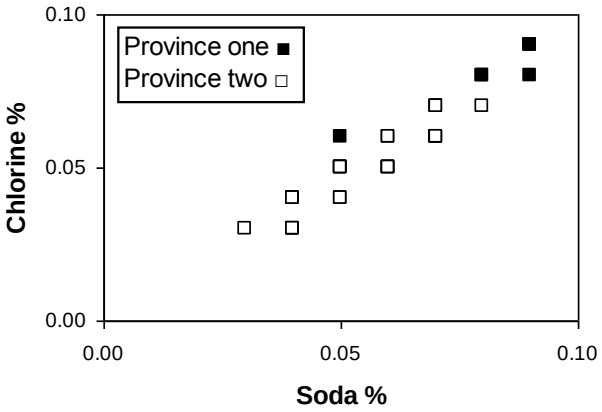

Fig. 3.6: Relationship between soda and chlorine in the study area

Titanium is relatively immobile compared to other elements during various sedimentary processes and may strongly represent the source rocks (McLennan *et al.,* 1993). Most of the studied samples have low TiO_2 contents. In province one, TiO_2 is strongly correlated with Fe_2O_3 (r = 0.90, Fig. 3.7) suggesting in agreement with Condie *et al.,* (1992) and Carranza-Edwards *et al.,* (2001) that Ti is contained in iron-titanium oxyhydroxides (rutile, magnetite, hematite and ilmenite). These correlations may be a result of sorting under control of the depositional environments (Abu El-Ella, 2006). In agreement with Shaltami (2012) this assumption seems to be eligible for the studied beach sands as confirmed by the positive correlation between TiO_2 and the traditional terrigenous elements such as Zr (r = 0.65, Fig. 3.8). In province one the TiO_2/Zr ratio ranges from 0.0032 to 0.0086, while in province two it ranges from 3 to 7.28. According to Garcia *et al.,* (1994), Asiedu *et al.,* (2000) and Malick and Ishiga (2015), mature sediments show a wide range of TiO_2/Zr variations whereas immature sediments show a more limited range of TiO_2/Zr variations.

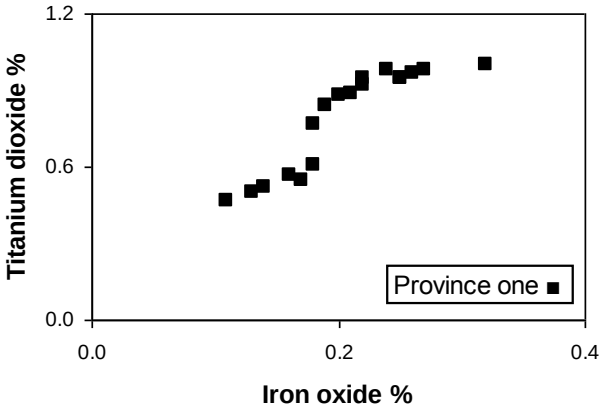

Fig. 3.7: Relationship between iron oxide and titanium dioxide in province one

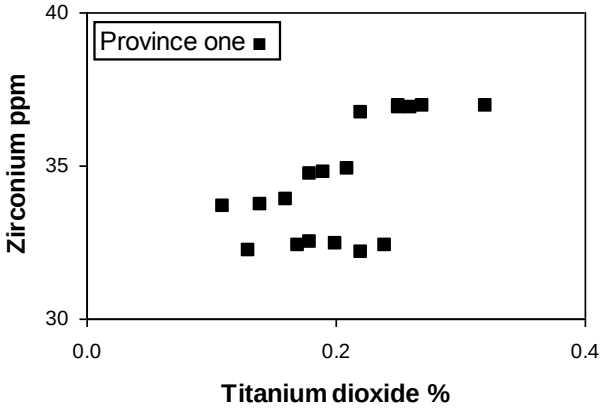

Fig. 3.8: Relationship between titanium dioxide and zirconium in province one

Froelich *et al.,* (1982) stated that there is an increasing amount of phosphorus, both organic and inorganic, supplied from the terrestrial to the marine environment, resulting in undesirable consequences for coastal ecosystems. Most of this increase can be traced to human activities. Information about the behavior of P in coastal regions is urgently needed in order to understand the impact of human activities on the coastal marine environment (Suzumural and Kamatani, 1995). In the present study, the P_2O_5 content ranges between 0.07 to 0.72 %, and it does not show clear coherence to Ce content (r = 0.16) suggesting in agreement with Shaltami (2012) that the potentiality of phosphate in the studied beach sands is not controlled by monazite. In agreement with Hanley *et al.,* (2014), the author believes that P_2O_5 distribution in the study area is related to anthropogenic activities.

3.4. Trace elements

The study of trace elements have become a vital part in modern petrology and more capable for discrimination between petrological processes than the major elements. The behavior of trace elements during sedimentary processes is complex due to many factors including weathering, physical sorting, adsorption, provenance, diagenesis, and metamorphism (Nebsitt *et al*., 1980; Wronkiewicz and Condie, 1987, Papadopoulos *et al.*, 2015). The differences in trace elements content in the beach environment is probably due to sorting effect of the sediments or differences in source rocks. The clay size fraction, being the finest and most capable of sorption, is the best accumulator of trace elements (Rollinson, 1993). Since the clay size is scarce or even absent in the beach sands under consideration, the silt size has been considered for chemical analysis.

3.4.1. Normalization to other beach sands

The average trace element concentrations of the studied samples are normalized to data of the beach sands along the Mediterranean Coast from Benghazi to Bin Jawwad, Northeast Libya as quoted by Shaltami (2012). The normalized data (Fig. 3.9) suggest the following inferences:

1) In all provinces, there are notable enrichments in Sr, Cr, Pb, Hf, Th, U and Y.

2) In all provinces, there are notable depletions in Ba, Cu, Zr and REE. According to Bopp *et al.*, (1993), in coastal areas high concentrations of Cu have been measured in sediments to depths of 54 cm.

The above arguments can be held as generalized geochemical signatures of the study area. The beach sands of the study area are obviously derived from different sources.

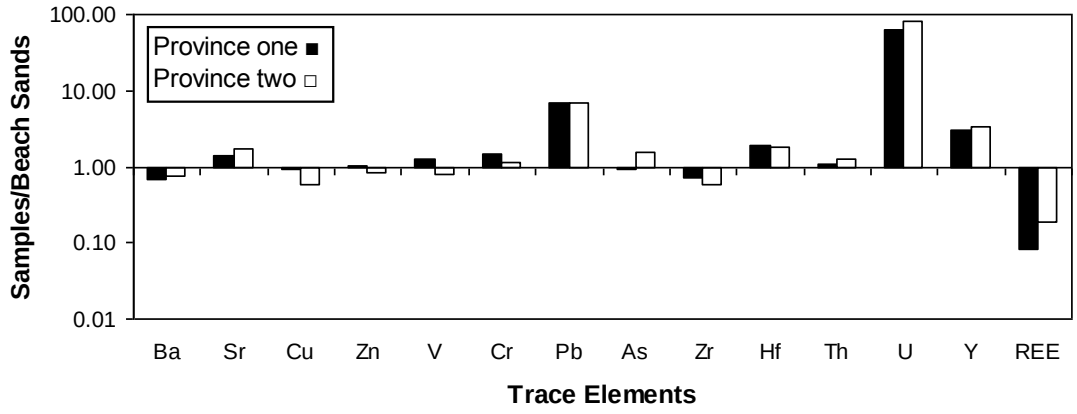

Fig. 3.9: Trace element contents of the studied sands normalized to data of the beach sands along the Mediterranean Coast from Benghazi to Bin Jawwad, Northeast Libya as quoted by Shaltami (2012)

3.4.2. Low field strength elements (LFSE)

They are large cations of small charge and tend to be compatible with major elements. The low ionic potential (ratio of charge to ionic radius) makes these elements relatively soluble in aqueous solution. Because of their solubility, they are quite mobile during metamorphism and weathering (White, 2001). In the studied samples, two LFSE, namely, Ba and Sr are analyzed. In all provinces, there is notable enrichment in these elements.

Sr and Ba are known to be relatively mobile in natural oxic and aqueous environments (Dupre *et al*., 1996; Gaillardet *et al*., 1999). The correlation matrix indicates that Ba and Sr are mutual (r = 0.99). Sr resides mainly in carbonate and feldspar (Yang *et al*., 2003). In agreement with Shaltami (2012) and Pease and Tchakerian (2014), the author believes that the abundance of Ba and Sr in the studied samples is basically controlled by the carbonate fraction which includes shell fragments and clastics of limestone. This assumption is confirmed by the strong correlation between CaO and both Ba and Sr (r = 0.96 and 0.97, Figs. 3.10-11, respectively).

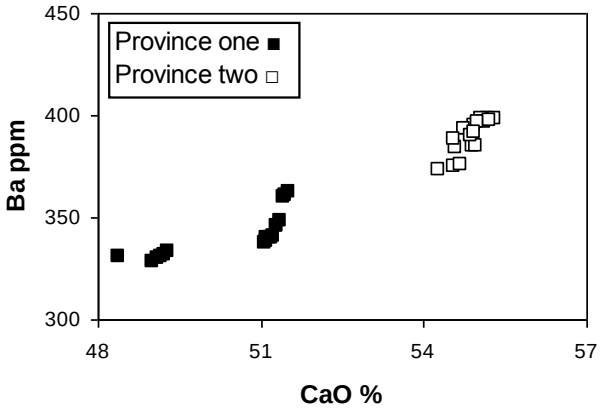

Fig. 3.10: Relationship between lime and barium in the study area

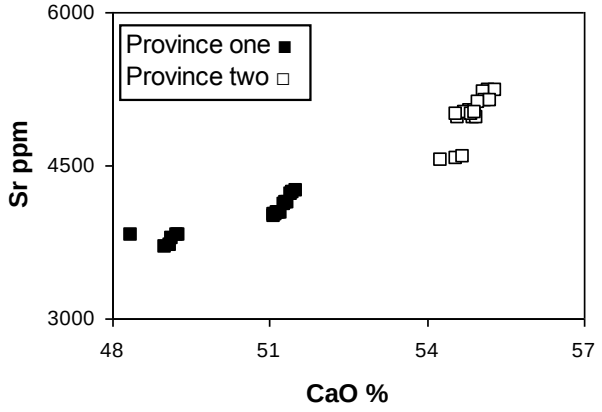

Fig. 3.11: Relationship between lime and strontium in the study area

The Sr content in carbonate minerals may be used as an important chemical characteristic to identify their genesis. According to Thomson *et al.,* (2004), the aragonitic carbonate sediments are better accumulator of Sr than the calcitic ones. In the studied beach sands, the Sr/Ca ratio ranges from $10*10^{-4}$ to $13*10^{-4}$. These ratios suggest that Sr is contained in both calcite and aragonite.

Sr^{2+} and Eu^{2+} are, sometimes, isovalents especially in plagioclase. The relationship between Sr and Eu is very weak (r = 0.01) and the Sr/Eu ratio ranges from 15826 to 377827. According to El-Kammar *et al.*, (2007), in beach sands the drastic increase in Sr relative to Eu can be interpreted to the preponderance of calcareous aragonitic and calcitic shell fragments. The relatively low Sr/Eu ratio can be explained to the lower quotient of shell fragments.

3.4.3. Heavy metals

According to Anderson (2003), heavy metals are stable metals or metalloids and cannot be degraded or destroyed. Therefore, they tend to accumulate in soils and sediments. However, anthropogenic activities have drastically altered the biochemical and geochemical cycles and the balance of some heavy metals. The analyzed heavy metals in the studied sands are Cu, Zn, Cr, V, As and Pb. The absence of strong correlations among some heavy metals can be interpreted to their derivation from different sources, but remobilization during chemical weathering is also possible.

Cu, Zn, Cr and V are normally associated with mafic rocks and could also be associated with felsic rock. Zn tends to replace Fe and Mg in the rock forming minerals. In all provinces, Cu, Zn, Cr and V are mutually correlated. The weak relationship between Zn and Fe_2O_3 (r = 0.56) and the negative correlation between Zn and MgO (r = -0.87) indicate that magnesium and iron minerals are not the sole carrier of Zn. In all provinces, Cu, Zn, V and Cr are strongly correlated with Al_2O_3 (r = 0.88, 0.90, 0.83 and 0.88, Figs. 3.12-15, respectively) suggesting, in agreement with Fedo *et al*., (1996) and Al Shariani (2006), their possible accommodation as alumino-silicates which can be concentrated during weathering.

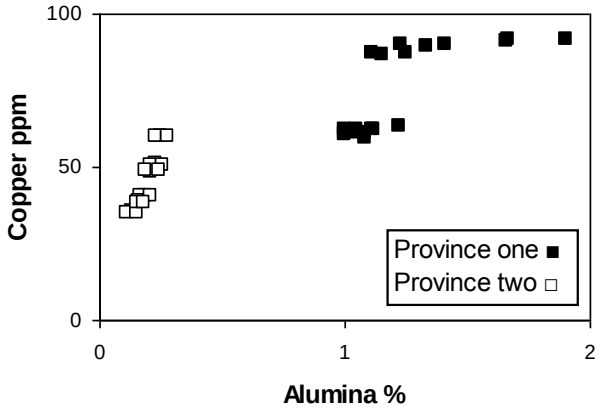

Fig. 3.12: Relationship between alumina and copper in the study area

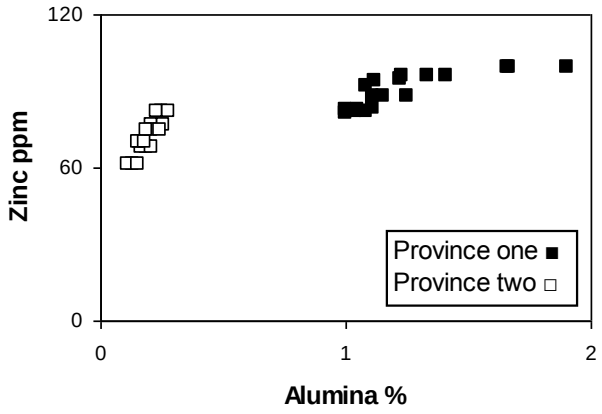

Fig. 3.13: Relationship between alumina and zinc in the study area

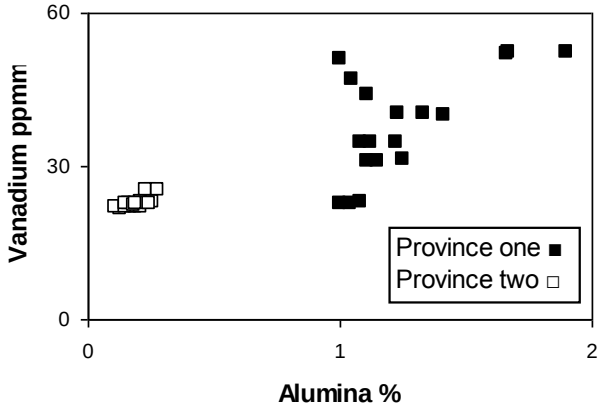

Fig. 3.14: Relationship between alumina and vanadium in the study area

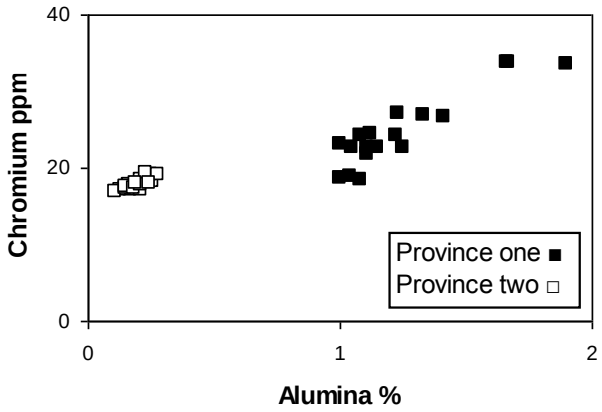

Fig. 3.15: Relationship between alumina and chromium in the study area

The Cu/Zn and V/Cr ratios are used as a redox parameter in many studies (e.g., Nagarajan *et al.*, 2007; Shaltami, 2012). According to Hallberg (1976) the increasing value of

the Cu/Zn ratio indicates a reducing depositional condition while decreasing Cu/Zn values suggest increased oxidizing conditions. Ratio of V/Cr above 2 indicates anoxic conditions, whereas values below 2 suggest more oxidizing conditions (Jones and Manning, 1994). Thus, the prevailing well oxidizing coastal environments are well expresses by the low Cu/Zn and V/Cr ratios (0.73 and 1.4 in average, respectively).

Lead precipitates with carbonate minerals, as stable solid compounds (Callahan. *et al.,* 1979). The independence of Pb distribution on CaO (r = -0.14) can be interpreted to its possibly anthropogenic source.

3.4.4. High field strength elements (HFSE)

They are highly charged cations and often have appropriate size for many cation sites in minerals. Their charge is too high and requires one or more coupled substitution to maintain charge balance; this is generally energetically unfavorable (White, 2001). Thus HFSE are incompatible elements as they have high ionic potential, they are insoluble and tend to be very immobile during weathering and metamorphism. In the studied samples, four HFSE, namely, Zr, Hf, Th and U are analyzed.

Lopez *et al.,* (2005) reported that the highest abundance of HFSE associates the silts which imply that accessory minerals, such as zircon and Nb-bearing phases are mainly concentrated in silt lithology. The high silica rocks tend to contain higher concentrations of HFSE than the basic rocks (Chandrajith, *et al.,* 2000).

The HFSE provide a series of the geochemical isovalents (Zr-Hf, Nb-Ta and Th-U). The mutual abundance and distribution of these isovalents in most geologic environments follow the popularly known Goldschmidt`s rule which is based on the charge and radius control (i.e., CHARAC). The non-CHARAC behavior of the isovalents is important in interpreting geological environments. The ratios between isovalents have the advantage that they do not change with time as isotopic ratios do (Condie, 2005). In the present study the ratios of the isovalents are summarized in table 3.4.

Table 3.4: Ratios of selected isovalents in the studied samples

Location	Zr/Hf	Th/U
East Tolmeita	9.74	2.68
Tolmeita	9.31	2.69
West Tolmeita	9.95	2.70
East Tukrah	9.19	2.70
Tukrah	9.97	2.68
West Tukrah	9.17	2.71
Daryana	9.33	2.38
West Daryana	7.56	2.38
East Sidi Khalifa	8.62	2.41
Sidi Khalifa	8.31	2.92
West Sidi Khalifa	8.67	2.38
Al Kuwifia	8.29	2.40

The concentration of Zr in sandstone is typically higher than that in both mudrocks and limestone. Zr is generally transported with terrigenous influx in the form of heavy mineral (zircon). The two elements; Zr and Hf with atomic numbers 40 and 72, respectively, form an excellent example of a pair of elements having almost complete chemical similarity in spite of very different total electron numbers and atomic weights. In the present study, Zr and Hf are strongly correlated (r = 0.93, Fig. 3.16), suggesting that these elements are controlled by zircon.

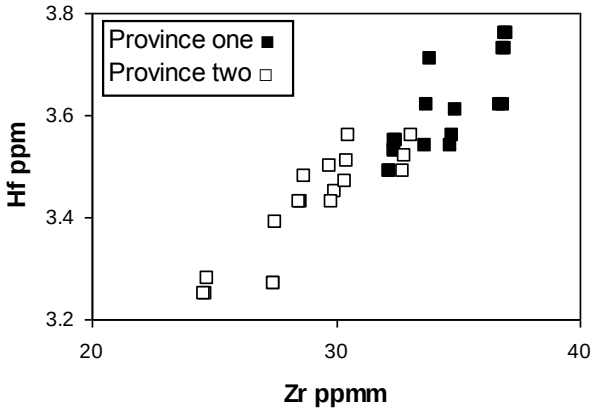

Fig. 3.16: Relationship between Zr and Hf in the study area

The Zr/Hf ratio in the studied samples ranges from 7.56 to 9.97, while the chondritic value is estimated to be 35 by Weyer *et al.*, (2002). Ahrnes and Erlank (1969) concluded that the Zr/Hf ratio of detrital zircon varies depending on its provenance, with an increase in Hf content from basic to acidic rocks.

Both natural and synthetic zircon crystals are commonly enriched in Y and HREE relative to LREE (Watson, 1980; Fujimaki, 1986; Hinton and Upton, 1991; Hanchar *et al.*, 2001). In the studied samples, Zr shows negative correlations with Th, U, Y and REE (r = -0.64, -0.77, -0.76 and -0.69, Figs. 3.17-20, respectively). These relationships mean that Th, U, Y and REE are not contained in zircon.

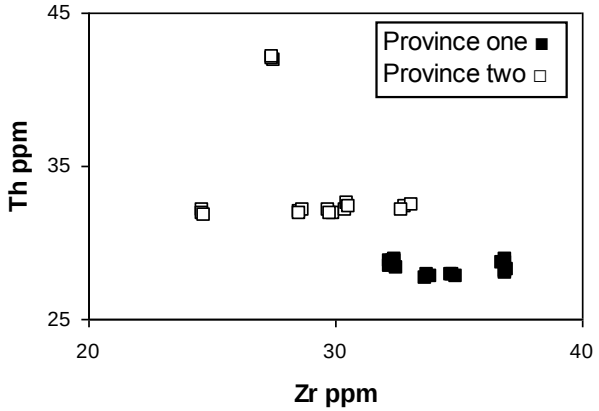

Fig. 3.17: Relationship between Zr and Th in the study area

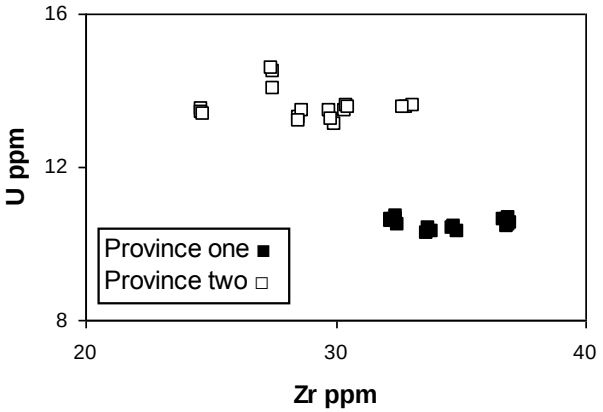

Fig. 3.18: Relationship between Zr and U in the study area

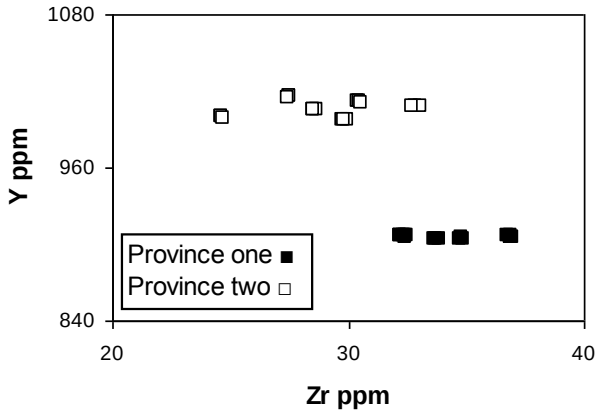

Fig. 3.19: Relationship between Zr and Y in the study area

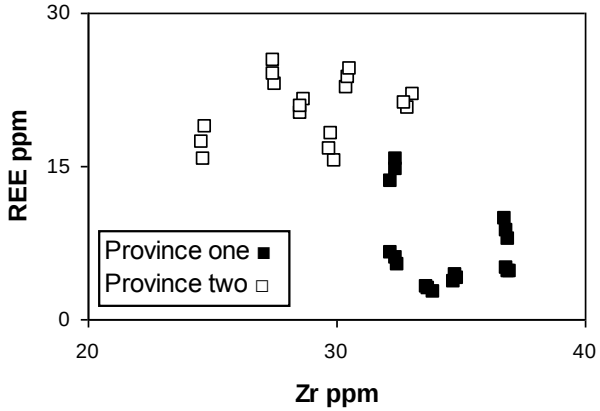

Fig. 3.20: Relationship between Zr and REE in the study area

In the studied samples, Th always dominates over U. Under the prevailing surface conditions, U is mobile due to its oxidation to the soluble hexavalent state, as compared to the relatively immobile Th, which is concentrated in residual materials. Thus, the intensively weathered sediments display high Th/U ratios. In the present study, Th and U are strongly correlated (r = 0.82, Fig. 3.21). The author believes that Th and U in the studied samples are basically controlled by the carbonate fraction which includes shell fragments and clastics of limestone. This assumption is confirmed by the positive correlation between CaO and both Th and U (r = 0.73 and 0.95, Figs. 3.22-23, respectively).

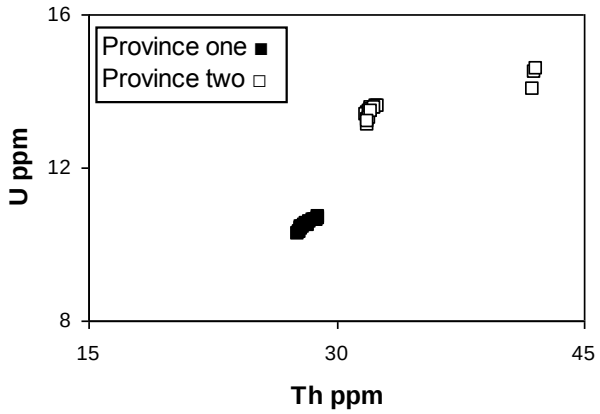

Fig. 3.21: Relationship between Th and U in the study area

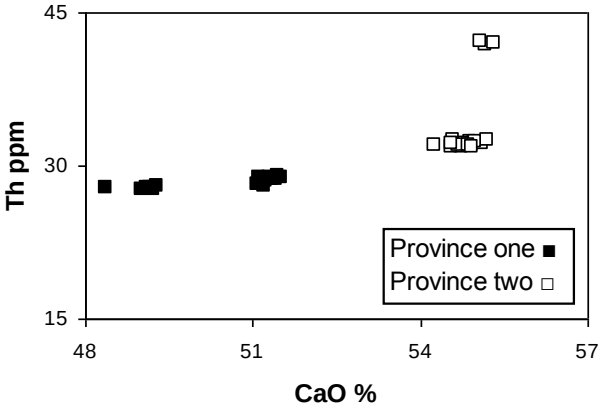

Fig. 3.22: Relationship between CaO and Th in the study area

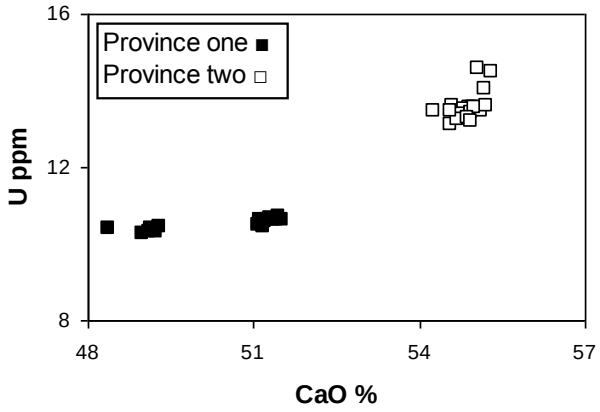

Fig. 3.23: Relationship between CaO and U in the study area

In the present study, the average value of Th/U (2.7) approximately resembles the chondritic value (3, by McLennan *et al.*, 1993). In most cases, weathering and sedimentary

recycling typically result in loss of U, leading to an elevation in the Th/U ratio. According to Asiedu *et al.,* (2000), in sedimentary rocks, Th/U values higher than 4 may indicate intense weathering in source areas or sediment recycling (i.e., derivation from older sedimentary rocks).

The U/Th ratio and authigenic uranium are used as a redox parameter in many studies (e.g., Jones and Manning, 1994; Nagarajan *et al.,* 2007; Shaltami, 2012). U/Th ratios below 1.25 suggest oxic conditions of deposition, whereas values above 1.25 indicate suboxic and anoxic conditions (Nath *et al.,* 1997). According to Nagarajan *et al.,* (2007), in the Arabian Sea, sediments below the oxygen minimum zone (OMZ) show high U/Th (>1.25) ratios, whereas the sediments above the OMZ exhibit low U/Th (<1.25) ratios. The authigenic uranium content is calculated as: (authigenic U) = [U – Th/3]. Values of authigenic U below 5 are thought to represent oxic depositional conditions, while values above 5 are indicative of suboxic and anoxic conditions (Nagarajan *et al.,* 2007). The studied limestone samples show low values of U/Th ratio (ranges from 0.34 to 0.42) and authigenic uranium (ranges from 0.07 to 2.82), which indicate that these sediments were deposited in oxic conditions.

3.4.5. Rare earth elements (REE)

The term rare earth elements describes the lanthanides (atomic numbers from 57 to 71), except the naturally unstable promethium (Pm, atomic number 61), that occur in Group IIIA of the Periodic Table. The REE include 14 elements namely; lanthanum (La), cerium (Ce), praseodymium (Pr), neodymium (Nd), samarium (Sm), europium (Eu), gadolinium (Gd), terbium (Tb), dysprosium (Dy), holmium (Ho), erbium (Er), thulium (Tm), ytterbium (Yb) and lutetium (Lu). The REE are divided into two groups, namely; the light rare earth elements (LREE), from La to Eu, and heavy rare earth elements (HREE), from Gd to Lu. Y and Sc have been recognized as pseudolanthanides. Geochemically, these two elements are traditionally considered as heavy rare earth elements, because their properties are similar to HREE. The commonest oxidation state of the REE is the trivalent, with Eu which may also exist in the divalent state and Ce in the tetravalent state. These two exceptions of Eu and Ce provide a significant tool for interpreting the redox controls. There is a gradual decrease in ionic radii with increasing atomic number, known as the lanthanide contraction.

The distribution of REE in marine waters, sediments and carbonate rocks has been discussed by many workers (e.g., Piper, 1974; Klinkhammer *et al.*, 1983; De Baar *et al.*, 1988; Elderfield *et al.*, 1990; Madhavaraju and Ramasamy, 1999; Nothdurft *et al.*, 2004; Madhavaraju and Lee, 2009; Madhavaraju and Gonzalez-Leon, 2012). The concentrations of REE in seawater

are principally influenced by different input sources (*e.g.*, terrestrial input from continental weathering and hydrothermal) and scavenging processes related to depth, salinity and oxygen levels (Greaves *et al.*, 1999). The unique feature of the seawater REE pattern reveals the uniform trivalent behavior of the elements (except Ce and Eu that exhibit multiple valences) and estuarine and marine scavenging processes (Nothdurft *et al.*, 2004).

The analyzed REE include all the naturally occurring 14 rare earth members. In general, the studied samples are enriched in the LREE over the HREE. The concentration of REE is less in province one samples than in the province two samples. The REE are normalized to Post-Archean Australian Shale (PAAS, Taylor and McLennan, 1985). PAAS-normalized REE patterns of the studied samples are shown in Fig. 3.24.

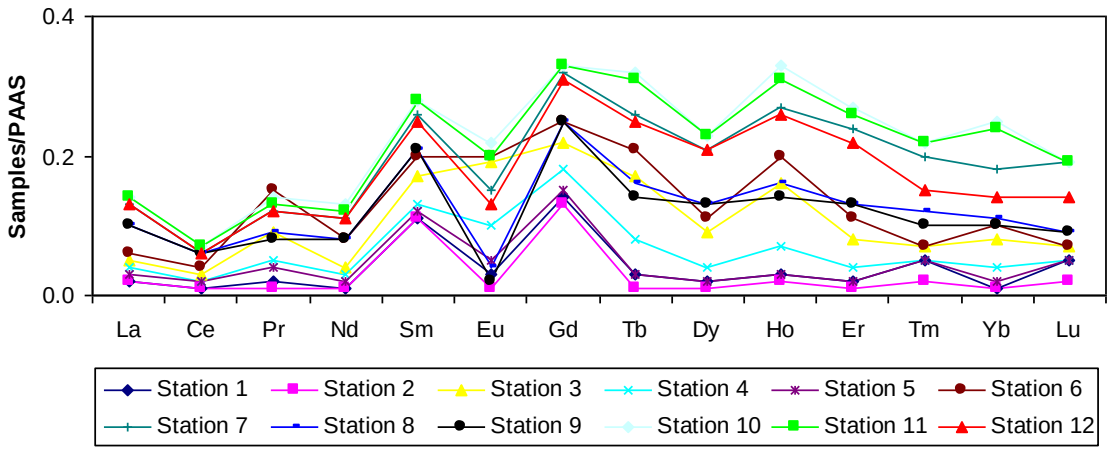

Fig. 3.24: PAAS normalized REE diagram for the studied samples

The REE parameters such as ∑REE, LREE/HREE ratios, Ce- and Eu- anomalies (Table 3.5) provide important clues concerning the source, provenance and transportation history of the studied sands.

The Ce anomaly (ΔCe) content is calculated as: ΔCe = Ce/(La + Pr)/2, while the Eu anomaly (ΔEu) content is calculated as: ΔEu = Eu/(Sm + Gd)/2. The contents of La, Pr, Ce, Sm, Eu and Gd used in these equations are PAAS normalized values.

Table 3.5: REE parameters in the studied samples

Location	LREE	HREE	∑REE	LREE/HREE	ΔCe	ΔEu	Y/Ho
East Tolmeita	3.08	0.88	3.96	3.50	0.67	0.22	30149.30
Tolmeita	2.18	0.76	2.94	2.87	0.70	0.08	52198.90
West Tolmeita	6.78	1.95	8.73	3.48	0.42	0.87	7759.32
East Tukrah	4.76	1.23	5.99	3.88	0.45	0.50	20421.80
Tukrah	3.79	0.99	4.78	3.83	0.50	0.31	24426.00
West Tukrah	11.54	3.06	14.60	3.78	0.35	0.92	3590.36
Daryana	16.83	4.47	21.30	3.77	0.51	0.56	3563.29
West Daryana	14.00	3.31	17.31	4.25	0.59	0.32	5136.76
East Sidi Khalifa	13.66	3.11	16.77	4.41	0.60	0.23	5839.58
Sidi Khalifa	18.89	5.24	24.13	3.61	0.49	0.81	2621.59
West Sidi Khalifa	18.60	5.04	23.64	3.69	0.50	0.75	2846.50
Al Kuwifia	16.52	4.28	20.80	3.87	0.52	0.50	3685.64

Province one shows more or less flat REE pattern with positive La and slightly negative Ce anomalies (ΔCe: 0.35 to 0.70, Table 3.5). Province two samples exhibit LREE-enriched but HREE-depleted patterns with slightly negative Ce anomalies (ΔCe: 0.49 to 0.60, Table 3.5). The studied samples show slight to mild positive Eu anomalies. Fig. (3.24) and table (3.5) show that the concentration of rare earth elements (REE) is less in province one than in province two. In agreement with Verma (2005) and Shaltami (2013), the author believes that the variations in REE concentrations in the studied sands are probably controlled by the amount of carbonate minerals. This is supported by the strong correlation between CaO and ΣREE (r = 0.93, Fig. 3.25).

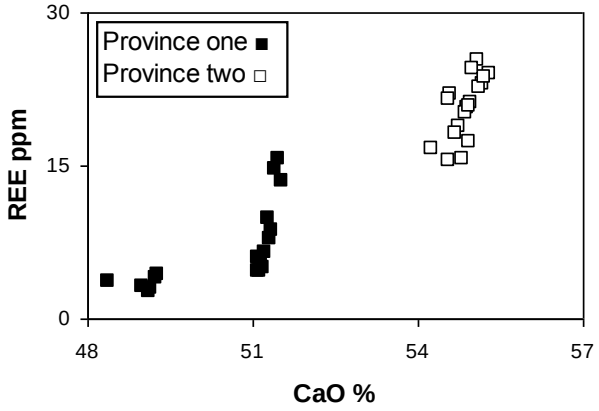

Fig. 3.25: Relationship between CaO and ΣREE in the study area

The depletion of Ce in oceanic water results from redox changes relative to the rest of REE series (Nath *et al.*, 1994). The studied sands show slightly negative Ce anomalies (Table

3.5). In oceanic water, ΔCe values range from <0.1 to 0.4 (Elderfield and Greaves, 1982; Piepgras and Jacobsen, 1992), whereas in average shale ΔCe is 1 (Murray *et al.*, 1991b). The observed negative Ce anomalies in the studied samples are smaller than in the Arabian Sea sediments (Nath *et al.*, 1997) and in deep-sea carbonates from the Indian Ocean (Nath *et al.*, 1992). In the present study, ΔCe values are not correlated with U content (r = 0.02) and ΔCe values show weak negative correlation with the amount of CaO (r = -0.21), which suggest in agreement with Madhavaraju and Lee (2009) and Shaltami (2013), that the ΔCe values in the studied beach sands are not related to the paleo-redox conditions.

Y is chemically similar to the HREE, especially its isovalent; Ho. The two elements have almost the same ionic radius and valence where Y/Ho ratio is very constant in the lithosphere and even in planetary materials. In the studied samples, Y is positively correlated with Ho (r = 0.77, Fig. 3.26). However, there is much evidence to show that these two elements are significantly fractionated in aqueous systems (Zhang *et al.*, 1994), indicating that Y has a different aqueous chemistry than those of the REE. However, the mechanism that fractionates these two elements has not yet been well documented (Zhang and Liu, 2004).

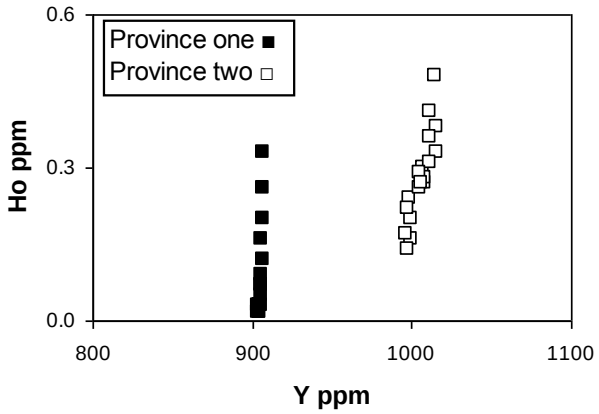

Fig. 3.26: Relationship between Y and Ho in the study area

The Y/Ho ratio in the studied samples ranges from 2621 to 52198, while the chondritic value is estimated to be 28 by Weyer *et al.*, (2002). According to Kawabe *et al*., (1991) and Miura *et al*., (1999), a large negative Ce anomaly, a small negative Eu anomaly and a high Y/Ho ratio (i.e., Y/Ho > 28) are typical characteristics of REE and Y patterns for marine limestones.

ENVIRONMENTAL GEOCHEMISTRY OF SILT FRACTION

4.1. Introduction

The Mediterranean is a typical model for regional sea calculations of fluxes and mass balances consisting of both naturally and anthropogenically derived materials. It is a semi-enclosed sea with deep basins and large-scale layered circulations; yet it has negligible tidal movements and local circulation patterns are basically wind-driven (Hopkins, 1978). The Mediterranean Sea is often considered as a representative model of the world`s ocean. Being semienclosed, it also records various signals of high anthropic pressures from surrounding countries and the industrialized North European countries. Although accounting for 1 % of the world`s ocean surface, it receives about 25 % of worldwide petroleum inputs to the ocean, with 750 x 10^3 ton yr^{-1} (Burns and Saliot, 1986).

The present chapter attempts to assess the environmental geochemistry of the silt fraction of the beach sands along the Mediterranean Coast from Benghazi outskirts (Al Kuwifia) to Tolmeita, NE Libya.

The quantification of the pollution magnitude in the aquatic system is a relatively new field of research. Human environment is tightly linked to the aquatic ecosystems hence will be subjected, by way or another, to the same pollutants. Heavy metals such as Cu, Zn, Cr, V, Pb, and As are normal constituents of marine environment. When additional quantities are introduced from industrial wastes or sewage they enter the biogeochemical cycle and, as a result of being potentially toxic, may interfere with the ecology of a particular environment. In different marine organisms, the behavior of these metals is described in terms of their absorption, storage, and excretion and when different concentrations are available in the environment. At higher concentrations, the detrimental effects of these metals become apparent and their different toxic effects (Bryan, 1971). The present work focuses on the possible toxicity of beach sands by trace metals, as a first step in the protection of the ecology of this ecosystem rather than as an inexpensive safeguard to man, although these aims are not mutually exclusive. Sediments conserve important environmental information (VonGunten *et al.,* 1997) and are increasingly as both a carrier and a possible source of contaminants in aquatic systems (Forstner and Salomons, 1991; Tessier *et al.,* 1994). Sediments act as sink for transition metal contaminants and risk increases with metals leachability. The impact of potentially toxic metals abnormality may extend to involve the water quality, food web and human health. Rulkens *et al.,* (1995)

characterized the physical states of pollutants in soils and sediments as being present as particulates, liquid films, adsorbed ions, absorbed ions and liquid phases in pores. According to Kunzendorf (1986), in the beach environment, metal-rich sands are generally found in the upper beach zone, or backshore, where waves lead to concentrations of high-density minerals that are not easily removed back to the sea by the low energy backwash flow.

The chemical analysis of the studied beach sands includes a group of environment-sensitive elements such as Cu, Zn, Cr, V, Pb, As, U and Th. The sources of these elements could be natural or anthropogenic. The natural sources include chemical weathering, while the most important sources of anthropogenic heavy metals in the studied sands include petroleum pollution (Fig. 4.1), sewage disposal and paints.

Fig. 4.1: Petroleum pollution at station no.12 (Al Kuwifia)

4.2. Heavy metals

The widespread use of heavy metals in industries ranging from large-scale mining to intensive agriculture has resulted in a variety of heavy metals being released into the environment with concentrations in excess of the natural background levels (Dryssen and Wedborg, 1980). The potential environmental damage might be comparatively small if these metals are ultimately fixed in sediments and pore-water concentrations are limited by their solubility (Zoumis *et al*., 2001). Information on the total concentrations of metals alone is not sufficient to assess the environmental impact of polluted sediments because heavy metals are

present as easily exchangeable metal carbonates, oxides, sulfides, organometallic compounds, ions in the crystal lattice of minerals etc. which determine their mobilization capacity and bioavailability (Soto-Jimenez *et al*., 2003). Environmental pollution by heavy metals is of concern, because they exhibit behavior consistent with those of persistent toxic chemicals (Clark, 1992). Sediments play a useful role in the assessment of heavy metal contamination (Forstner and Wittmann, 1981). Total concentrations of heavy metals in soils and sediments are dependent on a number of factors. The background concentrations, influenced by local bedrock geochemistry, may be supplemented to differing degrees by anthropogenic inputs.

In studied samples, Cu, Zn, Cr and V show positive correlations among themselves suggesting in agreement with Dalai *et al.*, (2004) and Suresh *et al.*, (2015), that a common mechanism regulates their abundance and reflect their derivation from common sources. Both As and Pb do not demonstrate any confident coherence to any of the analyzed elements. The author believes that As and Pb distributions in the study area are related to anthropogenic activities.

4.2.1. Lead (Pb)

Sediments contain considerably higher levels of lead than corresponding surface waters (Craig *et al.,* 1999). The average value of Pb in the studied samples (132.74 ppm) is clearly higher than the beach sands of some other studies (Table 4.1).

Table 4.1: Comparison of Pb concentration (ppm) in beach sands in the study area with previous studies

Studies of beach sands	Pb (average) ppm
Mansour (2000), Red Sea Coast, Egypt	19.81
El-Kammar *et al.,* (2007), Eastern side of the Gulf of Suez, Egypt	10.30
Abdallah (2008) Mediterranean Coast, Egypt	48.64
Schintu *et al.,* (2009), Western Mediterranean Coast, Sardinia	20.44
Shaltami (2012) Mediterranean Coast, Libya	19.80
Present study	132.74

The author believes that the possible anthropogenic sources of Pb pollution in the study area are variable, where leak of oil and its products seems to be the most influential, as pollution is reinforced in oil shipping areas and harbors. Pb is used as antiknocking additive in gasoline; hence, it is contributed by shipping and other anthropogenic activities. Pb is also used in the marine paints as lead chlorides, as weights for diving equipment and added to the marine environment with the oil wastes from the boats. The upper background of Pb (mean + standard deviation) is 153.78 ppm, while the lower background (mean - standard deviation) is 111.70 ppm. The upper background of Pb is much higher than the average continental crust (8 ppm, by Taylor and McLennan, 1985). It is important to note that all stations contain higher concentrations of Pb than continental crust (Fig. 4.2). According to Abu El-Ella (2006) the Maximum Permissible Limit of Pb in soil is not yet definite, but average of limestone, which is most comparable to the studied samples, is 9 ppm. The upper background of Pb in the studied samples (153.78 ppm) is approximately fifteen times the elemental composition of typical uncontaminated soil (10 ppm, http://www.dsa.unipr.it/ phytonet/fertilia/partners/tcan4.htm). The pollution limits of Pb in the study area are a serious matter and should be handled with enough care. According to the Agency for Toxic Substances and Disease Registry (ATSDR, 1990,1992) soil lead contamination from mine tailings may be less effective in increasing PbB (blood lead) levels than is lead contamination derived from urban lead pollution (paint, gasoline) or atmospheric lead fallout from lead smelting operations.

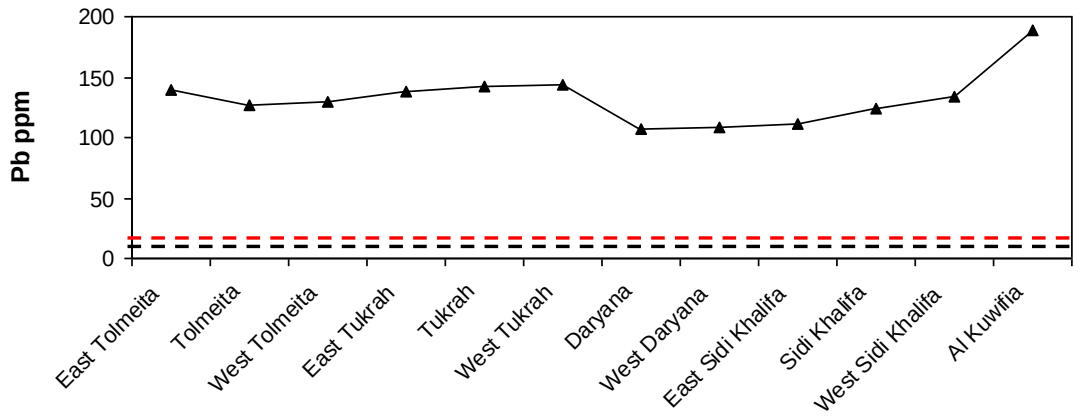

Fig. 4.2: Distribution of Pb in the study area (Black dashed line means average Continental Crust and red dashed line means elemental composition of typical uncontaminated soil)

4.2.2. Arsenic (As)

The average value of As in the studied samples (8 ppm), is slightly higher than the beach sands in the studies as quoted by El-Kammar *et al.,* (2007) and Shaltami (2012), while is much lower than the beach sands in the study as quoted by Moreira (1996, Table 4.2).

It is estimated that about 60% of As present in the environment is of anthropogenic origin (Nriagu, 1989). The author believes that in the study area, the anthropogenic sources of As are oil production and processing, and landfill/waste pile leaching. The upper background of As is 10.62 ppm which is much higher than the average Continental Crust (1 ppm, by Taylor and McLennan, 1985), while is slightly higher that the elemental composition of typical uncontaminated soil (6 ppm, http://www.dsa.unipr.it/phytonet/fertilia/partners/tcan4.htm). In the study area, all stations contain higher concentrations of As than continental crust (Fig. 4.3).

Table 4.2: Comparison of As concentration (ppm) in beach sands in the study area with previous studies

Studies of beach sands	As (average) ppm
Moreira (1996), Sepetiba Bay, Brazil	80.00
El-Kammar *et al.,* (2007), Eastern side of the Gulf of Suez, Egypt	5.00
Shaltami (2012) Mediterranean Coast, Libya	6.91
Present study	8

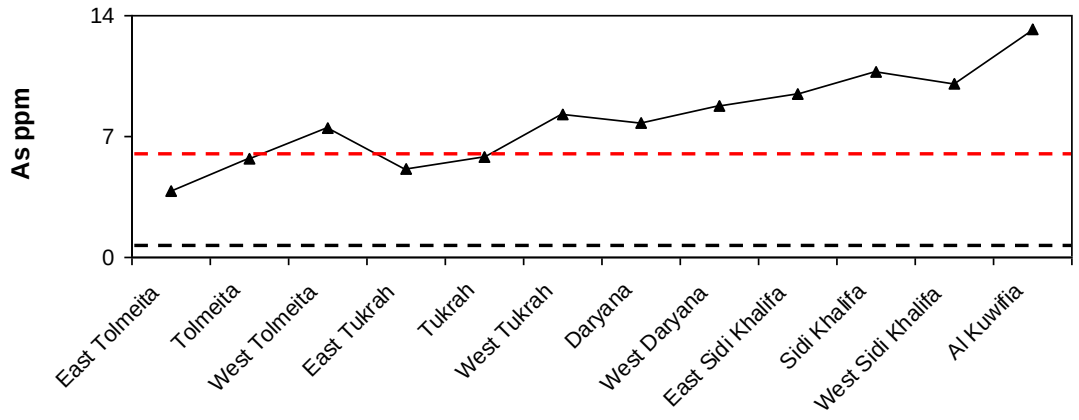

Fig. 4.3: Distribution of As in the study area (Black dashed line means average Continental Crust and red dashed line means elemental composition of typical uncontaminated soil)

4.2.3. Copper (Cu)

The average value of Cu in the studied samples (60.53 ppm), is much higher than the beach sands in the studies as quoted by El-Kammar *et al.,* (2007) and Schintu *et al.,* (2009), while is slightly lower than the beach sands in the study as quoted by Shaltami (2012, Table 4.3).

The author believes that the probable anthropogenic sources of Cu in the studied beach are the yard used in the ship constructions, renewing the old ships, removing rust and old metal parts and painting the ship bodies. Cu was used as nails in the ship constructions, as antifouling paints and removed as rust from the ship bodies. The upper background of Cu is 79.67 ppm, which is slightly higher than the average Continental Crust (75 ppm, by Taylor and McLennan, 1985). In the study area, all stations contain higher concentrations of Cu than the elemental composition of typical uncontaminated soil (20 ppm, http://www.dsa.unipr.it/phytonet/fertilia/partners/tcan4.htm, Fig. 4.4).

Table 4.3: Comparison of Cu concentration (ppm) in beach sands in the study area with previous studies

Studies of beach sands	Cu (average) ppm
El-Kammar *et al.,* (2007), Eastern side of the Gulf of Suez, Egypt	5.10
Schintu *et al.,* (2009), Western Mediterranean Coast, Sardinia	3.00
Shaltami (2012) Mediterranean Coast, Libya	76.15
Present study	60.53

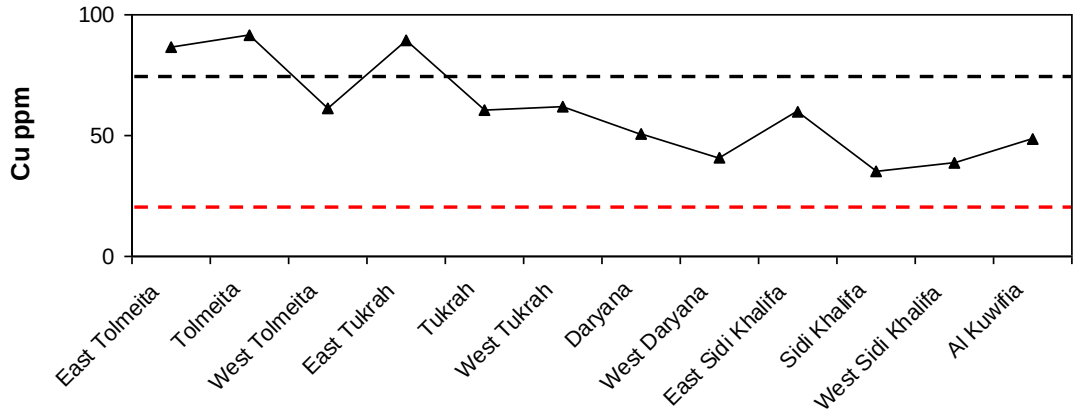

Fig. 4.4: Distribution of Cu in the study area (Black dashed line means average Continental Crust and red dashed line means elemental composition of typical uncontaminated soil)

4.2.4. Zinc (Zn)

The average value of Zn in the studied samples (81.13 ppm), is clearly higher than the beach sands in the studies as quoted by El-Kammar *et al.,* (2007) and Schintu *et al.,* (2009), while is slightly lower than the beach sands in the study as quoted by Shaltami (2012, Table 4.4).

The author believes that, in thy study area the anthropogenic sources of Zn include oil harbor and municipal. Zn is widely used as zinc sulfate in the initial stage of building and ship painting inside the coastal zone. Among all metals, Cu, Pb and Zn are in the closest relationship to humans (Narla, 1996). These elements are not only widely used in daily life, but they are also absorbed by other organisms (Fichet *et al.,* 1998; Babi *et al.,* 2001). The upper background of Zn is 92.53 ppm, which is slightly higher than the average Continental Crust (80 ppm, by Taylor and McLennan, 1985). In the study area, all stations contain higher concentrations of Zn than the elemental composition of typical uncontaminated soil (50 ppm, http://www.dsa.unipr.it/phytonet/fertilia/partners/tcan4.htm, Fig. 4.5).

Table 4.4: Comparison of Zn concentration (ppm) in beach sands in the study area with previous studies

Studies of beach sands	Zn (average) ppm
El-Kammar *et al.,* (2007), Eastern side of the Gulf of Suez, Egypt	28.68
Schintu *et al.,* (2009), Western Mediterranean Coast, Sardinia	40.31
Shaltami (2012) Mediterranean Coast, Libya	86.55
Present study	81.13

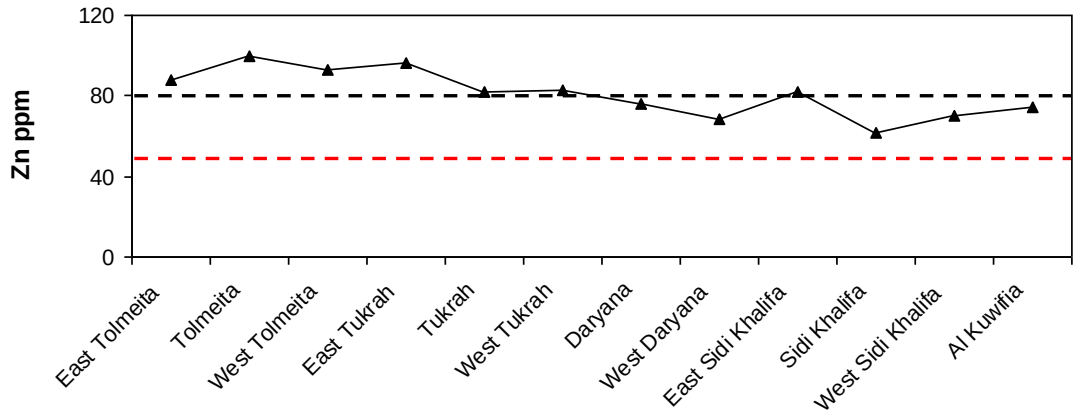

Fig. 4.5: Distribution of Zn in the study area (Black dashed line means average Continental Crust and red dashed line means elemental composition of typical uncontaminated soil)

4.2.5. Chromium (Cr) and Vanadium (V)

The average values of Cr and V in the studied samples (21.34 and 30.47 ppm, respectively) are slightly higher than the beach sands in the study as quoted by El-Kammar *et al.*, (2007), Schintu *et al.*, (2009) and Shaltami (2012, Table 4.5).

The author believes that, in the study area, combustion of fossil fuels, particularly fuel oils, and sewage discharges seem to be the main anthropogenic sources of Cr and V. The upper backgrounds of Cr and V (26.21 and 41 ppm, respectively) are much lower than the average Continental Crust (185 and 230 ppm, respectively, by Taylor and McLennan, 1985). El-Moselhy (2006) showed that the Red Sea sediments had a mean concentration of V higher than those of the Mediterranean. No data are available regarding biomagnification of V within the food chain, but human studies suggest that it is unlikely; most of the l%-2% V that appears to be absorbed by humans following ingestion is rapidly excreted in the urine with no evidence of long-term accumulation (Fox, 1987). In the study area, all stations contain lower concentrations of Cu and V than the elemental composition of typical uncontaminated soil (40 and 37 ppm, respectively, http://www.dsa.unipr.it/phytonet/ fertilia/partners/tcan4.htm).

Table 4.5: Comparison of Cr and V concentrations (ppm) in beach sands in the study area with previous studies

Studies of beach sands	Cr (average) ppm	V (average) ppm
El-Kammar *et al.,* (2007), Eastern side of the Gulf of Suez, Egypt	5.20	23.50
Schintu *et al.,* (2009), Western Mediterranean Coast, Sardinia	17.26	27.27
Shaltami (2012) Mediterranean Coast, Libya	15.86	28.80
Present study	21.34	30.47

4.3. Uranium (U) and Thorium (Th)

U and other actinides are of environmental concern. U is passively accumulated by microbes via electrostatic interaction between charged U species and functional groups on cells. U is toxic to cells due to its chemical properties rather than radioactivity (Huang *et al.*, 2015). U is also accumulated inside cells via an energy-independent transport system. Alternatively, intracellular U accumulation might be induced by increase in membrance permeability due to death of cells (Suzuki and Banfield, 2001). The average values of Th and U in the studied

samples (31 and 12 ppm, respectively) are clearly higher than the beach sands of some other studies (Table 4.6). The upper backgrounds of Th and U (34.87 and 13.63 ppm, respectively) are much higher than the Crustal averages (3.5 and 0.91 ppm, respectively, by Taylor and McLennan, 1985). This refers, in agreement with Ozmen *et al.*, (2014), to the significant and influential contamination with respect to Th and U. It is important to note that all the study areas are anomalous in Th and U with respect to Continental Crustal average (Figs. 4.6-7).

Table 4.6: Comparison of Th and U concentrations (ppm) in beach sands in the study area with previous studies

Studies of beach sands	Th (average) ppm	U (average) ppm
El-Kammar *et al.,* (2007), Eastern side of the Gulf of Suez, Egypt	15.10	5.45
Shaltami (2012) Mediterranean Coast, Libya	26.93	0.17
Present study	31.00	12.00

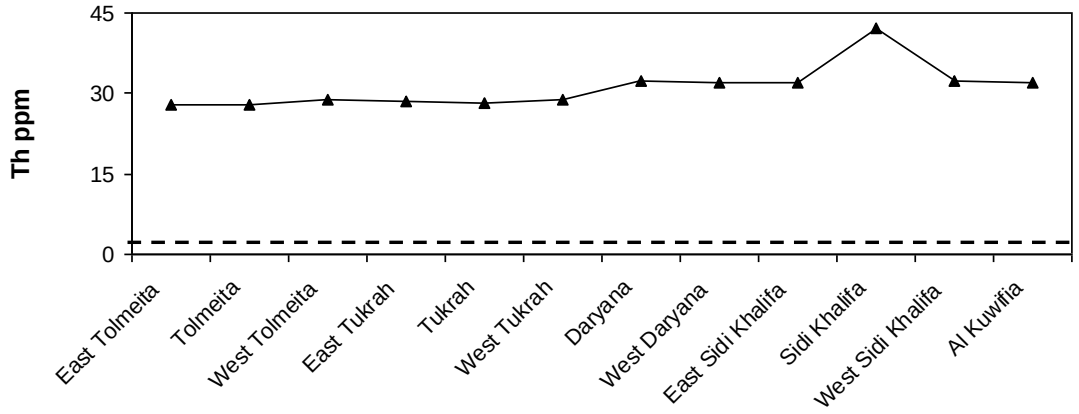

Fig. 4.6: Distribution of Th in the study area (Black dashed line means average Continental Crust)

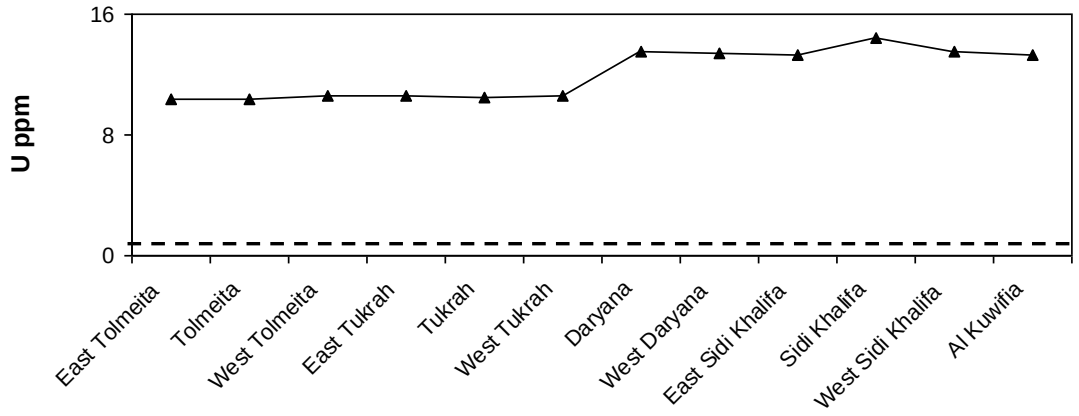

Fig. 4.7: Distribution of U in the study area (Black dashed line means average Continental Crust)

4.4. Contamination processes

The possibility of sediment contamination was assessed through the calculation of the metal enrichment factor (EF), which is the observed metal/normalizer ratio in the sample divided by the metal/normalizer ratio reported for a reference material (Salomons and Forstner, 1984; Zhang, 1995). Metals such as Al, Li and Fe have been largely used as geochemical normalizers (Daskalakis and O'Connor, 1995; Niencheski *et al.,* 2002; Dalai *et al.,* 2004; Leopold *et al.,* 2008; Shaltami, 2012; Mahu *et al.,* 2015). In relation to Fe, the author believes that the use of Al as geochemical normalizer seems to be more adequate. The main limitation of using Fe as a geochemical normalizer is the possibility of anthropogenic input of this element (Niencheski *et al.*, 2002). Metal concentrations in the studied beach sands is a net result of variability in source rock composition, sediment texture, adsorption/desorption, sediment transport, mineral sorting and anthropogenic activity. Contributions of metals to sediments from non-lithogenic sources can be gauged by calculating their enrichment factors (EF). According to Ergin *et al.,* (1991) and Rubio *et al.,* (2000) the metal enrichment factor (EF) is defined as: $(EF) = [(X/Al)_{sample}/(X/Al)_{Upper\ Continental\ Crust}]$, where, X is the concentration of any element. Metal concentrations of average continental crust (Taylor and McLennan, 1985) are used as for calculation of EF.

According to Reimann and de Caritat (2005), there is no accepted pollution ranking system or categorization of degree of pollution on the EF analysis. It cannot provide a reliable assessment of the degree of human interference with the global environment, but only indicate lithogenic or anthropogenic origin of the contaminants. Real-world examples of regional geochemical surveys demonstrate that EF is influenced by a number of factors of which contamination is but one (Dragovic *et al.,* 2008). According to Grousset *et al*., (1995), a value of $EF \leq 2$ can be considered to be of lithogenic origin for a metal whereas $EF > 2$ is suggestive of sources such as biogenic and anthropogenic. In addition, strong correlations with aluminum and enrichment factors (close to one) represent elements present in sediments due to natural weathering (Krupadam *et al.,* 2006). Metals analyzed in this study, except Cr and V in some locations (Table 4.7), have $EF > 2$ suggesting that they are mainly of anthropogenic origin and that natural activities exert little influence on their abundances.

Table 4.7: Enrichment factor (EF) of metals in the study area

Location	EFCu	EFZn	EFV	EFCr	EFPb	EFAs	EFTh	EFU
East Tolmeita	15.79	14.99	1.87	1.67	25.09	6.12	11.25	16.78
Tolmeita	11.16	11.37	2.10	1.66	15.22	6.18	7.55	11.22
West Tolmeita	11.46	16.28	2.13	1.83	23.90	12.36	11.93	17.64
East Tukrah	14.43	14.47	2.14	1.75	22.00	7.39	10.19	15.10
Tukrah	12.42	15.62	1.52	1.54	28.63	10.50	12.76	19.05
West Tukrah	12.52	15.66	3.15	1.84	28.62	14.83	12.93	19.10
Daryana	46.41	65.58	6.96	6.81	97.35	62.99	65.77	110.51
West Daryana	45.55	71.68	8.14	7.81	121.00	88.05	79.92	134.38
East Sidi Khalifa	50.63	64.61	7.03	6.54	92.54	71.08	59.87	99.47
Sidi Khalifa	58.41	95.18	11.93	11.49	203.50	157.40	154.90	211.93
West Sidi Khalifa	50.31	85.46	9.68	9.29	172.61	116.60	93.89	157.35
Al Kuwifia	48.85	70.04	7.49	7.28	186.67	117.91	71.37	118.79

Another approach of quantitative assessment of metal pollution in sediments is to determine geo-accumulation index (I_{geo}) of metals as proposed originally by Muller (1979). I_{geo} is expressed as: $(I_{geo}) = [\log_2 C_n / 1.5B_n]$, where C_n and B_n are the measured and background concentrations of the metal *n* respectively; and 1.5 is the correction factor used to account for possible variability in the background data due to lithological variation. Metal concentrations of average continental crust (Taylor and McLennan, 1985) are used as the background concentrations for metals. According to Loska *et al.,* (2003) and Das *et al.,* (2008), I_{geo} classified pollution levels into 6 grades, namely, unpolluted (grade 1, $I_{geo} < 1$), very lightly polluted (grade 2, $1 < I_{geo} < 2$), lightly polluted (grade 3, $2 < I_{geo} < 3$), moderately polluted (grade 4, $3 < I_{geo} < 4$), highly polluted (grade 5, $4 < I_{geo} < 5$) and very highly polluted (grade 6, $I_{geo} > 5$). The I_{geo} values (Table 4.8) suggest that the studied samples are unpolluted with Cu, Zn, V, Cr, Pb and Th, very lightly polluted to lightly polluted with As and lightly polluted with U.

4.5. Gadolinium anomaly (ΔGd)

According to Elbaz-Poulichet *et al.,* (2002) and Kulaksiz and Bau (2007), except at the surface, seawater shows positive anomalies of Gd. These anomalies result primarily from the lower solubility of Gd complexes compared to those of their respective neighbors in the REE series. According to Knappe *et al*., (1999) and Ogata and Terakado (2006), the extent of the ΔGd in seawater is only small (from 1 to 1.2).

Table 4.8: Geo-accumulation index (I_{geo}) of metals in the study area

Location	Igeo Cu	Igeo Zn	Igeo V	Igeo Cr	Igeo Pb	Igeo As	Igeo Th	Igeo U
East Tolmeita	0.06	0.05	0.01	0.02	0.59	1.28	0.91	2.47
Tolmeita	0.06	0.06	0.02	0.02	0.58	1.67	0.91	2.47
West Tolmeita	0.05	0.05	0.01	0.02	0.58	1.93	0.92	2.50
East Tukrah	0.06	0.05	0.02	0.02	0.59	1.58	0.92	2.49
Tukrah	0.05	0.05	0.01	0.02	0.60	1.69	0.92	2.48
West Tukrah	0.05	0.05	0.02	0.02	0.60	2.03	0.92	2.50
Daryana	0.05	0.05	0.01	0.02	0.56	1.97	0.95	2.76
West Daryana	0.05	0.05	0.01	0.01	0.56	2.09	0.95	2.75
East Sidi Khalifa	0.05	0.05	0.01	0.02	0.57	2.16	0.95	2.73
Sidi Khalifa	0.05	0.05	0.01	0.01	0.58	2.28	1.03	2.82
West Sidi Khalifa	0.05	0.05	0.01	0.01	0.59	2.22	0.96	2.75
Al Kuwifia	0.05	0.05	0.01	0.02	0.63	2.48	0.95	2.74

According to Bolhara and Van Kranendonkb (2007), the ΔGd content is calculated as: ΔGd = Gd/(2Tb–Dy). The values of the REE used in this equation are normalized to Post-Archean Australian Shale (PAAS. Table (4.9) shows that the studied samples display both negative and positive Gd-anomalies. According to Zhu *et al.*, (2004) positive Gd anomaly in coastal areas was artificially caused by anthropogenic sources where Gd derived from domestic wastewaters and from its use in medical facilities.

Table 4.9: Gadolinium anomaly in the study area

Location	ΔGd
East Tolmeita	3.60
Tolmeita	6.62
West Tolmeita	1.04
East Tukrah	3.08
Tukrah	4.52
West Tukrah	0.70
Daryana	0.96
West Daryana	1.18
East Sidi Khalifa	1.30
Sidi Khalifa	0.66
West Sidi Khalifa	0.72
Al Kuwifia	1.02

SUMMARY AND CONCLUSIONS

This work aims to characterize the mineralogy, geochemistry and environmental geochemistry of the beach sands along the Mediterranean Coast from Benghazi outskirts (Al Kuwifia) to Tolmeita, NE Libya, with especial emphases on the provenance. The exposed facies surrounded in the study area is mainly limestones range in age from the Lower Eocene which is represented in the Apolonia Formation to the Upper Miocene which is represented in the Wadi al Qattarah Formation. The Quaternary deposits observed in the study area are extended along the coastal plain to the shoreline. These deposits are represented in red soil, gravels, sabkha sediments, beach sands and calcarenites.

Twelve stations were sampled along the beach of the study area (S1 - S12). This beach is surrounded by Al Jabal Al Akhdar (Green Mountain) from the first to the forth stations (S1-S4), and it is getting to be open from the fifth station (S5) to the southwest. There are two beach types; sandy and rocky beaches.

The studied beach sands are basically a mixture of carbonate and non-carbonate materials. The microscopic examination indicates abundance of carbonates, quartz, glauconite, feldspars and evaporites. Carbonate grains are mainly represented by biogenic grains made of aragonite and/or calcite. Biogenic grains are composed of whole shell fragments of macrofauna (mollusks) and microfaunal shells, mostly of foraminifera and algae and other, not clearly classifiable biogenic fragments. Aragonite occurs as ooids and tritiform, whereas calcite occurs as rectangular and irregular shapes. Calcite is usually colorless and exhibits gleaming interference colors of very high orders. The EDX microanalysis shows that the detected calcite is low-Mg calcite. It is an excellent accumulator of barium, strontium and yttrium.

Quartz is commonly colorless and contains inclusions, namely, opaques. It is mostly monocrystalline with uniform and undulatory extinction, and occurs either in the form of angular grains or as rounded grains. Dust rims in most quartz grains have long been recognized as an indicator for sediment recycling. Some quartz grains show cracks, which could either be the feature inherited from the source material or could be due to long distance of transportation.

The detected evaporites are gypsum and halite. Gypsum occurs as prismatic grains, whereas halite occurs as cubic grains. The EDX microanalyses show that gypsum and halite are good accumulators of Ni.

Feldspars, glauconite and heavy minerals are only detected in the eastern side (from east Tolmeita to west Tukrah) of the studied beach, while they are lacking in the western side. Microcline and orthoclase are common feldspars. Glauconite occurs as irregular dark green grains. The microscopic examination shows that the detected heavy minerals in the study area are opaques, zircon, augite, tourmaline, rutile, biotite, garnet, monazite, titanite, hornblende and pistachite.

Zircon represents the most abundant heavy mineral among the non-opaques. Microscopic observations of zircon enabled the recognition of different shapes of zircon, such as; the oval with zoned structure, prismatic with bipyramidal terminations and broken. It occurs as colorless and smoky grains. The EDX microanalysis data shows that zircon is enriched in uranium, thorium and heavy rare earth elements (ytterbium), and the Hf/Zr ratio is about 0.03.

Titanite is the second common non-opaque mineral. The honey titanite is the only detected type. It is uncommon, imperfect cleavage is observed in few titanite grains. Augite is the only detected pyroxene mineral. It is mostly prismatic in shape. It has yellowish brown color and exhibits perfect cleavage. Biotite is commonly light brown. It is mostly sub-rounded in shape. Fine inclusions of opaque minerals are sometimes frequent. Hornblende is the only detected amphibole mineral. It is commonly light green. It displays diagnostic perfect cleavage that appears imperfect in some cases. It is mostly prismatic in shape. The encountered garnet grains are cubic form but occasionally prismatic. The most common grains are colorless. The EDX microanalysis shows that garnet mostly of almandite variety.

Tourmaline grains are mostly zoneless, subrounded to well-rounded but sometimes prismatic in shape. The occurrence of a rounded to well-rounded tourmaline variety suggests that the sediments were reworked from older sedimentary precursor. The yellowish brown and brown tourmalines are the only detected types. It is characterized by its strong pleochrism.

Pistachite is the only detected epidote mineral. It occurs mostly as sub-rounded to rounded grains. It is commonly pale yellowish green in color. The EDX microanalysis indicates that

pistachite contains more Fe than Mg. It has Ca/Mg ratio about 3.29 and relatively rich in Ti, where the Ti/Al ratio measures 0.41.

The detected opaque minerals in the study area are magnetite, ilmenite, hematite, goethite, limonite and pyrite. Magnetite occurs as homogeneous and altered grains. Homogeneous magnetite is commonly pale grey in color with pinkish tint. The pre-depositional textures of magnetite are martitization, replacement by titanite and alteration to rutile and hematite, while the post-depositional texture is alteration to goethite and limonite.

Ilmenite occurs as homogeneous and altered grains. Homogeneous ilmenite is usually paler in color being grey with brownish tint. It is commonly prismatic in shape. The pre-depositional texture of ilmenite is alteration to rutile and hematite, while the post-depositional texture is alteration to goethite and limonite.

The detected pyrite is framboidal pyrite. It commonly replaces magnetite grains along their boundaries, replaces magnetite along their cracks or completely replaces goethite. Glauconite occurred together with pyrite. They both need reducing conditions to form which is probably caused by the presence of decaying organic matter which consumes all free oxygen.

Based on the mineral composition, two distinct types or groups of sediments were extracted and defined as:

1) Province one (from East Tolmeita (station no. 1) to West Tukrah (station no. 6)): This province contains high concentration of quartz (from 5.55 to 9.12). It is also characterized by the presence of feldspars, glauconite and heavy minerals.

2) Province two (Daryana (station no. 7) to Al Kuwifia (station no. 12)): This province contains low concentration of quartz (from 1.52 to 2.81). It is also characterized by the absence of feldspars, glauconite and heavy minerals.

Based upon the difference in minerals concentrations between the two provinces, and regards to the mineralogy of the surrounded areas, the beach sands of province one (closed beach) are derived from the sea accumulation (carbonates and evaporites), surrounded carbonate rocks

(glauconite) and terra rossa, while the beach sands of province two (open beach) are mainly derived from the sea accumulation, while bearing in mind that the provenance of the heavy minerals and some light minerals (feldspars) can be derived from the aeolian sands which have been produced by weathering of the igneous and metamorphic rocks that are distributed in many part of Libya such as Jabal Al Tibisti, Harouj, As Sawda, etc. These aeolian sands can be transported by wind from the source and deposited on the surrounded rocks, and then to the beach as terra rossa?

The correlation matrix suggests that the heavy metals are possibly of different sources. The Th and U as well as the REE and Y are essentially related to marine and terrestrial inputs. Lime, silica, alumina and magnesia are the main constituents of the studied samples. The correlation coefficients among the analyzed major oxides points to the intimate coherence among them, except for lime and magnesia. Silica, alumina, iron oxides, soda and potash are most probably accommodated within silicate clastics. Lime, which expresses the carbonate sediments in the studied coastal zone, seems to be the main diluents of the terrestrial admixture. The plot of silica versus alumina suggests that silica and alumina are strongly correlated in province two, while their weak correlated in province one. This reflects the occurrence of silica in both silicate and free silica modes.

The distribution of CaO is clearly opposite to that of SiO_2 (r = -0.95). Silica is likely to represent mineral components especially quartz, while lime may be mainly derived from shell fragments, which are abundant in the studied beach. CaO is strongly correlated with MgO (r = 0.93). The relationship means that calcite is the sole carrier of MgO. The studied samples show very low MgO/CaO ratio (~0.01). This low value indicates that the studied samples are not dolomitized.

K_2O is strongly correlated with Al_2O_3 (r = 0.90) suggesting that these elements are almost entirely associated with detrital admixture. In province one, the K_2O/Al_2O_3 ratio ranges from 0.47 to 0.96, indicates that feldspars have a major role in the distribution of aluminum in this province. The strong positive correlation between Na_2O and Cl (r = 0.95) supports their accommodation in the form of halite.

Most of the studied samples have low TiO_2 contents. In province one, TiO_2 is strongly correlated with Fe_2O_3 (r = 0.90) suggesting that Ti is contained in iron-titanium oxyhydroxides (rutile, magnetite, hematite and ilmenite). This assumption confirmed by the positive correlation

between TiO_2 and the traditional terrigenous elements such as Zr (r = 0.65). In province one the TiO_2/Zr ratio ranges from 32.7 to 86.56, while in province two it ranges from 3 to 7.28.

In the present study, the P_2O_5 content ranges between 0.07 to 0.72 %, and it does not show clear coherence to Ce content (r = 0.16) suggesting that the potentiality of phosphate is not controlled by monazite. P_2O_5 distribution in the study area is related to anthropogenic activities.

The abundance of Ba and Sr is basically controlled by the carbonate fraction which includes shell fragments and clastics of limestone. This assumption is confirmed by the strong correlation between CaO and both Ba and Sr (r = 0.96 and 0.97, respectively).

In all provinces, Cu, Zn, V and Cr are strongly correlated with Al_2O_3 (r = 0.88, 0.90, 0.83 and 0.88, respectively) suggesting their possible accommodation as alumino-silicates which can be concentrated during weathering.

Zr shows negative correlations with Th, U, Y and REE (r = -0.64, -0.77, -0.76 and -0.69, respectively). These relationships mean that Th, U, Y and REE are not contained in zircon. Th and U are strongly correlated (r = 0.82) indicating that Th and U are basically controlled by the carbonate fraction which includes shell fragments and clastics of limestone. This assumption is confirmed by the positive correlation between CaO and both Th and U (r = 0.73 and 0.95, respectively).

The prevailing well oxidizing coastal environments are well expresses by the low Cu/Zn, V/Cr and U/Th ratios and authigenic uranium (0.73, 1.4, 0.39 and 1.7 in average, respectively).

Province one shows more or less flat REE pattern with positive La and slightly negative Ce anomalies (ΔCe: 0.35 to 0.70). Province two samples exhibit LREE-enriched but HREE-depleted patterns with slightly negative Ce anomalies (ΔCe: 0.49 to 0.60). The samples show slight to mild positive Eu anomalies, and the concentration of rare earth elements (REE) is less in province one than in province two. The variations in REE concentrations are probably controlled by the amount of carbonate minerals. This is supported by the strong correlation between CaO and ΣREE (r = 0.93). ΔCe values are not correlated with U content (r = 0.02) and ΔCe values show weak negative correlation with the amount of CaO (r = -0.21), which suggest that the ΔCe values are not related to

the paleo-redox conditions. The Y/Ho ratio in the studied samples ranges from 2621 to 52198. Negative Ce anomaly, a small negative Eu anomaly and a high Y/Ho ratio (i.e., Y/Ho > 28) are typical characteristics of REE and Y patterns for marine limestones.

The sources of the toxic elements could be natural or anthropogenic. The natural sources include chemical weathering, while the most important sources of anthropogenic heavy metals in the studied sands include petroleum pollution, sewage disposal and paints.

Cu, Zn, Cr and V show positive correlations among themselves, whereas As and Pb do not demonstrate any confident coherence to any of the analyzed elements. This indicating that As and Pb distributions in the study area are related to anthropogenic activities.

Metals analyzed in this study, except Cr and V in some locations, have EF > 2 suggesting that they are mainly of anthropogenic origin.

The I_{geo} values suggest that the studied samples are unpolluted with Cu, Zn, V, Cr, Pb and Th ($I_{geo} < 1$), very lightly polluted to lightly polluted with As ($1 < I_{geo} < 3$) and lightly polluted with U ($2 < I_{geo} < 3$).

The studied samples display both negative and positive Gd-anomalies. The positive Gd anomaly in the studied beach is suggested to be artificially caused by anthropogenic sources where Gd derived from domestic wastewaters and from its use in medical facilities.

References

Abdel Gawad, A. M. (1966): X-ray Spectrographic Determination of Zirconium-Hafnium Ratio in Zirconium Minerals. Amer Mineral; 51:464.

Abu El-Ella, N. A. (2006): Sedimentological, mineralogical and geomorphological studies on the Quaternary sediments of coastal area, W. Tripoli, Libya. PH.D. Thesis. Cairo Univ. Cairo, Egypt.

Agency for Toxic Substances and disease Registry (ATSDR) (1990): Case studies in environmental medicine: Lead toxicity.

Agency for Toxic Substances and Disease Registry (ATSDR) (1992): Toxicological profile for lead, ATSDR/TP-88/17.

Ahrens, L. H. and Erlank, A. J. (1969): Hafnium, Section B-O, in Wedephol, K.H., ed., Handbook of Geochemistry (Vol. 11/5): New York, Springer-Verlag.

Akimoto, T.; Kinoshita, H. and Furuta, T. (1984): Electron probe microanalysis study on process of iow-temperature oxidation of titanomagnetite. Earth Planet. Sci. Lett., 71, 263-278**.**

Albardeiro, L.; Pereira, M. F.; Gama, C.; Chichorro, M.; Hofmann, M. and Linnemann, U. (2014): Provenance study of Pliocene–Pleistocene sands based on ancient detrital zircons (Alvalade Basin, SW Iberian Atlantic coast). Sedimentary Geology; 307: 47–58.

Ali, L. H.; El Jawashi, S. A.; Ejbali, A. A. and Garbaj, M. J. (1998): Investigations on organics in the Libyan beach sand and water: extraction, spectroscopy and gas chromatography, Zwarah to East Tripoli coastline. Water studies series; 3:133-144.

Al Shariani, T. A. K. (2006): Composition and environmental geochemistry of sediment encroachment controlled by dams in the United Arab Emirates. PH.D. Thesis. Cairo Univ., Cairo, Egypt.

Anderson, D. (2003): Introduction to heavy metal monitoring. Natural Environmental Research Council. CEH. 1p.

Anfuso, G.; Achab, M.; Cultrone, G. and Lopez - Aguayo, F. (1999): Utility of heavy minerals distribution and granulometric analyses in the study of coastal dynamics: Application to the littoral between Sanlucar de Barrameda and Rota (Cadiz, southwest Iberian Peninsula). Bol. Inst. Esp. Oceanogr; 15(1-4): 243-250.

Angusamy, N.; Loveson, V. J. and Rajamanickam, G. V. (2004): Zircon and ilmenite from the beach placers of southern coast of Tamil Nadu, east coast of India. Indian Journal of Marine Sciences; 33(2): 138-149.

Asiedu, D. K.; Suzuki, S.; Nogami, K. and Shibata, T. (2000): Geochemistry of Lower Cretaceous sediments, Inner Zone of Southwest Japan: Constraints on provenance and tectonic environment. Geochemical Journal; 34: 155-173.

Assaf, H. S.; Hangari, K. M. and Baegi, M.B. (1994): A1 Awaynat surficial uranium mineralization, south-western Libya, a new approach to its origin. Journal of African Earth Sciences; 19: 85-90.

Atkinson, K. and Waugh, B (2007): Morphology and mineralogy of red desert soils in the Libyan Sahara. Earth Surface Processes; 4(2): 103-115.

Babi, D.; Vasjari, M. and Lazo, P. (2001): Determination of heavy metals content in hair in different collectives of Albania. Asian J Chem; 13(3):837–843.

Basu, A. (1985): Reading provenance from detrital quartz, in Zuffa G.G.I., Provenance of Arenites: Nato Series C.; 148: 231-247.

Basu, A.; Young, S. W.; Suttner, L. J.; James, W. C. and Mack, G. H. (1975): Reevaluation of the use of undulatory extinction and polycrystallinity in detrital quartz foe provenance interpretation: Journal of Sedimentary Petrology; 45: 873-882.

Bird, E .C. F. and Schwartz, M. L. (1985): The World's Coastline, Van Norstrand Rheinhold, New York; 1071 pp.

Blatt, H.; Middleton, G. and Murray, R. (1972): Origin of sedimentary rocks, Prentice Hall Inc., Englewood Cliffs, New Jersey; 634p.

Bolhara, R. and Van Kranendonkb, M. J. (2007): A non-marine depositional setting for the northern Fortescue Group, Pilbara Craton, inferred from trace element geochemistry of stromatolitic carbonat. Precambrian Research; 155: 229-250.

Bopp, R. F.; Simpson, H. J. and Chillrud, S. N. (1993): Sediment-derived chronologies of persistent contaminants in Jamaica Bay, New York. Estuaries; 16 (3B): 608–616.

Bryan, G. W., (1971): The effects of heavy metals (other than mercury) on marine and estuarine organisms. Proc. R. Soc. Lond. 177: 1.

Burns, K. A. and Saliot, A., (1986): Petroleum hydrocarbons in the Mediterranean Sea: A mass balance. Marine Chemistry; 20: 141–157.

Butler, J. R. and Thompson, A. J. (1965): Zirconium: Hafnium Ratio in Some Igneous Rocks. Geochim Cosmochim Acta; 29:197.

Callahan, M. A.; Slimak, M. W. and Gable, N. W. (1979): Water-related fate of 129 priority pollutants. Washington, DC: U.S. Environmental Protection Agency, Office of Water Planning and Standards. EPA-440/4-79-029a.

Carlson, W. D. and Schwarze, E. (1997): Petrological significance of prograde homogenization of growth zoning in garnet: an example from the Llano Uplift. J Metam Geol; 15:631–644.

Carranza-Edwards, A.; Bocanegra-Garcia, G.; Rosales-Hoz, L. and Galan, L. D. (1998): Beach sands from Baja California Peninsula, Mexico. Sedimentary Geology; 119(3-4): 263-274.

Carranza-Edwards, A.; Centeno-García, L.; Rosales-Hoz, L. and Lozano-Santa Cruz, R. (2001): Provenance of beach gray sands from western México: Journal of South American Earth Sciences; 14: 291-301.

Carranza-Edwards, A.; Kasper-Zubillaga, J. J.; Rosales-Hoz, L.; Morales-de la Garza, E. A. and Lozano-Santa Cruz, R. (2009): Beach sand composition and provenance in a sector of the southwestern Mexican Pacific. Revista Mexicana de Ciencias Geológicas; 26(2): 433-447.

Carter, R. W. G. (1982): Some problems associated with the analysis and interpretation of mixed carbonate and quartz beach sands, illustrated by examples from North-West Ireland. Sedimentary Geology; 33: 35-56.

Chandrajiath, R.; Dissanayake, C. B. and Tobschall, H. J. (2000): Enrichment of high-field strength elements in stream sediments of a granulite terrain in Sri Lanka-evidence for a mineralized belt. Chem. Geol; 175: 259-271.

Chang, L. L. Y.; Howie, R. A. and Zussman, J. (1996): Rock-forming minerals. Non-silicates. vol 5B. Longman, London.

Chang, S. S.; Shau, Y. H.; Wang, M. K.; Ku, C. T. and Chiang, P. N. (2008): Mineralogy and occurrence of glauconite in central Taiwan. Applied Clay Science; 42: 74–80.

Chave, K. E. (1954b): Aspects of the biogeochemistry of magnesium. Part 2. Calcareous scdimcnts and rocks. J. Geol; 62: 587-599.

Chave, K. E. (1962): Processes of carbonate sedimentation. Narragansett Marine Lab. Occ. Publ.; 1: 77-85.

Chen, J.; Wang, F. and Chen, J. (1994): Relation of aquatic particulate grain size to heavy metals concentrations in Eastern Chinese Rivers. Acta Scientiae Circumstantiae; 14: 419-425.

Cherian, A.; Chandrasekar, N. and Rajamanickam, V. (2004): Light minerals of beach sediments from Southern Tamilnadu, south east coast of India. Oceanologia; 46 (2): 233–252.

Clark, R. B. (1992): Marine Pollution. Clarendon Press, Oxford, UK, pp. 61–79.

Condie, K. C. (2005): High field strength element ratios in Archean basalts: a window to evolving sources of mantle plumes. Lithos; 79: 491-504.

Condie, K. C.; Boryta, M. D.; Liu, J. and Quian, X., (1992): The origin of khondalites: geochemical evidence from the Archean to Early Proterozoic granulitic belt in the North China Craton: Precambrian Research; 59(3-4), 207-223.

Cox, R.; Low, D. R. and Cullers, R. L. (1995): The influence of sediment recycling and basement composition on evolution of mudrock chemistry in the southwestern United States. Geochimica et Cosmochimica Acta; 59: 2919–2940.

Craig, J. R.; Rimstidt, J. D. and Bonnaffon, C. A. (1999): Surface water transport of lead at shooting range. Bull Environ Contam Toxicol; 63:312-319.

Curtis, C. E.; Doney, L. M. and Johnson, J. R. (1954): Some properties of hafnium oxide, hafnium silicate, calcium hafnate and hafnium carbide. Jour. Am. Ceram. Soc.; 37: 458-465.

Dalai, T. K.; Rengarajan, R. and Patel, P. P. (2004): Sediment geochemistry of the Yamuna River System in the Himalaya: Implications to weathering and transport. Geochemical Journal; 38: 441-453.

Das, S. K.; Routh, J.; Roychoudhury, A. N. and Klump, J. V. (2008): Major and trace element geochemistry in Zeekoevlei, South Africa: A lacustrine record of present and past processes. Applied Geochemistry; 23: 2496–2511.

Daskalakis, K. D. and O'Connor, T. P. (1995): Distribution of chemical concentrations in US coastal and estuarine sediment. Marine Environmental Research; 40: 381–398.

De Baar, H. J. W.; German, C. G.; Elderfield, H. and van Gaans, P. (1988): Rare earth elements distributions in anoxic waters of the Cariaco Trench. Geochimica et Cosmochimica Acta; 52: 1203-1219.

De Meijer, R. J.; James, I. R.; Jennings, P. J. and Koeyers, J. E. (2001): Cluster analysis of radionuclide concentrations in beach sand. Applied Radiation and Isotopes. Volume 54, Issue 3, P. 535-542.

Desio, A. (1970): The Sebkha of Marada. L esplorazione mineraria della Libya. Ispi, Milano; pp. 170-262.

Dickinson, W. W. and Milliken, K. L. (1995): The diagenetic role of brittle deformation in compaction and pressure solution, Etjo Sandstone, Namibia: Journal of Geology; 103: 339-347.

Dragovic, S.; Mihailovic, N. and Gajic, B. (2008): Heavy metals in soils: Distribution, relationship with soil characteristics and radionuclides and multivariate assessment of contamination sources. Chemosphere; 72: 491–495.

Dryssen, D. and Wedborg, M. (1980): Major and minor elements, chemical speciation in estuarine waters. Chemistry and Biogeochemistry of Estuaries (Olausson, E. and Cato, I., eds.), 71–119, Wiley, Chichester.

Dupre, B.; Gaillardet, J.; Rousseau, D. and Allegre, C. J. (1996): Major and trace element of river-born material: the Congo basin. Geochim. Cosmochim. Acta; 60: 1301–1321.

El-Amamy, M. M.; Page, A. L. and Abudelgawad, G. (1982): Chemical and Mineralogical Properties of Glauconitic Soil as Related to Potassium Depletion. Soil Sci Soc Am J; 46:426-430.

Elbaz-Poulichet, F.; Seidel, J. L. and Othoniel, C. (2002): Occurrence of an anthropogenic gadolinium anomaly in river and coastal waters of Southern France. Water Research; 36: 1102-1105.

Elderfield, H. and Greaves, M. J. (1982): The rare earth elements in seawater. Nature; 296: 214-219.

Elderfield, H.; Upstill-Goddard R. and Sholkovitz, E. R. (1990): The rare earth elements in rivers, estuaries and coastal seas and their significance to the composition of ocean waters. Geochimica et Cosmochimica Acta; 54: 971-991.

El-Ghawi, U. M.; Al-Fakhri, S. M.; Al-Sadeq, A. A.; Bejey, M. M. and Doubali, K. K. (2007): The level of selenium and some other trace elements in different Libyan arable soils using instrumental neutron activation analysis. Biol Trace Elem Res; 119(1):89-96.

El-Ghawi, U. M.; Bejey, M. M.; Al-Fakhri, S. M.; Al-Sadeq, A. A. and Doubali, K. K. (2005): Analysis of Libyan arable soils by means of thermal and epithermal NAA. The Arabian Journal for Science and Engineering; 30: 147-153.

EL HAWAT, A. S. (1980): Intertidal and Storm Sedimentation from Wadi al Qattarah Member, Ar Rajmah Formation (Middle Miocene), Al Jabal al Akhdar. In: M.J. Salem, M.T. Busrewil (eds.), The Geology of Libya, Academic Press, London vol. II: 449-461.

EL HAWAT, A. S. & ABDULSAMAD, E. O. (2004): The geology of Cyrenaica a field seminar. Sedimentary basins of Libya, Earth Sci. Soc. Libya, Tripoli. 130p.

EL HAWAT, A. S., BARGHATHI, H. & OBEIDI, A. (2004): Cyrenaica - Transect VII. In: W. Cavazza, W. Roure, F., Spakman, W., Stampfli, G. & Ziegler, P. (eds.),

The TRANSMED Atlas: the Mediterranean Region from Crust to Mantel. CD Rom, Springer-Verlag.

El-Hawat, A. S. and Pawellek, T. (2005): A field guidebook to the geology of Sirte Basin, Libya. REW Dea North Africa / Middle East GmbH / Libya branch; 93: 5-38.

EL Hawat, A. S. & Salem, M. J. (1987): A Case Study of the stratigraphic subdivision of Ar Rajmah Fm. and its Implication on the Miocene of Nern Libya. In: Proc. **VIII**th Cong. Med. Neogene Stratig., Budapest. Ann. Inst. Geol. Publ. Hung., Budapest. **LXX**: 173-184.

El-Hinnawi, E. (1964): Mineralogical and Geochemical Studies on Egyptian Black Sands. Beitr Mineral Petrol; 9:519.

El Hinshery, A. K. and Kumar, N. S. (1992): Lead levels in settled dusts of Tripoli, Libya. The Science of The Total Environment; 119: 51-56.

El-Kameesy, S. U.; Abd El-Ghany, S.; El-Minyawi, S. M.; Miligy, Z. and El-Mabrouk, E.M. (2008): Natural Radioactivity of Beach Sand Samples in the Tripoli Region, Northwest Libya. Turkish J. Eng. Env. Sci.; 32: 1–7.

El-Kammar, A. M.; Arafa, I.H. and El-Sheltami, O. R. (2007): Mineral composition and environmental geochemistry of the beach sediments along the eastern side of the Gulf of Suez, Egypt. Journal of African Earth Sciences; 49: 103–114.

El-Moselhy, K. M. (2006): Distribution of vanadium in bottom sediments from the marine coastal area of the Egyptian Seas. Egyptian Journal of Aquatic Research; 32(1): 12-21.

El Werfalli, A. O., Muftah, A. M. and El Hawat, A. S. (2000). A Guidebook on the Geology of Al Jabal Al Akhdar, Cyrenaica, NE Libya. Gutenberg Press, Malta; 71: 6.

Emelyanov, E. M. and Shinmkus, K. M. (1986): Geochemistry of the Mediterranean Sea, Dordrecht. D. Reidel Publ.

Ergin, M.; Saydam, C.; Basturk, O.; Erdem, E. and Yoruk, R. (1991): Heavy metal concentrations in surface sediments from the two coastal inlets (Golden Horn Estuary and Izmit Bay) of the northeastern Sea of Marmara. Chem. Geo.; 91: 269–285.

Fedo, C. M.; Eriksson, K. and Krogstad, E. J. (1996): Geochemistry of shale from the Archean (~ 3.0 Ga) Buhwa Greenstone belt, Zimbabwe: Implications for provenance and source area weathering. Geochimica et Cosmochimica Acta; 60(10): 1751-1763.

Fichet, D.; Radenac, G. and Miramand, P. (1998): Experimental studies of impacts of harbor sediments resuspension to marine invertebrates lavae: bioavailibility of Cd, Cu, Pb and Zn and toxicity. Mar Pollut Bull; 36(7):509–518.

Fipke, C. E. (1991): Significance of chromite, G5 Mg-almandine garnet, zircon and tourmaline in heavy mineral detection of diamond bearing lamproite. Proceedings of the International Kimberlite Conference; 5: 97-100.

Folk, R. L. (1978): Petrology of Sedimentary Rocks: Austin Texas, Hemphil Public. 182p.

Force, E. R. (1980): The Provenance of Rutile. Journal of Sedimentary Petrology; 50(2): 485-488.

Force, E. R. (1991): Geology of titanium-mineral deposits, Geol. Soc. Am. Spec. Pap; 259: 11–18.

Forst, M. T.; Grey, I.E; Harrowfield, I. R. and Mason, K (1983): The dependence of alumina and silica contents on the alteration of weathered ilmenites from western Australia. Mineral Mag; 47: 201-208.

Forstner, U. and Salomons, W. (1991): Mobilization of metals from sediments. In: Merian, E (ed.), Metals and Their Compounds in the Environment, pp. 379–398. VCH, Weinheim.

Forstner, U. and Wittmann, G. T. W. (1981): Metal Pollution in the Aquatic Environment (2nd edn.). Springer, Berlin, Germany.

Fox, M. R. (1987): Assessment of cadmium, lead and vanadium status of large animals as related to the human food chain. J Anim Sci; 65:1744-1752.

Frihy, O. E. and Komar, P. D. (1993): Long-term shoreline changes and the concentration of heavy minerals in beach sands of the Nile Delta, Egypt. Mar. Geol; 115: 253-261.

Froelich, P. N.; Bender, M. L; Luedtke, N. A.; Heath, G. R. and Devries, T. (1982): The marine phosphorus cycle. Am. J. Sci.; 282: 474-511.

Frost, B. R.; Chamberlain, K. R. and Schuhmacher, J. C. (2000): Sphene (titanite) Phase relations and role as a geochronometer, Chem. Geol; 172: 131–148.

Fujimaki, H. (1986): Partition coefficients of Hf, Zr, and REE between zircon, apatite, and liquid. Contributions to Mineralogy and Petrology; 94: 42–45.

Gaillardet, J.; Dupre, B. and Allegre, C.J. (1999): Global silicate weathering and CO_2 consumption rates deduced from the chemistry of large rivers. Chem. Geol.; 159: 3–30.

Gandhi, M. S. and Raja, M. (2014): Heavy mineral distribution and geochemical studies of coastal sediments between Besant Nagar and Marakkanam, Tamil Nadu, India. Journal of Radiation Research and Applied Sciences; 7: 256-268.

Garcia, D., Fonteilles, M. and Moutte, J. (1994): Sedimentary fractionations between Al, Ti, and Zr and the genesis of strongly peraluminous granites. J. Geol.; 102: 411–422.

Garming, J. F. L.; Bleil, U. and Riedinger, N. (2005): Alteration of magnetic mineralogy at the sulfate–methane transition: Analysis of sediments from the Argentine continental slope. Physics of The Earth and Planetary Interiors. Volume 151, Issues 3-4 , 15 P. 290-308.

Garzanti, E., Ando, S.; Vezzoli, G.; Abdel Megid, A. A. and El Kammar, A. M. (2006): Petrology of Nile River sands (Ethiopia and Sudan): Sediment budgets and erosion patterns. Earth and Planetary Science Letters; 252: 327–341.

Garzanti, E., Vermeesch, P.; Ando, S.; Lustrino, M.; Padoan, M. and Vezzoli, G. (2014): Ultra-long distance littoral transport of Orange sand and provenance of the Skeleton Coast Erg (Namibia). Marine Geology; 357: 25-36.

Golik, A.; Weber, K.; Salihoglu, I.; Yilmaz, A. and Loizides, L. (1988): Pelagic tar in the Mediterranean Sea. Marine Pollution Bulletin; 19(11): 567-572.

Greaves, M. J.; Elderfield, H. and Sholkovitz, E. R. (1999): Aeolian sources of rare earth elements to the Western Pacific Ocean. Marine Chemistry; 68: 31-38.

Grousset, F. E., Quetel, Q. E.; Thomas, B., Donard, O. F. X., Lambert, C. E., Guillard, F. and Monaco, A. (1995): Anthropogenic vs. lithogenic origins of trace elements (As, Cd, Pb, Rb, Sb, Sc, Sn, Zn) in water column particles: northwestern Medierranean Sea. Mar. Chem.; 48: 291–310.

Hallberg, R. O. (1976): A geochemical method for investigation of palaeoredox conditions in sediments: Ambio, Special Report; 4: 139-147.

Hamouda, M. S. and Wilson, J. G. (1989): Levels of heavy metals along the Libyan coastline. Marine Pollution Bulletin; 20(12): 621-624.

Hanchar, J. M.; Finch, R. J.; Hoskin, P. W. O.; Watson, E. B.; Cherniak, D. J., and Mariano, A.N. (2001): Rare earth elements in synthetic zircon: Part 1. Synthesis, and rare-earth element and phosphorous doping of zircon. American Mineralogist; 86: 667–680.

Hanley, M. E.; Hoggart, S. P. G.; Simmonds, D. J.; Bichot, A.; Colangelo, M. A.; Bozzeda, F.; Heurtefeux, H.; Ondiviela, B.; Ostrowski, R.; Recio, M.; Trude, R.; Zawadzka-Kahlau, E. and Thompson, R. C. (2014): Shifting sands? Coastal protection by sand banks, beaches and dunes. Coastal Engineering; 87: 136-146.

Hegde, V. S.; Shalini, G. and Gosavi Kanchanagouri, D. (2006): Provenance of heavy minerals with special reference to ilmenite of the Honnavar beach, central west coast of India. Current Science; 91(5), 10.

Hernandez Arana, H. A.; Attrill, M. J.; Hartley, R. and Bouchot, G. G. (2005): Transitional carbonate-terrigenous shelf sub-environments inferred from textural characteristics of surficial sediments in the Southern Gulf of Mexico, Cont. Shelf Res.; 25(15): 1836–1852.

Hey, R. W. (1963): Pleistocene screes in Cyrenaica (Libya). Eiszeitalter und Gegenwart; 14: 77.

Hinton, R. W. and Upton, B. G. J. (1991): The chemistry of zircon: Variations within and between large crystals from syenite and alkali basalt xenoliths. Geochimica et Cosmochimica Acta; 55: 3287–3302.

Hopkins, T. S. (1978): Physical processes in the Mediterranean basins. In: Kjerfve, B. (Ed.), Estuarine Transport Processes. University of South Carolina Press, Columbia, SC, pp. 269–310.

Huang, Y.; Lu, X.; Ding, X. and Feng, T. (2015): Natural radioactivity level in beach sand along the coast of Xiamen Island, China. Marine Pollution Bulletin; 91: 357-361.

Hugo, V. E. and Cornell, D. H. (1991): Altered ilmenites in Holocene dunes from Zulu land, South Africa; petrologic evidence for multistage alteration. S. Afr. J. Geol.; 94: 365–378.

Jakovljevic, Z. (1984): Geological Map of Libya; 1:250,000 sheet: Al Awaynat NH 32-12. Explanatory Booklet, Ind. Res. Centre, Tripoli. 119p.

Jones, B. and Manning, D. C. (1994): Comparison of geochemical indices used for the interpretation of paleo-redox conditions in Ancient mudstones: Chemical Geology; 111(1-4): 111-129.

Kasper-Zubillaga, J. J. (2009): Roundness in quartz grains from inland and coastal dune sands, Altar Desert, Sonora, Mexico. Boletín de la Sociedad GeolóGica Mexicana; 61(1): 1-12.

Kasper-Zubillaga, J. J., Dickinson, W. W., Carranza-Edwards, A. and Hornelas-Orozco, Y. (2005): Petrography of quartz grains in beach and dune sands of Northland, North Island, New Zealand: Journal of Geology and Geophysics; 48: 649-660.

Katongo, C., Koeberl, C., Witzke, B. J., Hammond, R. H. and Anderson, R. R. (2004): Geochemistry and shock petrography of the Crow Creek Member, South Dakota, USA: Ejecta from the 74-Ma Manson impact structure. Meteoritics and Planetary Science; 39(1): 31–51.

Kawabe, I., Kitahara, Y. and Naito, K. (1991): Non-chondritic yttrium/holmium ratio and lanthanide tetrad effect observed in Pre-Cenozoic limestones. Geochem. J.; 25: 31–41.

Kitano, Y. and Furutsu, T. (1959): The state of magnesium contained in calcareous shells. Bull. Chem. Soc. Japan; 33: 1-4.

Klinkhammer, G. P., Elderfield, H. and Hudson, A. (1983): Rare earth elements in seawater near hydrothermal vents. Nature; 305: 185-188.

Knappe, A., Jarmersted, C. S., Pekdeger, A., Bau, M. and Dulski, P. (1999): Gadolinium in aquatic systems as indicator for sewage water contamination.

Geochemistry of the Earth's Surface (Armannsson, H., ed.), 187–190, Balkema, Rotterdam.

Krinsley, D. H. and Tovey, N. K. (1978): Cathodoluminescence in quartz sand grains. Scanning Electron Microscopy; 1: 887-894.

Krumbein, W. C. and Sloss, L. L. (1963): Stratigraphy and Sedimentation. W.H. Freedman and Co. San Francisco, U.S.A., 660.

Krupadam, R. J.; Smita, P. and Wate, S. R. (2006): Geochemical fractionation of heavy metals in sediments of the Tapi estuary. Geochemical Journal; 40: 513- 522.

Kulaksiz, S. and Bau, M. (2007): Contrasting behavior of anthropogenic gadolinium and natural rare earth elements in estuaries and the gadolinium input into the North Sea. Earth and Planetary Science Letters; 260: 361-371.

Kunzendorf, H. E. (1986): Marine Mineral Exploration (Elsevier Oceanography Series). Elsevier, Amsterdam, p. 300.

Lashhab, M. I.; West, I. M. and El Zarough, R. (2002): Origin and diagenesis of the evaporites in the Jir Formation, Jabal Waddan and Western Sirt Basin, Libya. 6th International Conference on the Geology of the Arab World, Cairo University, pp. 623-632. (Written by Dr. Mokhtar Lashhab mainly on the basis of his thesis on this topic in 1992, and supervised by Ian West.).

Leopold, E. N.; Jung, M. C.; Auguste, O.; Ngatcha, N.; Georges, E. and Lape, M. (2008): Metals pollution in freshly deposited sediments from river Mingoa, main tributary to the Municipal lake of Yaounde, Cameroon. Geosciences Journal; 12(4): 337 − 347.

Lihou, J. C. and Mange-Rajetzky, M. A. (1996): Provenance of the Sardona Flysch, eastern Swiss Alps: example of high-resolution heavy mineral analysis applied to an ultrastable assemblage. Sedimentary Geology; 105: 141-157.

Lipova, I. M. and Mayeva, M. M. (1971): The relation of Zr/Hf ratio in zircon to crystal morphology. Geochem. Int.; 8: 785-791.

Locock, A. J. (2008): An Excel spreadsheet to recast analyses of garnet into end-member components, and a synopsis of the crystal chemistry of natural silicate garnets. Computers and Geosciences; 34: 1769– 1780.

Lopez, J. M. G.; Bauluz, B.; Fernández-Nieto, C. and Oliete, A. Y. (2005): Factors controlling the trace-element distribution in fine-grained rocks: the Albian kaolinite-rich deposits of the Oliete Basin (NE Spain). Chemical Geology; 214 (1-2, 3): 1-19.

Loska, K.; Wiechuła, D.; Barska, B.; Cebula, E. and Chojnecka, A. (2003): Assessment of Arsenic Enrichment of Cultivated Soils in Southern Poland. Polish Journal of Environmental Studies; 12(2): 187-192.

Luzar-Oberiter, B.; Pavlakovic, S. M.; Crnjakovic, M. and Babic, L. (2008): Variable sources of beach sands of north Adriatic islands: examples from Rab and Susak. Geologia Croatica; 61(2–3): 379–384.

Macquaker, J. H. S.; Curtis, C. D. and Coleman, M. L. (1997): The role of iron in mudstone diagenesis: comparison of Kimmeridge Clay Formation mudstones from onshore and offshore (UKCS) localities. J. Sedim. Res.; 67: 871–878.

Madhavaraju, J. and Gonzalez-Leon, C. M. (2012): Depositional conditions and source of rare earth elements in carbonate strata of the Aptian-Albian Mural Formation, Pitaycachi section, northeastern Sonora, Mexico. Revista Mexicana de Ciencias Geológicas; 29(2): 478-491.

Madhavaraju, J. and Lee, Y. I. (2009): Geochemistry of the Dalmiapuram Formation of the Uttatur Group (Early Cretaceous), Cauvery basin, southeastern India: Implications on provenance and paleo-redox conditions. Revista Mexicana de Ciencias Geológicas; 26(2): 380-394.

Madhavaraju, J. and Ramasamy, S. (1999): Rare earth elements in limestones of Kallankurichchi Formation of Ariyalur Group, Tiruchirapalli Cretaceous, Tamil Nadu. Journal of the Geological Society of India; 54: 291-301.

Mahu, E.; Nyarko, E.; Hulme, S. and Coale, K. H. (2015): Distribution and enrichment of trace metals in marine sediments from the Eastern Equatorial Atlantic, off the Coast of Ghana in the Gulf of Guinea. Marine Pollution Bulletin; 98: 301-307.

Maksimovic, Z. and Eskangi, A. M. (1978): Trace elements in groundwaters of the Kufra Basin. Extrait du Bulletin T. LXI de l Academie serbe des Sciences et des Arts Classe Sciences mathematiques et naturelles, No. 17.

Malick, B. M. L. and Ishiga, H. (2015): Geochemical maturity of pocket beach sands from the Sanin region of southwest Japan. Earth Science Research; 4(2): 45-61.

Mange, M. A. and Maurer, H. F. W. (1992): Heavy minerals in colour. Chapman and Hall, London, 147 p.

Margineanu, R. M., Blebea-Apostu, A. M., Celarel, A., Gomoiu, C. M., Costea, C., Dumitras, D., Ion, A. and Duliu, O. G. (2014): Radiometric, SEM and XRD investigation of the Chituc black sands, southern Danube Delta, Romania. Journal of Environmental Radioactivity; 138: 72–79.

Mcburney C. B. M. & H E Y R.W. (1 9 5 5): Prehistory and Pleistocene geology in Cyrenaica Libya. Cambridge University Press; 315.

McLennan, S. M.; Hemming, S., McDaniel, D. K. and Hanson, G. N. (1993): Geochemical approaches to sedimentation, provenance, and tectonics, in Johnson, M.J., Basu, A. (eds.), Processes Controlling the Composition of Clastic Sediments: Geological Society of America, Special Paper; 284: 21-40.

Mikesell, L. R., Schaetzl, R. J. and Velbel, M. A. (2004): Hornblende etching and quartz/feldspar ratios as weathering and soil development indicators in some Michigan soils. Quaternary Research; 62: 162-171.

Mohapatra, S., Behera, P. and Das, S. K. (2015): Heavy mineral potentiality and alteration. Studies for ilmenite in Astaranga beach sands, District Puri, Odisha, India. Journal of Geoscience and Environment Protection; 3: 31-37**.**

Moreira, J. C. (1996): Threats by heavy metals: Human and environmental contamination in Brazil. Sci Total Environ; 188(Suppl 1):S61-S71.

Morton, A. C. (1984): Stability of Detrital Heavy Minerals in Tertiary Sandstones from the North-Sea Basin. Clay Minerals; 19(3): 287-308.

Morton, A. C. and Hallsworth, C. R. (1994): Identifying provenance-specific features of detrital heavy mineral assemblages in sandstones. Sedimentary Geology; 90: 241-256.

Morton, A. C. and Hallsworth, C. R. (1999): Processes controlling the composition of heavy mineral assemblages in sandstones. Sediment Geology; 124: 3–29.

Mount, J. F. (1985): Mixed siliciclastic and carbonate sediments: a proposed first-order textural and compositional classification. Sedimentology; 32(3): 435–442.

Muhs, D. R. (1982): A soil chronosequence on Quaternary marine terraces, San Clemente Island, California, Geoderma; 28: 257–283.

Muller, G. (1979): Schwermetalle in den sedimenten des Rheins-Veranderungen seit 1971. Umschau; 79: 778–783.

Murray, R.W., Ten Brink, M. R. B., Gerlach, D. C., Russ III, G. P. and Jones, D. L. (1991b): Rare earth, major and trace elements in chert from the Franciscan complex and Monterey Group, California: Assessing REE sources to fine grained marine sediments. Geochimica et Cosmochimica Acta; 55: 1875-1895.

Nagarajan, R., Madhavaraju, J., Nagendra, R., Armstrong-Altrin, J. S. and Moutte, J. (2007): Geochemistry of Neoproterozoic shales of the Rabanpalli Formation, Bhima Basin, Northern Karnataka, southern India: implications for

provenance and paleoredox conditions. Revista Mexicana de Ciencias Geológicas; 24 (2): 150-160.

Nakada, S. (1991): Magmatic processes in titanite-bearing dacites, central Andes of Chile and Bolivia, Am. Mineral; 76: 548–560.

Narla, A. K. (1996): Manganese and copper-zinc superoxide dismutases in the human olfactory mucosa: increased immunoreactivity in Alzheimer's disease. Exp Neurol; 140(2):115–125.

Nath, B. N., Bau, M., Ramlingeswara-Rao, B. and Rao, C. M., (1997): Trace and rare earth elemental variation in Arabian Sea sediments through a transect across the oxygen minimum zone. Geochimica et Cosmochimica Acta; 61: 2375-2388.

Nath, B. N., Roelandts, I., Sudhakar, M. and Plueger, W. L. (1992): Rare earth element patterns of the Central Indian Basin sediments related to their lithology. Geophysical Research Letters; 19: 1197-1200.

Nath, B. N., Roelandts, I., Sudhakar, M., Plueger, W. L. and Balaram, V. (1994): Cerium anomaly variations in ferromanganese nodules and crusts from the Indian Ocean. Marine Geology; 120: 385-400.

Nebsitt, H. W., Markovics, G. and Price, R. C. (1980): Chemical processes affecting alkalis and alkali earths during continental weathering. Geochim. Cosmochim. Acta; 44: 1659–1666.

Nebsitt, H. W. and Markovics, G. (1997): Weathering of granodioritic crust, longterm storage of elements in weathering profiles, and petrogenesis of siliciclastic sediments. Geochimica et Cosmochimica Acta; 61: 1653–1670.

Niencheski, L. F. H., Baraj, B., Franca, R. G. and Mirlean, N. (2002): Lithium as a normalizer for assessment of anthropogenic metal contamination of sediments of the southern area of Patos Lagoon. Aquatic Ecosystem Health and Management; 5: 473–483.

Nilgun, O. and Betel, E. (2005): Source of the basinal sediments in the Marmara Sea investigated using heavy minerals in the modern beach sands. Marine geology; 216(1-2): 1-15.

Nothdurft, L. D., Webb, G. E. and Kamber, B. S. (2004): Rare earth element geochemistry of Late Devonian reefal carbonates, Canning Basin, Western Australia: Confirmation of seawater REE proxy in ancient limestones. Geochimica et Cosmochimica Acta; 68: 263-283.

Nriagu, J. O. (1989): A global assessment of natural sources of atmospheric trace metals. Nature, 338, 47.

Ogata, T. and Terakado, Y. (2006): Rare earth element abundances in some seawaters and related river waters from the Osaka Bay area, Japan: Significance of anthropogenic gadolinium. Geochemical Journal; 40: 463-474.

Overstreet, W. C. (1967): The geological occurrence of monazite. US Geol Surv Prof Paper; 530:1–327.

Owen, M. R. (1987): Hafnium content of detrital zircons, a new tool for provenance study. Sedimentary Petrology; 57(5): 824-830.

Ozdemir, O. and Dunlop, D. J. (2000): Intermediate magnetite formation during dehydration of goethite. Earth and Planetary Science Letters; 177: 59-67.

Ozmen, S. F.; Cesur, A.; Boztosun, I. and Yavuz, M. (2014): Distribution of natural and anthropogenic radionuclides in beach sand samples from Mediterranean Coast of Turkey. Radiation Physics and Chemistry; 103: 37-44.

Papadopoulos, A.; Christofides, G.; Pe-Piper, G.; Koroneos, A. and Papadopoulou, L. (2015): Geochemistry of beach sands from Sithonia Peninsula (Chalkidiki, Northern Greece). Mineralogy and Petrology; 109: 53-66.

Parra, J. G.; Marsaglia, K. M.; Rivera, K. S.; Dawson, S. T. and Walsh, J. P. (2012): Provenance of sand on the Poverty Bay shelf, the link between source and sink sectors of the Waipaoa River sedimentary system. Sedimentary Geology; 280: 208-233.

Patyk-Kara, N.G.; Andrianova, E. A. and Dubinchuk, V. T. (2007): Secondary Alterations of Zircons in Placers. Doklady Earth Sciences; 419(2): 253–256.

Pavicic, L.; Babic, L.; Crnjakovic, M. and Zupanic, J. (2000): The provenance of sands on North Dalmatian beaches: Between ignorance and the need for coastal zone management. Periodicum Biologorum; 102: 349-354.

Perchuk, A. L.; Burchard, M.; Schertl, H. P.; Maresch, W. V.; Gerya, T. V.; Bernhardt, H. J. and Vidal, O. (2009): Diffusion of divalent cations in garnet: multi-couple experiments. Contrib Mineral Petrol; 157:573–592.

Peterson, C. D.; Komar, P. D. and Schneidegger, K. F. (1986): Distribution, geometry and origin of heavy mineral placer deposits on Oregon beaches. Journal of Sedimentary Petrology; 56: 67-77.

Petersen, N. T.; Smith, P. L.; Mortensen, J. K.; Creaser, R. A. and Tipper, H. W. (2004): Provenance of Jurassic sedimentary rocks of south-central Quesnellia, British Columbia: implications for paleogeography. Can. J. Earth Sci.; 41: 103-125.

Piepgras, D. J. and Jacobsen, S. B. (1992): The behaviour of rare earth elements in seawater: precise determination of variations in the North Pacific water column. Geochimica et Cosmochimica Acta; 56: 1851-1862.

Pilkey, O. H. (1963): Heavy minerals of the U.S. South Atlantic shelf and slope. Geol. Soc. Am. Bull; 74:641-648.

Piper, D. Z. (1974): Rare earth elements in the sedimentary cycle. Chemical Geology; 14: 285-304.

Pirrone, N.; Costa, P.; Pacyna, J. M. and Ferrara, R. (2001): Mercury emissions to the atmosphere from natural and anthropogenic sources in the Mediterranean region. Atmospheric Environment; 35(17): 2997-3006.

Pointer, C. M.; Ashworth, J. R. and Ixer, R. A. (1988): The Zircon-Thorite Mineral Group in Metasomatized Granite, Ririwai, Nigeria. Mineralogy and Petrology; 39: 21-37.

Polozek, K. (2000): Distribution of heavy minerals in CRP-2/2A, Victoria Land Basin, Antarctica. Terra Antartica; 7(4): 567-573.

Polozek, K. and Ehrmann, W. (1998): Distribution of heavy minerals in CRP- 1. Terra Antartica; 5(3): 633-638.

Potter, P. E. (1994): Modern sands of South America: composition, provenance and global signifi cance. – Geol. Rundsch; 83: 212–232.

Preda, M. and Cox, M. E. (2005): Chemical and mineralogical composition of marine sediments, and relation to their source and transport, Gulf of Carpentaria, Northern Australia. Journal of Marine Systems; 53: 169– 186.

Premaratne, W. A. P. J. and Rowson, N. A. (2003): The processing of beach sand from Sri Lanka for the recovery of titanium using magnetic separation. Physical Separation in Science and Engineering; 12(1): 13–22.

Pupin, J. P. (1985): Magmatic zoning of zircon from the Hercynian granitoids in France based on typology. Schweiz. Mineral. Petrogr. Mitt; 65: 29-56.

Pyokari, M. (1997): The provenance of beach sediments on Rhodes, southeastern Greece, indicated by sediment texture, composition and roundness. Geomorphology; 18: 315-332.

Quinby-Hunt, M. S.; Wilde, P. and Berry, W. B. N. (1991): The provenance of low-calcic black shales. Mineralium Deposita; 26: 113–121.

Rahman, M. A.; Alam, M. S. and Shine, F. M. M. (2004): Roundness and Sphericity of Calstic Sediments of Apical Part of the Tista Fan in Panchagarh District, Bangladesh. Rajshahi University Studies, Part-B.

Rasmussen, B. and Muhling, J. R. (2007): Monazite begets monazite: evidence for dissolution of detrital monazite and reprecipitation of syntectonic monazite during low-grade regional metamorphism. Contrib Mineral Petrol; 154:675–689.

Reimann, C. and de Caritat, P. (2005): Distinguishing between natural and anthropogenic sources for elements in the environment: regional geochemical surveys versus enrichment factors. Sci. Total Environ.; 337: 91–107.

Reyneke, L. and Van Der Westhuizen, W. G. (2001): Characterization of a heavy mineral-bearing sample from India and the relevance of intrinsic mineralogical features to mineral beneficiation. Minerals Engineering; 14(12): 1589-1600.

Robertson S., (2011): Direct Estimation of Organic Matter by Loss on Ignition. Property of SFU Soil Science Lab. P.1.

Rollinson, H. R. (1993): Using geochemical data: evaluation, presentation and interpretation. Longman Group Ltd., 352p.

Rubio, B.; Nombela, M. A. and Vilas, F. (2000): Geochemistry of major and trace elements in sediments of the Ria de Vigo (NW Spain) an assessment of metal pollution. Marine Pollution Bulletin; 40(11): 968-980.

Rulkens, W. H.; Grotenhuis, J. T. C. and Tichy, R. (1995): Methods for cleaning contaminated solis and sediments. In (W. Salomous; U. Forstner and P. Mader, Eds), Heavy metals: Problems and Solutions. Springer, Berlin, pp. 196-191.

Sabeen, H. M.; Ramanujam, N. and Morton, A. C. (2002): The provenance of garnet: constraints provided by studies of coastal sediments from southern India. Sedimentary Geology; 152: 4279-287.

Sagga, A. M. S. (1993): Roundness of sand grains of longitudinal dunes in Saudi Arabia: Sedimentary Geology; 87: 63-68.

Salomons, W. and Forstner, U. (1984): Metals in the Hydrocycle. Springer-Verlag, Berlin.

Sanderson, I. D. (1984): Recognition and significance of inherited quartz overgrowths in quartz arenites: Journal of Sedimentary Petrology; 54: 473-486.

Schintu, M.; Marras, B.; Maccioni, A.; Puddu, D.; Meloni, P. and Contu, A. (2009): Monitoring of trace metals in coastal sediments from sites around Sardinia, Western Mediterranean. Marine Pollution Bulletin; 58(10): 1577-1583.

Schwartz, J. J. and Gromet, P. L. (2004): Provenance of a late Proterozoic-early Cambrian basin, Sierras de Córdoba, Argentina. Precambrian Reserch;129:1-21.

Shaltami, O. R. (2007): Characteristics of heavy metals in the red soil (terra rossa) along the coastal plain of Al Jabal Al Akhdar, NE Libya. Trace Elements in the Environment; 5: 513-531.

Shaltami O. R. (2012): Mineral composition and environmental geochemistry of the beach sediments along the Mediterranean Coast from Benghazi to Bin Jawwad, Northeast Libya. PH.D. Thesis. Cairo Univ. Cairo, Egypt.

Shaltami, O. R. (2013): Mineralogical and geochemical characteristics of the Al Hilal Formation, Ras Al Hilal Area, Al Jabal Al Akhdar, NE Libya. Scientific Benghazi University Journal; 1: 41-56.

Shenber, M. A. and Eriksson, A. (1993): Sorption behaviour of cesium in various soils. Journal of Environmental Radioactivity; 19(1): 41-51.

Shenber, M. A.; El Shamis, E. E.; Bader, A. R.; El Ayan, M. N. and El Kikli, A. T. (2001): Measurement of radioactivity levels of the Sirt Gulf, Libya: Section A:

Environmental Studies. International journal of environmental studies; 58(5): 625-629.

Shine, F. M. M. (2006): Shape Analysis of Detrital Quartz Grains and its Environment of Deposition in Holocene Sediments along the Karotoya River, Bogra, Bangladesh. Journal of Geo-Environment; 6: 54-63.

Shuster, D. L.; Farley, K. A.; Vasconcelos, P. M.; Balco, G.; Monteiro, H. S.; Waltenberg, K. and Stone, J. O. (2012): Cosmogenic 3He in hematite and goethite from Brazilian "canga" duricrust demonstrates the extreme stability of these surfaces. Earth and Planetary Science Letters; 329: 41-50.

Skiba, M.; Maj-Szeliga, K.; Szymanski, W. and Blachowski, A. (2014): Weathering of glauconite in soils of temperate climate as exemplified by a Luvisol profile from Gora Pulawska, Poland. Geoderma; 235-236: 212-226.

Smith, A. L. (1970): Sphene, perovskite and coexisting Fe-Ti oxide minerals, American Mineralogist; 55: 264–269.

Soto-Jimenez, M. F.; Paez-Osuna, F. and Ruiz-Fernandez, A. C. (2003): Geochemical evidences of the anthropogenic alterations of trace metal composition of the sediments of Chiricahueto marsh (SE Gulf of California). Environ. Pollut.;125: 423–432.

Speer, J. A. (1982): Zircon. Reviews in Mineralogy 5, 2nd edn: 67-112.

Sukumaran, P. V. and Nambiar, A. R. (1994): Geochemistry of ilmenites from Ratnagiri coast, Maharashtra. Curr. Sci.; 67: 105–106.

Sundararajan, M.; Bhat, K. H.; Babu, N.; Janaki, M. E. K. and Mohan Das, P. N. (2009): Characterization studies on ilmenite of Ullal and Suratkal along Karnataka Coastline, West Coast of India. Journal of Minerals and Materials Characterization and Engineering; 8(6): 479-493.

Suresh, G.; Ramasamy, V.; Sundarrajan, M. and Paramasivam, K. (2015): Spatial and vertical distributions of heavy metals and their potential toxicity levels in various beach sediments from high background radiation area, Kerala, India. Marine Pollution Bulletin; 91: 389-400.

Suzuki, Y. and Banfield, J. F. (2001): Aerobic Microbial Interaction with Uranium: Resistance and Accumulation. Eleventh Annual V. M. Goldschmidt Conference (2001) 3533.pdf.

Suzumural, M. and Kamatani, A. (1995): Origin and distribution of inositol hexaphosphate in estuarine and coastal sediments. Limnol. Oceanogr; 40(7): 1254-1261.

Szefer, P.; Szefer, K.; Glasby, G. P.; Pempkowiak, J. and Kaliszan, R. (1996): Heavy metal pollution in surficial sediments from the southern Baltic Sea off Poland. Journal of Environmental Science and Health; A 31(10): 2723-2754.

Taylor, S. R. and McLennan, S. M. (1985): The Continental Crust: its composition and evolution. Blackwell Scientific Publishers, Oxford.

Tessier, A.; Carignan, R. and Belzile, N. (1994): Processes occurring at the sediment-water interface: emphasis on trace elements. In: Buffle, J. and De Vitre, R.R. (eds.), Chemical and Biological Regulation of Aquatic Processes, pp: 137–175. Lewis Publishers, Chelsea.

Thomson, J.; Crudeli, D.; De Lange, G. J.; Slomp, C. P.; Erba, E. and Corselli, C. (2004): *Florisphaera profunda* and the origin and diagenesis of carbonate phases in eastern Mediterranean sapropel units. *Paleoceanography 9*, PA3003, doi:10.1029/2003PA000976.

Trevena, A. S. and Nash, W. P. (1979): Chemistry and provenance of detrital plagioclase. Geology; 7: 475-478.

Turner, R. J. (2005): Provenance and depositional history of late Pleistocene New Jersey Shelf Sediments. MS.C. Thesis. Georgia State University. USA.

Veizer, J. (1983): Trace elements and isotopes in sedimentary carbonates, in Reeder, R.J. (ed.), Carbonates: Mineralogy and Chemistry: U.S.A, Mineralogical Society of America, Reviews of Mineralogy; 11: 265-299.

Verma, S. P. (2005): Estadística Básica para el Manejo de Datos Experimentales: Aplicación en la Geoquímica (Geoguimiometría): México, D.F., Universidad Nacional Autónoma de México, 186p.

Voegborlo, R. B. and Chirgawi, M. B. (2007): Heavy metals accumulation in roadside soil and vegetation along a major highway in Libya. Journal of Science and Technology (Ghana); 27(2): 86-97.

VonGunten, H. R.; Sturm, M. and Moser, R. N. (1997): 200-year record of metals in lake sediments and natural background concentrations. Envir. Sci. Technol.; 31(8): 2193–2197.

Watson, E. B. (1980): Some experimentally determined zircon/liquid partition coefficients for the rare earth elements. Geochimica et Cosmochimica Acta; 44: 895–897.

Weibel, R. (1998): Diagenesis in oxidising and locally reducing conditions-an example from the Triassic Skagerrak Formation, Denmark. Sedimentary Geology; 121: 259–276.

Weibel, R. and Friis, H. (2004): Opaque minerals as keys for distinguishing oxidising and reducing diagenetic conditions in the Lower Triassic Bunter Sandstone, North German Basin. Sedimentary Geology; 169: 129-149.

Weyer, S.; Munker, C.; Rehkomper, M.; and Mezger, K. (2002): Determination of ultra-low Nb, Ta, Zr and Hf concentrations and the chondritic Zr/Hf and Nb/Ta ratios

by isotope dilution analyses with multiple collector ICP-MS,Chem, Geol.; 187(3-4): 295-313.

White, W. M. (2001): Geochemistry: An on-line textbook. John-Hopkins University Press, 700 p.

Wilkin, R. T. and Barnes, H. L. (1997): Formation processes of framboidal pyrite. Geochimica et Cosmochimica Acta. Volume 61, Issue 2, P. 323-339.

Wronkiewicz, D. J. and Condie, K. C. (1987): Geochemistry of Archean shales from the Witwatersrand Supergroup, South Africa: source-area weathering and provenance, Geochim. Cosmochim. Acta; 51: 2401–2416.

Yang, S.; Jung, H. S. and Li, C. (2003): Two unique weathering regimes in the Changjiang and Huanghe drainage basins: geochemical evidence from river sediments. Sedimentary Geology; 164(1-2): 1-178.

Younis, A. M.; Kilcoyne, S. H.; Yacob, M. and Goodman, B. A. (1999): Soils from the Jabal Al-Akhdar region of North East Libya: Characterisation of the iron using chemical methods and Mössbauer spectroscopy. Hyperfine Interactions; 122 (3-4): 259-268.

Zack, T.; von Eynatten, H. and Kronz, A. (2004): Rutile geochemistry and its potential use in uantitative provenance studies. Sedimentary Geology; 171: 37-58.

Zaghloul, M. N.; Reddad, H. and Critelli, S. (2009): Source area controls on the composition of beach and fluvial sands on the southern side of the Gibraltar Strait and Western Alboran Sea (Flysch Basin, Internal and External, Domains, Northern Rif Chain). Journal of African Earth Sciences; 55: 36-46.

Zankl, H. (1993): The origin of High-Mg-Calcite microbialites in cryptic habitats of Caribbean coral reefs—Their dependence on light and turbulence. Facies; 29: 55-59.

Zhang, J. (1995): Geochemistry of trace metals from chinese river/estuary systems: An overview. Estuarine, Coastal and Shelf Science; 41: 631–658.

Zhang, K., J. (2004): Secular geochemical variations of the Lower Cretaceous siliciclastic rocks from central Tibet (China) indicate a tectonic transition from continental collision to back-arc rifting. Earth and Planetary Science Letters; 229: 73-89.

Zhang, J.; Amakawa, H. and Nozaki, Y. (1994): The comparative behaviors of yttrium and lanthanides in the seawater of the North Pacific, Geophys. Res. Lett.; 21: 2677–2680.

Zhang, J. and Liu, C. Q. (2004): Major and rare earth elements in rainwaters from Japan and East China Sea: Natural and anthropogenic sources. Chemical Geology; 209(3-4): 315-326.

Zhu, Y.; Hoshino, M.; Yamada, H.; Itoh, A. and Haraguchi, H. (2004): Gadolinium Anomaly in the Distributions of Rare Earth Elements Observed for Coastal Seawater and River Waters around Nagoya City. Bulletin of the Chemical Society of Japan; 77(10): 1835-1842.

Zoumis, T.; Schmidt, A.; Grigorova, L. and Calmano, W. (2001): Contaminants in sediments: remobilization and demobilization. Sci. Total Environ.; 266: 195–202.